Development of Fast Activation Method using Microwave-Induced Plasma for Preparation of High-Surface-Area Activated Carbon

Purichaya Kuptajit

2021

Table of Contents

Introduction

1. Introductory Remarks

Activated carbon is a porous carbon material, which can be used in various kinds of applications. In conventional processes, activated carbon with a specific surface area above 1000 m^2 g^{-1} can be produced using various activating agents. Typically, carbon precursors are mixed with the activating agents before being heated at 500 °C or higher for 1-4 h. [1] Among them, an activation method using potassium hydroxide (KOH) [2,3] can be used to produce activated carbon with a high degree of porosity.

The conventional activation methods require a long activation time (hour-day level) to produce activated carbon with a high specific surface area, resulting in high energy consumption. Therefore, this research aims to shorten activation time by developing a novel method, which leads to efficient production with reduced energy consumption. To reduce activation time, many research works have been paying attention to the microwave heating method and trying to apply it to KOH activation. When the microwave heating method applies to KOH activation, one of the short activation time recorded is 5 min, [4] which is one to two orders of magnitude shorter than conventional activation time.

As mentioned above, the activation time could be shortened by using microwave heating with KOH activation. This study aims to use microwave heating with KOH activation to open the possibility to develop a continuous system, which could lead to less energy consumption and less harm to the environment.

2. Activated Carbon

Activated carbon, often known as activated charcoal, is a kind of carbon material. It has a random, uneven structure that is highly porous and has a wide range of pore sizes. The porous structure of activated carbon provides a high surface area, allowing the activated carbon to adsorb various chemicals with a wide range of molecular size. Activated carbon is utilized in a variety of chemical processes. It can be used as adsorbents in water treatment, [5] purification of biotechnological xylitol from *Candida tropicalis* fermentation, [6] indoor air purification, [7] methylene blue removal, [8] and catalytic supports in lactic acid production from glucose, [9] methane dry reformation, [10] and other applications. Some applications of activated carbon show in **Figure 1**.

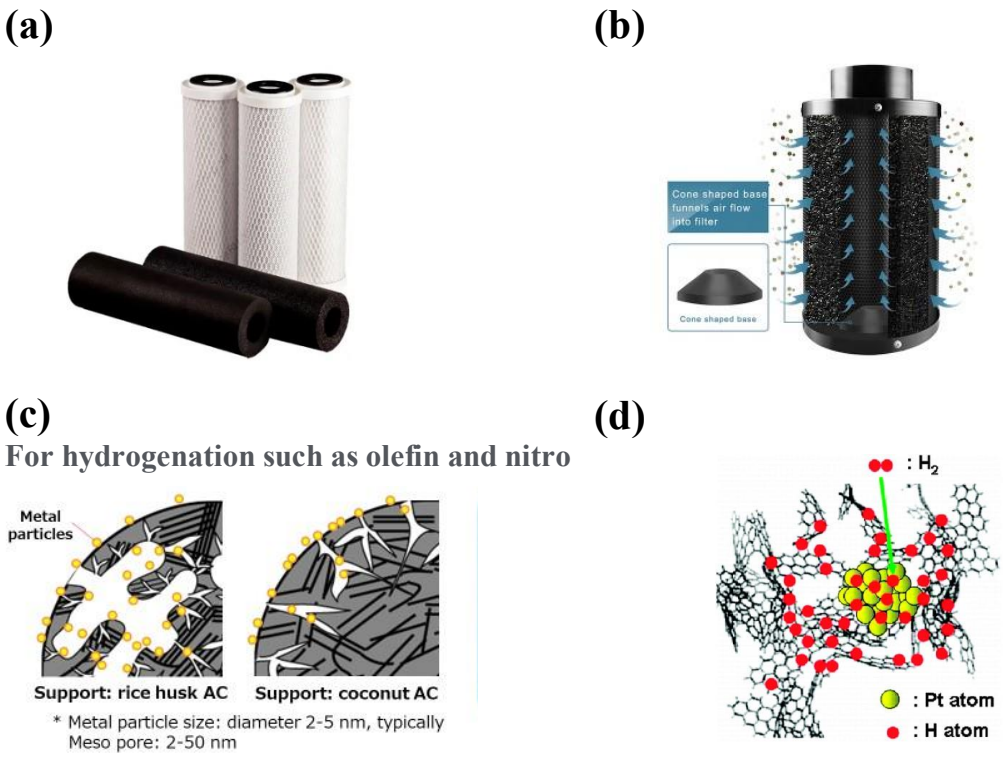

Figure 1 Some application of activated carbon: (a) water purification,[11] (b) air purification,[12] (c) catalyst support,[13] and (d) hydrogen storage. [14]

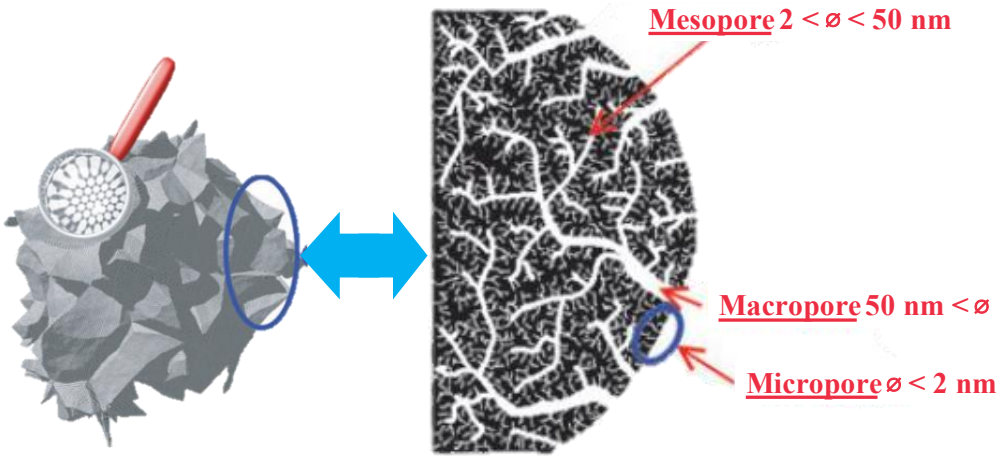

Figure 2 Activated carbon and its porous structure. [21]

Conventionally, activated carbon has a specific surface area in the range of 500 to 3000 m^2 g^{-1}. The structure of the activated carbon consists of micropores (pore diameter < 2 nm), mesopores (2 nm < pore diameter < 50 nm), and macropores (pore diameter > 50 nm) as shown in **Figure 2**. [15–19] The pore size was classified accordingly to IUPAC. [20]

Various carbon precursors can be used as feed material to prepare activated carbon, such as shaddock peel, [22] bamboo, [23] co-carbonization of waste truck tires and spent tea leaves, [24] coffee residue, [25] polyvinylidene chloride (PVDC) resin, [26] and yeast biomass waste. [27] Some examples of carbon precursor is presented in **Figure 3**.

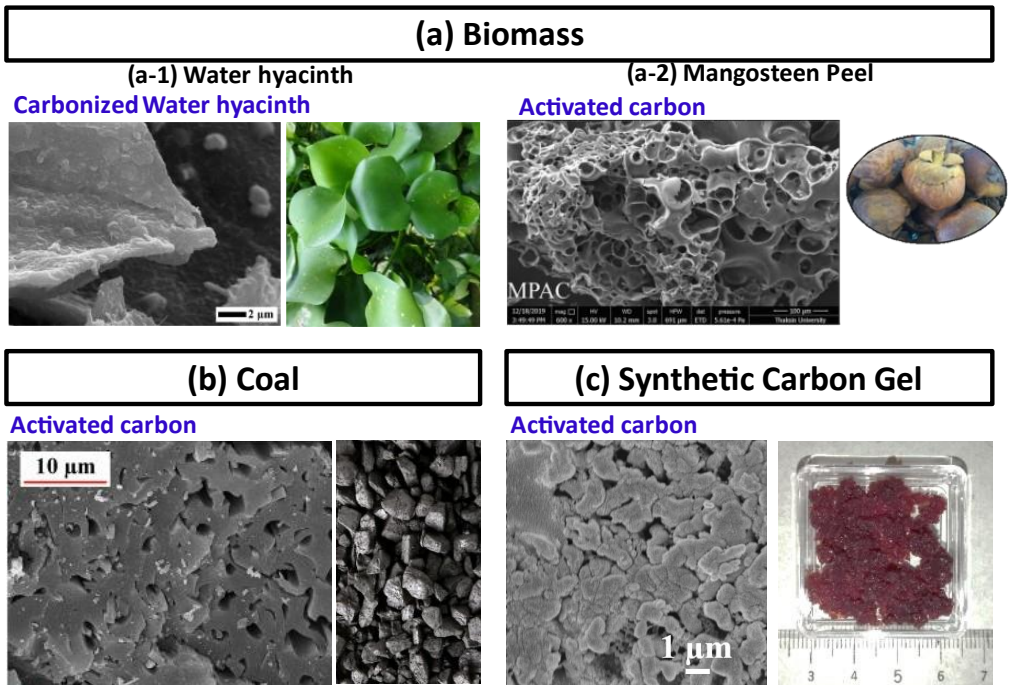

Figure 3 Some carbon precursors that can be used as a feed materials to prepare activated carbon: (a) biomass such as (a-1) water hyacinth and (a-2) mangosteen peel[28], (b) coal[29], and (c) synthetic carbon gel.

Typically, carbon precursors are mixed with a variety of activating agents, for example, gas activating agents such as steam [30] and carbon dioxide (CO_2), [31,32] or chemical activating agents such as zinc chloride ($ZnCl_2$), [33] sodium hydroxide (NaOH), [34,35] KOH, and potassium carbonate (K_2CO_3) [36]. The advantages and disadvantages of the activation method using gas and chemical activating agents are compared and summarized in Table 1. Then, the mixture of carbon precursor and activating agents is heated at designated temperature and time. The activation period using gas activating agents and chemical activating agents are summarized in **Figure 4**.

Table 1 Comparison of advantages and disadvantages of activation using gas and chemical activating agents.

	Advantage	Disadvantage
Gas activating agents	Inexpensive and easy to handle	Ineffective to generate micropores
Chemical activating agents	Effectively to generate microporous structure	Expensive and difficult to handle due to corrosiveness

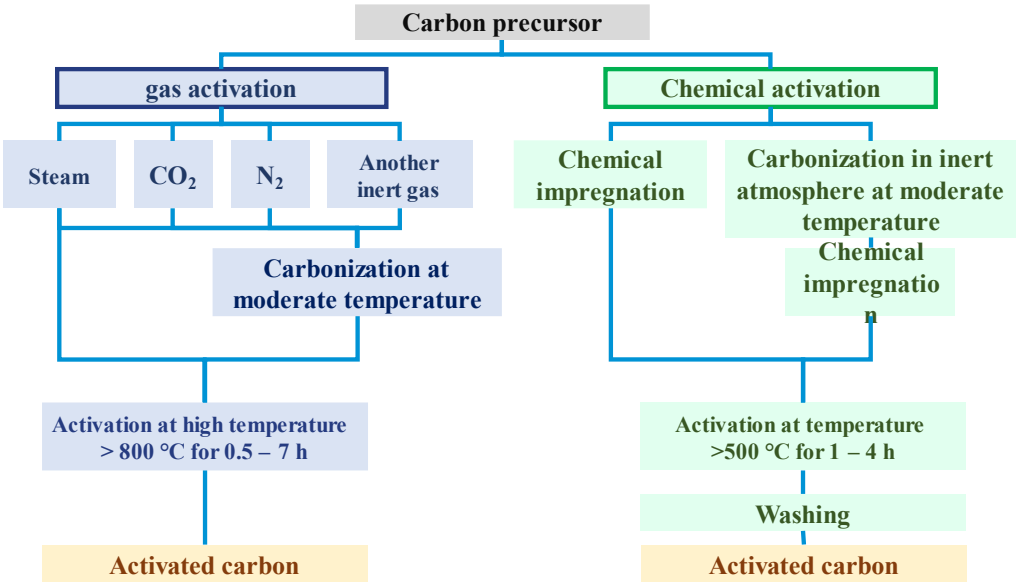

Figure 4 Summary of activation using gas and chemical activating agents.[1]

3. Reactor design for Production of Activated Carbon

3.1 Conventional Reactors

Rotary kiln and fluidized bed are normally used for activated carbon production on an inductrial scale. [37] It is important that the reactors are operated under high temperature and inert atmosphere e.g. argon (Ar) and nitrogen (N_2). It is also necessary to have a purge line in order to prevent a build-up of the pressure inside the reactor. Normally, the temperature limit of the heating part varies by the installed resistor of the reactor. [38] However, a maximun temperature of 900 °C is ideal for most reactors especially when chemical activation is used.

For example, Satya Sai, *et al.* [39] prepared activated carbon from coconut shell for iodine adsorption. In this work, a fluidized bed reactor with diameter

of 100 mm was employed. Steam and/or carbon dioxide had been used as activating agents. The optimal operating condition observing in this work is a reaction time of 1.5 h and particle size of 1.55 mm at a temperature of 850 °C, using steam as the fluidizing medium.

Mohaddespour, *et al.* [40] developed an induction heated fluidized bed reactor to make activated carbon from resorcinol–formaldehyde aerogels. Carbon dioxide was served as an activating agent in this research. The results show that the developed reactor can markedly reduce the activation time (from hours to minutes) by improving heat and mass transfer effieciency. The development of this reactor can contribute to the scale-up of the activation process.

Tiegam, *et al.* [41] studied a production process of activated carbon from cocoa pods by KOH activation in a batch sytstem and assessed its sustainability by using Life Cycle Assessment (LCA). This study demonstrated that this process has a high electrical consumption, that potentially be harmful to the ecosystem.

3.2 Microwave Reactor

A microwave is an electromagnetic wave, which is normally operated at 2.45 GHz for heating purposes. It is known that microwave heating has two mechanisms. One mechanism is the excitation of the dipole for dielectric materials. For example, water can be heated by microwave irradiation by this mechanism. For the activation to produce activated carbon with KOH addition, the temperature of KOH can be raised by this mechanism. Another mechanism is the absorption by free electrons in conductive materials, generating eddy current in them and causes Joule heating. [42] For example, high crystallinity carbon can be heated by this mechanism. When amorphous carbon receives microwave at room temperature, the heating by this mechanism is not significant. But when its temperature become high, its conductivity can be increased, [43] and the electrical conductivity of such carbon may become high enough to be heated by the second mechanism.

Microwave reactors, as opposed to conventional reactors, can provide a high temperature-elevation rate. A previous studies suggested that the activation time is mostly determined by the type of precursor and can be altered greatly by particle size and heat transfer mechanism. In addition, operating conditions can have significant effects on pore properties and yield of the activated carbon. For example, the activation temperature, heating rate, type of activating agent, activation atmosphere, microwave irradiation power, sample weight, and gas flowrate can pose strong influences on the surface

area and pore structure of the produced activated carbon. Moreover, the yield of activated carbon is affected by the sample's washing procedures, activation temperature, overall handling, etc.

Canales-Flores, *et al.* [44] produced activated carbon from barley husk, corn cob, and *Agave salmiana* leaves using phosphoric acid impregnation with microwave heating. The produced activated carbon showed significant removal efficiencies of methylene blue, which could be influences of the activation agent and microwave.

Brazil *et al.* [45] reported the optimization of the activated carbon production based on conventional and microwave processes. In this research, Kraft lignin was used as a feed material. Activated carbon was prepared using phosphoric acid impregnation under oxidizing atmosphere. The experimental results indicated that activated carbon with a specific surface area of 1,030 $m^2 g^{-1}$ can be prepared with the lignin : acid ratio of 1:2. In addition, the activated carbon prepared by the microwave process is more efficient in the methylene blue removal than the activated carbon prepared by the conventional process.

3.3 Comparison between Conventional and Microwave Reactors

It is desired to develop a reactor which contributes to a sustainable society. Such a reactor should be able to produce activated carbon on a large scale and can be operated in a continuous process in order to reduce energy consumption and time with acceptable production yield. For the production of activated carbon, conventional reactors, particularly rotary kilns and fluidized bed reactors, are used on a large scale. [37,46] They are mostly employed in the industry because of their ease of use, good control over the temperature gradient, and inexpensive installation cost. This type of reactor can be used to perform carbonization and activation in one step.

The microwave reactor is a promising technology because it allows fast heating and conversion of raw materials to activated carbon with a short activation period, leading to less energy consumption. However, more research into more energy efficiency is recommended for this method. Also, a large-scale microwave reactor for activated carbon production would be expensive, and large-scale deployment has yet to be established. Furthermore, precise temperature monitoring in a microwave reactor is difficult. As a result, temperature control is required for the commercialization of this technique for activated carbon production; otherwise, hot spots can cause non-homogeneous heating, compromising the quality of the final activated carbon product.

Both conventional and microwave reactors can generate activated carbon with a high surface area and promising pore properties. Here, this study focuses on microwave reactor to obtain high-surface-area activated carbon because the author expects that the activation time can be shortened than the conventional one, resulting in less energy consumption. Despite the fact that conventional reactors driven by electric heating or fossil fuel combustion have attained technological maturity, they nevertheless have a number of drawbacks, including environmental concerns and limited efficiency.

4. Plasma and its influences on Chemical Reaction

Plasma is the fourth state of matter (states of matter are solid, liquid, gas, and plasma). Plasma can be used widely in chemical engineering work because of its properties that can intense chemical processes including improve process efficiency and stimulate chemical reactions that are not possible in the conventional method. The plasma can be classified according to the temperature of plasma components including electron temperature (T_e), ion temperature (T_i), gas temperature (T_g), and electron density (n_e). Schematic explanations of plasma classification is illustrated in **Figure 5**.

Plasma can be categorized by electron temperature into low- and high-temperature plasma (electron temperature > 10^7 K). The low-temperature plasma can be categorized into thermal and non-thermal plasma. For thermal plasma, electron temperature, ion temperature, and gas temperature are similar. Therefore, the thermal plasma can be defined as in local thermodynamic equilibrium. On the contrary, for non-thermal plasma, the electron temperature is much higher than the ion temperature. In addition, previous studies reported that gliding arc and microwave discharge can provide properties of both thermal plasmas (large electron densities, currents, and power) and non-thermal plasmas (low gas temperature).[47] The non-thermal plasma can be categorized by electron temperature into warm (gas temperature ~10^3 K) and cold plasma (gas temperature ~10^2 K). A previous study illustrates that plasma can be used for intense chemical processes. However, practical use of a chemical process in a plasma system needs to be in a reactor with good phase contact and optimal plasma parameters.

4.1 Thermal plasma

Thermal plasma can provide extremely high temperature in the range of 10^3~10^4 K, which is not easy to reach in normal environments for chemical reactions. The thermal plasma can be generated from various kinds of reactors such as microwave plasma, RF-induced plasma, and arc plasma. The high

temperature can be realized when the gas molecules expose to a strong electric field. Then, the charged particles collide with each other and release heat, resulting in direct heat reductive and oxidative on the gas and its mixtures.

The features of thermal plasma, which mentioned earlier can be used to realize cleaner chemical processes. For example, one-step conversion from coal to acetylene, waste treatment, and nanomaterials fabrication. On the contrary, extremely high temperature of the thermal plasma makes a big challenge on the reactor design.

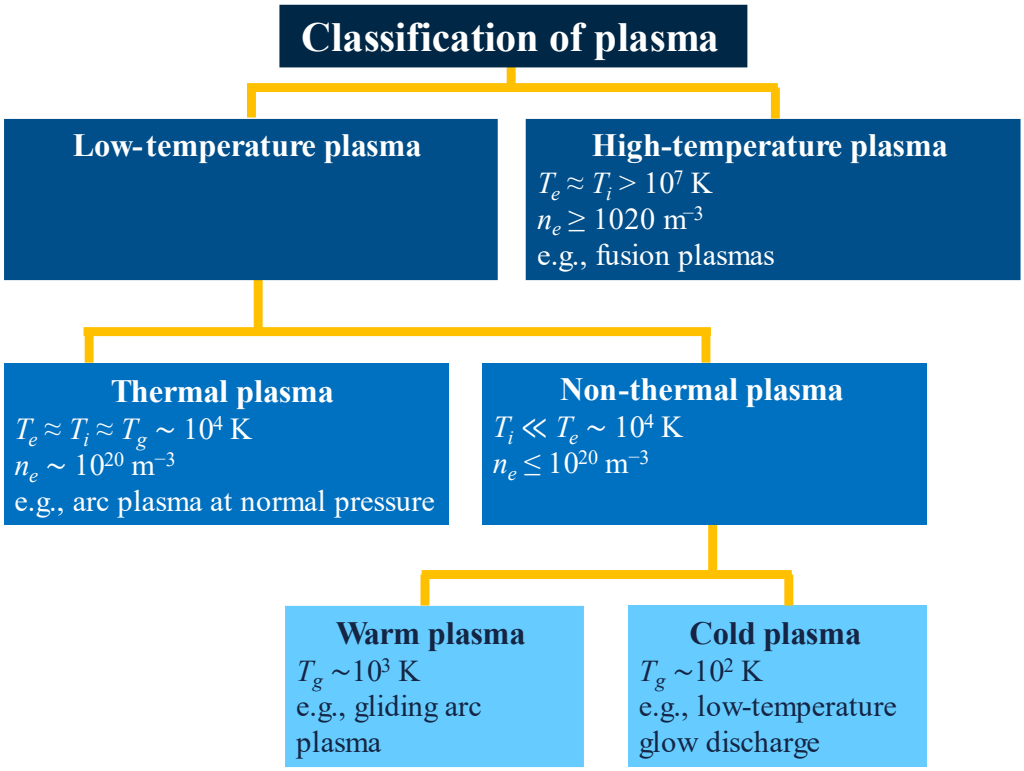

Figure 5 Classification of Plasma. [47]

4.2 Non-thermal plasma

Different from thermal plasma, non-thermal plasma cannot be defined as in local thermodynamic equilibrium because electron temperature is much higher than ion temperature. It consists of various components, which are highly reactive such as charged particles, excited molecules, radicals, etc. In such non-equilibrium plasma likes non-thermal plasma, it can be directly determined by electron temperature because the electron temperature is significantly higher than the temperature of heavy particles like ion temperature. Non-thermal plasma can be made from various types of pulsed

discharge such as corona discharge, glow discharge, dielectric barrier discharge. The non-thermal plasma also can be generated from microwave and RF discharges. Since non-thermal plasma has a lower temperature than thermal plasma, it can be combined with a catalysis reaction. In order to generate non-thermal plasma by discharge, operating parameters such as operating pressure and gas temperature need to be optimized for a specific applications.

5. Objective of This Work

This dissertation aims to open the possibility to develop a new continuous reactor design concept for activated carbon preparation by combining microwave-induced plasma with the KOH activation. Here, this activation is referred to as MiWP-KOH activation. This MiWP-KOH activation can realize the extremely fast preparation of activated carbon with a high surface area and controlled pore structure.

In Chapter 1, the development of MiWP-KOH activation (batch-operation) to obtain activated carbon within several minutes is reported. It is remarkable that the investigated method can reduce the activation time by one to two orders of magnitude in comparison to conventional heat-conduction activation. Emission spectra from the plasma are also discussed here.

In Chapter 2, the effect of temperature-elevation rate on pore formation of activated carbon prepared by MiWP-KOH activation operated in the batch system is discussed. The measurement of temperature change of the feed material in the MiWP-KOH activation is included. The microporous and mesoporous structure of activated carbon produced by the MiWP-KOH activation is investigated to understand the effect of rapid temperature-elevation rate on pore generation of a micropore-dominating structure. For the discussion, activated carbon is prepared using a conventional heat-conduction activation with various temperature-elevation programs, and the results of pore-structural analysis from these experiments are compared with those observed in activated carbon prepared by MiWP-KOH activation. The investigation on activated carbon prepared by MiWP-KOH activation and conventional heat-conduction activation with a similar temperature changing program is conducted to confirm the effects of microwave irradiation to enhance the pore formation.

In Chapter 3, the hypothesizes that microwave-irradiation time and KOH concentration in the feed mixture as important factors governing the pore formation is investigated. The operating conditions of the MiWP-KOH activation operated in the batch system have been adjusted to modify and

increase the surface area of activated carbon and to keep the repeatability of the activated carbon.

In Chapter 4, a new pseudo-continuous reactor for MiWP-KOH activation is examined. The specific surface area and pore structure of the produced activated carbon is investigated by varying microwave-retention time. In addition, an average mass yield percentage of the activated carbon synthesized by the proposed method is reported. In this chapter, the reaction mechanism is discussed based on the influence of the microwave retention time.

Chapter 1 MiWP-KOH Activation: Batch Operation

1.1 Introduction

Many researchers have been paying attention to the fundamentals and applications of plasma owing to its unique properties including high reactivity and high temperature, which can be useful for material fabrications. [52] Microwave-induced plasma can be generated by irradiating microwave to conductive porous materials, such as carbonized powders. The conductive porous materials can easily facilitate the generation of plasma because electrons can be discharged in the microstructure of the porous materials when a microwave is applied. [53] Previous studies reported the generation of microwave-induced microplasmas in porous carbon materials, resulting in the production of selective catalysts. [54,55] Because microwave can rapidly heat materials which are good microwave absorbers, such as carbon materials, the microwave has been applied to a process of opening small pores on these materials to prepare activated carbon to reduce the activation time. [4] Before the present study, the shortest record of activation time is 5 min to obtain activated carbon with a relatively small surface area of 708 $m^2\ g^{-1}$ when a microwave is applied. [56,57]

Activated carbon is a porous carbon material with a surface area in the range of 500–3000 $m^2\ g^{-1}$. Due to the porous structure of activated carbon, it has been used in various purification processes based on adsorption, including water and gas purifications. [58–62] Activated carbon can be produced by heating carbon precursors with activating agents, such as KOH, NaOH, and K_2CO_3 at an elevated temperature. [63,64] Nowadays, in industries, the process to prepare activated carbon is limited to only batch operation because of its long activation time. [65–69] The drastic reduction of activation time can make an evolutional change in the reactor design concept for activated carbon preparation by switching the batch operation to continuous operation. This situation motivates us to conduct this study to reduce the activation time by applying MiWP-KOH activation.

1.2 Materials and Methods

The procedure to obtain activated carbon examined in this study is described as follows. Firstly, a synthetic carbon gel was prepared according to the method reported by Mukai *et al.* [70] Here, phenol was mixed with formaldehyde in distilled water in the presence of sodium carbonate which served as the catalyst. The concentration of phenol was fixed at 500 mol m^{-3}. Molar ratios of phenol to formaldehyde and sodium carbonate were fixed at

0.5 and 1.5, respectively. The mixture was heated at 95 °C for 72 h before being left at room temperature for another 72 h to complete polymerization, and the gel formed by this polymerization was washed with distilled water for 1 h. The obtained carbon gel was dried at 110 °C (1 °C min^{-1} to reach 110 °C) for 1 h and was carbonized at 700 °C (10 °C min^{-1} to reach 700 °C) for 1 h under nitrogen atmosphere before being cooled naturally to obtain carbonized carbon gel (CCG).

The CCG was ground with KOH at a mass ratio of KOH to CCG = 1:10, 1:1, and 6:1. Among of CCG was fixed at 0.1 g. The mixture of CCG and KOH was heated for 40–330 s by a modified microwave oven [Sanyo Electric, EM-LA1(HL)] as shown in **Figure 1.1**. The inside dimension of the microwave oven is 350 mm × 425 mm ×198 mm. The inside dimension and length of the quartz tube is 42 mm and 139 mm, respectively. The inside dimension of the alumina container is 14 mm × 17 mm × 11 mm. The diameter of the microwave emission port is 15 mm. The modified microwave oven was operated at 2.45 GHz, 500 W.

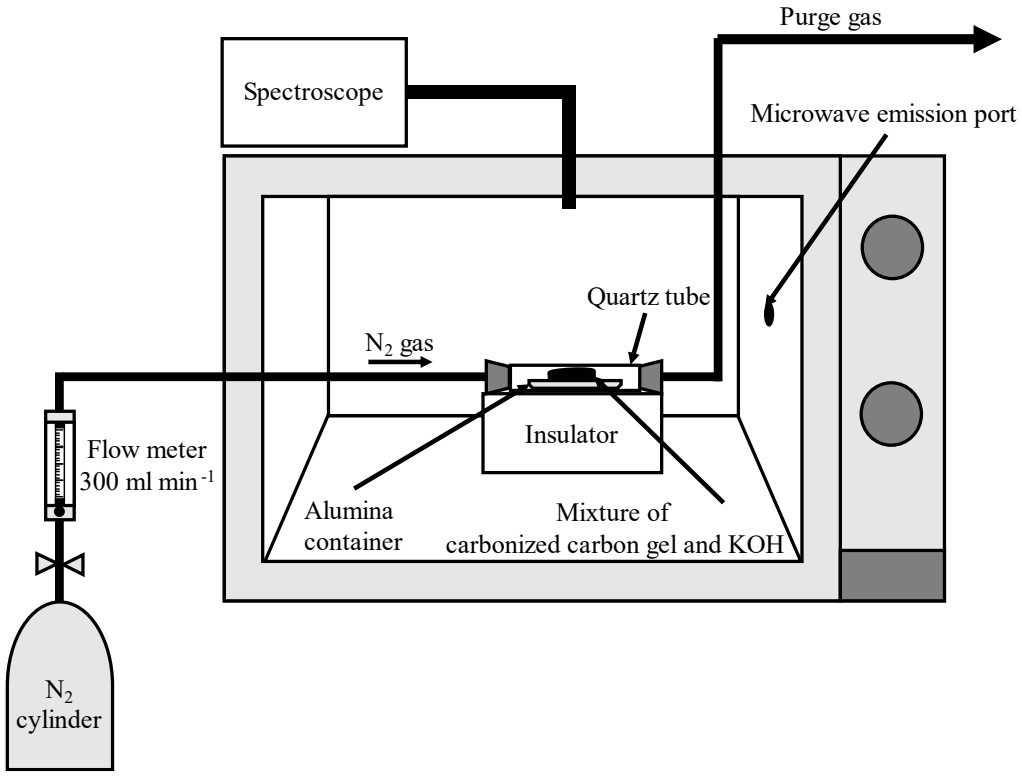

Figure 1.1 Experimental setup for microwave-induced plasma used in extremely fast activation.

To compare the MiWP-KOH activation and the conventional activation using an electric furnace, the mixture of CCG and KOH was heated up to 1000 °C by an electric furnace using two heating patterns, with a temperature-elevation rate of 10 and 50 °C min^{-1}, and holding time for 5 and 0 min, respectively.

1.3 Results and Discussion

1.3.1 Temperature-distribution in the microwave oven

Microwave irradiation normally provides ununiform heating. To identify the suitable location to perform MiWP-KOH activation, COMSOL multiphysics© software had been used to calculate electric field in the reactor as presented in **Figure 1.2**. To validate the calculation results from COMSOL multiphysics© software and identify a location to perform MiWP-KOH activation, flakes of cheese were put in the tray with the same size as the microwave oven (350 mm × 425 mm) before being heated by microwave for 20 s. The image of heated cheese is illustrated in **Figure 1.3**.

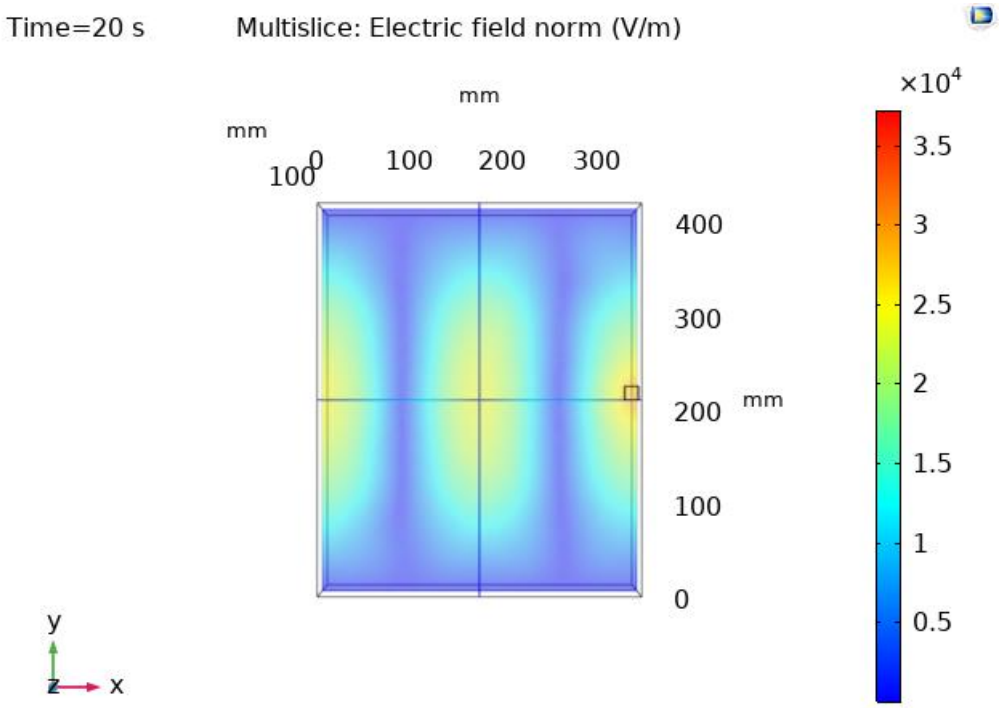

Figure 1.2 Electric field in the reactor for MiWP-KOH activation calculated from COMSOL multiphysics© software.

Figure 1.3 Flakes of cheese heated by microwave for 20 s.

1.3.2 Plasma-Temperature Evaluation

When the MiWP-KOH activation was used on the powder bed with a mass ratio of KOH to CCG = 1:1 and 6:1, a uniquely bright plasma was clearly observed above the powder bed. It should be noted that the plasma cannot be observed when the mixture of KOH to CCG with a mass ratio of KOH to CCG = 1:10. The size of the observed plasma was much larger than the microscale reported previously as microwave-driven plasma in porous carbon. [54,55] The emission spectra of the microwave-induced plasma were measured using a spectroscope [Ocean Optics, USB2000] as presented in **Figure 1.4**.

The optical fiber was fixed at a constant position, but the lighting plasma was moving around on the surface of the KOH–carbon gel mixture bed. Because of this situation, the sensitivity of the measurement of the optical emission spectra was not stable, and the plasma evolution with time could not

be obtained. Nevertheless, we can show the spectra obtained when the light was introduced to the optical fiber well so that the sensitivity is high and when less light was introduced to the optical fiber causing relatively low sensitivity. In the spectrum with low sensitivity, the prominent peaks can be seen at about 595 nm and about 770 nm, indicating atomic Na and K, respectively. [71,72] Na might come from the remaining sodium carbonate catalyst to form carbon gel or impurities contained in the KOH reagent (0.5 wt%). In the spectrum with high sensitivity, small peaks suggesting K are also seen at about 410 nm and 700 nm. [73] The plasma temperature was estimated using the intensities of these small K peaks with relatively comparable intensities by Eq. (1.1).

For this temperature estimation, the physical parameters, A_{ki}, g_k, and E_k are taken from the Kurucz atomic spectral line database. [73] T is thermodynamic temperature, artificially chosen as 10^4 K and k_B is Boltzmann constant 8.617330310×10^{-5} eV·K^{-1}. As a result, the temperature estimated by this way turned out to be 16500 K.

$$\text{Intensity} = A_{ki}g_k \exp(-E_k/(Tk_B)) \qquad (1.1)$$

In the spectrum with high sensitivity, a broad peak with a maximum wavelength of about 500 nm can be seen. When Wien's displacement law [74] of Eq. (1.2) is used, the temperature is estimated to be 5770 K.

$$\lambda_{max}T = 0.2884 \text{ cm K} \qquad (1.2)$$

where, λ_{max} represents wavelength at the highest intensity of the black body radiation spectrum, and T represents the temperature of a radiating object. The calculated temperature here is considered to be in the same range as the typical microwave-induced plasma temperature previously reported. [75] The inconsistency of the temperatures above may indicate that atmospheric-pressure non-thermal plasma was generated in our system. It should be noted that the temperature of the fed particle mixture (CCG and KOH) should not exceed the range of 500–1000 °C, which is a known range of activation temperature for the synthesis of activated carbon. [56,57]

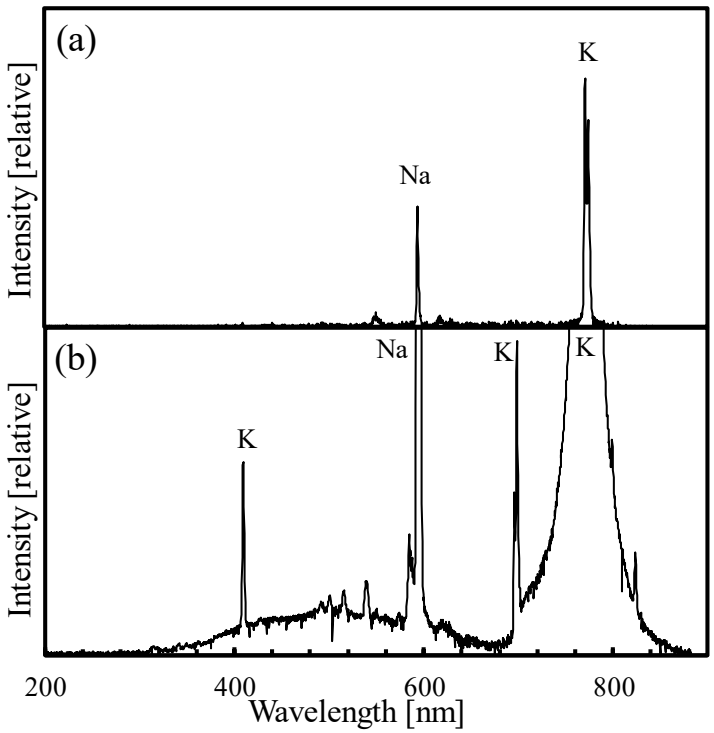

Figure 1.4 Emission spectra of microwave-induced plasma observed from MiWP-KOH activation (a) when plasma moved from the focus point of the optical fiber so that the sensitivity of spectrum measurement is reduced and (b) when light emitted from plasma was well introduced to optical fiber.

1.3.3 Specific Surface Area of Activated Carbon

A specific surface area of each resultant activated carbon was evaluated by the Brunauer–Emmett–Teller (BET) method with nitrogen using an automated physisorption surface area analyzer [MicrotracBEL, BELSORP-miniII-S] at 77 K. The specific surface area of the activated carbon obtained from MiWP-KOH activation with a microwave-irradiation time in the range of 40–330 s is presented in **Figure 1.5**.

It is shown here that the specific surface area of the activated carbon tends to increase with the increase in microwave-irradiation time. This tendency is reasonable as the pore opening reaction takes time to proceed. The point regarded as significant is that the increasing rate of the specific surface area of the products is extremely high. One can see in this figure that the specific surface area reaches 1,007, 1,888, and 2,084 $m^2\ g^{-1}$ within 80, 270, and 330 s. On the other hand, the activated carbon prepared using an electric furnace by heating at 1,000 °C with a temperature-elevation rate of 10 and 50 °C min^{-1} possesses a specific surface area of 1,913 and 1,607 $m^2\ g^{-1}$, respectively. It is commonly known that the conventional

activation operated using an electric furnace requires several hours to prepare activated carbon with a specific surface area that is higher than 1000 m^2 g^{-1}. [56,57]

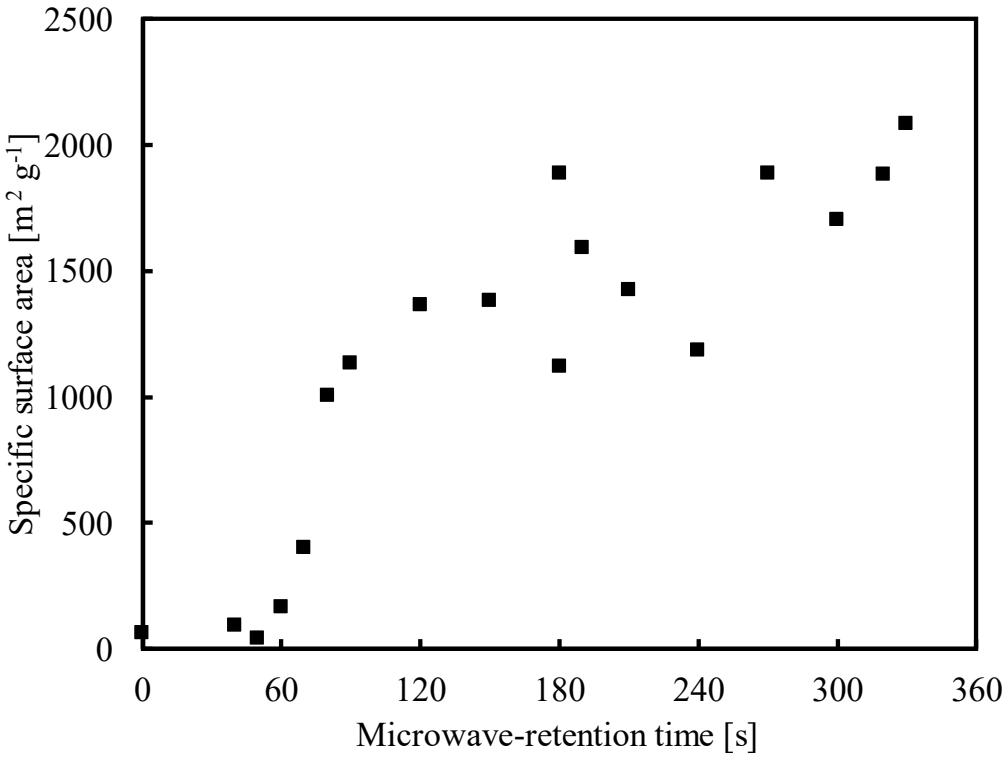

Figure 1.5 Effect of microwave-irradiation time on the specific surface area of activated carbon prepared by MiWP-KOH activation.

The long activation time limits the operation mode of activation only in the batch system. The method investigated here can drastically reduce the activation time by one to two orders of magnitude. Thus, this result will make an epoch-making change in reactor design concept by switching the operating mode from a batch system to a continuous system.

1.3.4 Nitrogen Adsorption-Desorption Isotherm

Figure 1.6 illustrates nitrogen adsorption-desorption isotherm of CCG and activated carbon derived from an electric furnace with a heating rate of 10 and 50 °C min^{-1}, and activated carbon obtained from the MiWP-KOH activation using a microwave-irradiation time of 270 s. According to **Figure 1.6**, nitrogen adsorption-desorption isotherm of activated carbon derived from an electric furnace with a temperature-elevation rate of 50 °C min^{-1} and activated carbon obtained from MiWP-KOH activation show a similar shape. However, the shape of the nitrogen adsorption-desorption isotherm of

activated carbon derived from the electric furnace with a temperature-elevation rate of 10 °C min^{-1} is different from the others. It should be noted that the shape of nitrogen adsorption-desorption isotherm represents pore structure. [76] Therefore, the pore structure of activated carbon derived from the electric furnace with a relatively high temperature-elevation rate of 50 °C min^{-1} and activated carbon obtained from MiWP-KOH activation may be similar, while the pore structure of activated carbon derived from the electric furnace with a relatively low temperature-elevation rate of 10 °C min^{-1} is different from the others.

The volumes of mesopores (2 nm < pore diameter < 50 nm) v_{meso} calculated from adsorption isotherms based on the Dollimore–Heal method [77] and those of the micropores (pore diameter <2 nm) v_{micro} based on the Horvath–Kawazoe 9method [78] are shown in **Table 1.1**. The ratio of v_{micro}/v_{meso} is commonly as large as 3.6–3.8 in the activated carbon derived from relatively fast activation using a 50 °C min^{-1} of the temperature-elevation rate in the furnace and the MiWP-KOH activation with a microwave-irradiation time of 270 s, while this ratio becomes as small as 1.6 when the temperature-elevation rate is as low as 10 °C min^{-1} in the electric furnace. The pore size becomes larger when the activation time is longer because the pores may merge together if the pore opening reaction on carbon takes a long time.

In addition, one can see in this table that the specific surface area and v_{micro}/v_{meso} ratio of the activated carbon tend to increase with the increase in the concentration of KOH in the mixture of KOH and CCG. It can be implied that activated carbon with a high ratio of v_{micro}/v_{meso} has a high degree of porosity. The results indicate that KOH plays an important role in the creation of a porous structure. When the concentration of KOH is higher, a degree of porosity in the structure of the activated carbon is higher, resulting in a higher specific surface area.

As mentioned above, the activated carbon with a large surface area derived from the MiWP-KOH activation has the feature that the micropores dominate over the mesopores. This result indicates that the hot microwave-induced plasma contacted with the precursor powder bed may contribute to the rapid increase in temperature of the precursors, resulting in the production of micropore-dominating activated carbon. Here, it should be recognized that, in our observation, the plasma is difficult to generate when the same microwave is irradiated to the carbon gel powders without mixing with KOH. Also, plasma generation is difficult when the microwave is irradiated with only KOH. Thus, the appropriate mixing ratio between carbon and KOH

should be necessary to realize this plasma generation. The optimization work to find the best mixing ratio is described in Chapter 3.

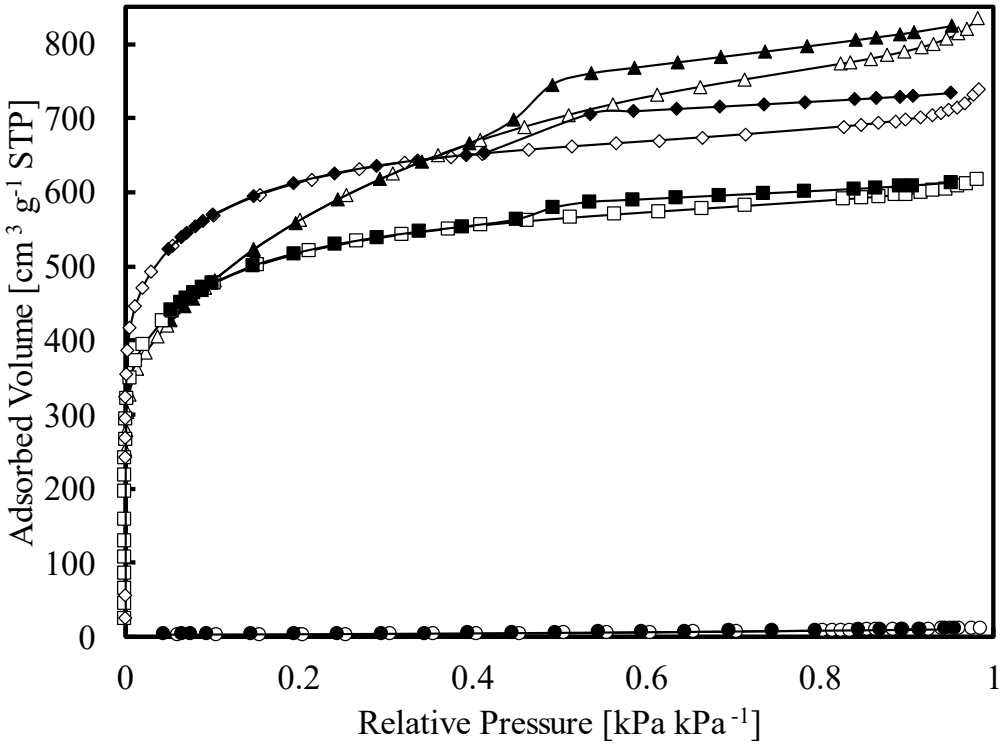

Figure 1.6 Nitrogen adsorption-desorption isotherms of (○-●) CCG, (△–▲) activated carbon prepared by activation using an electric furnace at 1000 °C with a temperature-elevation rate of 10 °C min^{-1}, (□ – ■) activated carbon prepared by activation using an electric furnace at 1000 °C with a temperature-elevation rate of 50 °C min^{-1}, and (◇ – ◆) activated carbon obtained prepared by MiWP-KOH activation with a microwave-irradiation time of 270 s.

Table 1.1 Summary of pore structural analyses using nitrogen adsorption-desorption isotherm at 77 K.

Activation method	Specific surface area [$m^2\ g^{-1}$]	Micropore volume, v_{micro} [$m^3\ g^{-1}$]	Mesopore volume, v_{meso} [$m^3\ g^{-1}$]	v_{micro}/v_{meso}
MiWP-KOH activation with retention time of 80 s and mass ratio of KOH to CCG of 1:10.	11	0.0012	0.02	0.2
MiWP-KOH activation with retention time of 80 s and mass ratio of KOH to CCG of 1:1.	108	0.05	0.06	0.85
MiWP-KOH activation with retention time of 80 s and mass ratio of KOH to CCG of 6:1.	1007	0.52	0.15	3.5
MiWP-KOH activation with retention time of 270 s and mass ratio of KOH to CCG of 6:1.	1888	1	0.26	3.8
Conventional activation at 1000 °C with elevation rate of 10 °C min^{-1} and mass ratio of KOH to CCG of 6:1.	1913	1.07	0.67	1.6
Conventional activation at 1000 °C with elevation rate of 50 °C min^{-1} and mass ratio of KOH to CCG of 6:1.	1607	0.86	0.24	3.6

1.3.5 SEM and TEM Images

Field emission scanning electron microscope [SEM; JEOL, JSM-6700F] and transmission electron microscope [TEM; JEOL, JEM−1010] were used to observe the surface morphology and pore structure of each particular sample. **Figure 1.7** presents the surface morphology and pore structure of **(a)**, **(e)** CCG, activated carbon derived from the electric furnace with a temperature-elevation rate of **(b)**, **(f)** 10 and **(c)**, **(g)** 50 °C min^{-1}, and **(d)**, **(h)** activated carbon obtained from the MiWP-KOH activation with a microwave-irradiation time of 270 s. One can see that the CCG without activation and the activated carbon derived from an electric furnace with a temperature-elevation rate of 10 °C min^{-1} show a similar surface structure in the SEM images. However, the pore structure of the CCG and the activated carbon derived from the electric furnace with a temperature-elevation rate of 10 °C min^{-1} are different in the nitrogen adsorption analysis. No porous structure was observed on the CCG in the TEM image. In comparison with CCG and the activated carbon derived from the electric furnace with a temperature-elevation rate of 10 °C min^{-1}, activated carbon derived from the electric furnace with a temperature-elevation rate of 50 °C min^{-1} and activated carbon obtained from MiWP-KOH activation with a microwave-irradiation time of 270 s show the porous structures including micropores and distinct surface structures in the microscopic observation. These results confirm that the temperature-elevation rate used in the MiWP-KOH activation affects the surface structure of the activated carbon.

1.4 Conclusion

In summary, microwave-induced plasma with KOH activation can be used for extremely fast preparation of activated carbon, so-called MiWP-KOH activation. The temperature of the plasma above the precursor powder bed, including powdery CCG mixed with KOH, was estimated to be higher than 5000 °C from black body radiation spectrum analysis, resulting in the energy input to the precursors to realize the extremely fast activation. From the analysis of emission spectra, the plasma was considered to be non-thermal. By this fast activation, the specific surface area of the activated carbon can reach 1,007, 1,888, and 2,084 m^2 g^{-1} within 80, 270, and 330 s, respectively. This MiWP-KOH activation can reduce activation time by one to two orders of magnitude compared to conventional activation. This result can raise expectations that an epoch-making change will occur in the reactor design concept in the preparation of activated carbon by changing the operating mode from a batch system to a continuous system. Furthermore,

nitrogen adsorption-desorption analyses and microscopic observation reveal that temperature-elevation rate can have influences on the pore structure of the activated carbon. It is revealed that the micropores dominate the mesopores in the activated carbon obtained from MiWP-KOH activation when an appropriate KOH/carbon ratio is used.

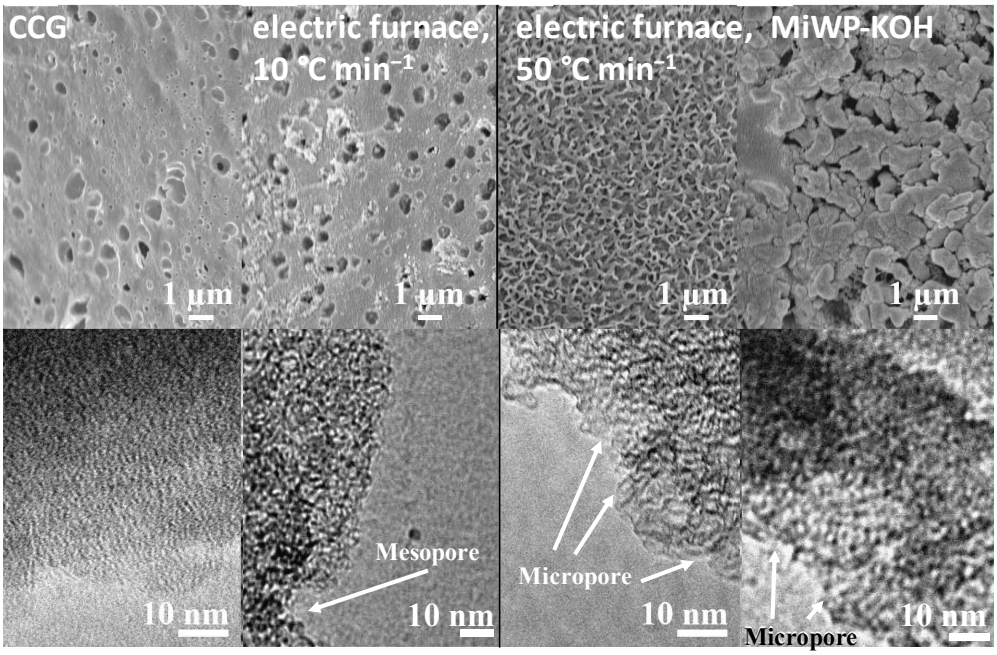

Figure 1.7 SEM images of surface structure: (a) CCG, (b) activated carbon prepared using an electric furnace at 1,000 °C with a temperature-elevation rate of 10 °C min^{-1}, (c) activated carbon prepared using an electric furnace at 1,000 °C with a temperature-elevation rate of 50 °C min^{-1}, and (d) activated carbon obtained using MiWP-KOH activation with a microwave-irradiation time of 270 s. TEM images of surface structure: (e) CCG, (f) activated carbon prepared using an electric furnace at 1,000 °C with a temperature-elevation rate of 10 °C min^{-1}, (g) activated carbon prepared using an electric furnace at 1,000 °C with a temperature-elevation rate of 50 °C min^{-1}, and (h) activated carbon obtained using MiWP-KOH activation with a microwave-irradiation time of 270 s.

Chapter 2 Effect of Temperature-Elevation Rate

2.1 Introduction

It was reported that some kinds of plasma such as dielectric barrier discharge plasma [79,80] and microwave-induced plasma [81,82] can be used to modify surface structures of activated carbon. Microwave-induced plasma can be made by irradiating microwave to electrically conductive materials with specific structures such as metals with sharp-edge or porous carbon materials. In case of the porous carbon materials, it can facilitate plasma generation because electrons can be discharged in microporous structures.

A previous study reported that microwave-induced CO_2 activation within 90 min can be used to prepare activated carbon with a specific surface area of 1,036 $m^2 g^{-1}$, where plasma generation was not reported. [83] In contrast, the present work uses a plasma-generating microwave system, so-called MiWP-KOH activation, aiming to produce activated carbon of which specific surface area is approaching 2,000 $m^2 g^{-1}$ with the drastically-reduced activation time within 80-330 s as reported in Chapter 1. For its short reaction time, the results are expected to cause a revolutionary change in the reactor design concept by changing the activated carbon preparation process from batch to continuous system. To develop a new reactor system using MiWP-KOH activation, the mechanism of this method must be investigated.

Temperature-elevation rate can be one of the important factors governing the pore formation in activated carbon prepared by MiWP-KOH activation because microwave-induced plasma is expected to rise up the temperature of reacting carbon material rapidly. Therefore, the effect of temperature-elevation rate on the pore formation of activated carbon was investigated in this work. To discuss this effect, the pore structure analysis on the activated carbon prepared by MiWP-KOH activation is compared with the results obtained from the activation by the conventional heat-conduction method. Here, the micropores and mesopores are focused to investigate because these pores mainly contribute to realizing high surface area and important adsorption characteristics.

2.2 Materials and Methods

2.2.1 Preparation of Activated Carbon

Here, carbonized carbon gel (CCG) was used as a precursor material to prepare activated carbon. The synthetic carbon gel was prepared as explained in Chapter 1. The CCG was ground with KOH solid pellets to make a

powdery mixture. The mass ratio of KOH to CCG was fixed at 6. The activation on CCG was conducted by microwave irradiation to this CCG-KOH mixture as described below.

2.2.1.1 Activated Carbon Synthesis by MiWP-KOH Activation

This CCG-KOH mixture was put in an alumina container, which was placed in a quartz tube. The quartz tube was filled with nitrogen (300 mL min^{-1}) and located in the middle of a modified household microwave-oven [Sanyo Electric, EM-LA1(HL)] operated at 2.45 GHz and 500 W. The inside dimension of the microwave oven is 350 mm × 425 mm ×198 mm. The mixture was heated by this oven for 40-600 s. Temperature-change in MiWP-KOH activation was measured by a radiation thermometer [Japan Sensor, FTHX-0200S V-1563] as shown in **Figure 2.1 (a)**. It suggests that the maximum temperature occurred in MiWP-KOH activation is around 750-850 °C. Here, the temperature-elevation rate was calculated using the period of time used to raise the temperature from 500 °C to the maximum temperature. In MiWP-KOH activation, temperature-elevation rate varies from 90-700 °C min^{-1}. The resultant activated carbon was washed with distilled water until the filtrate became neutral (pH ~7). Then, it was dried at 50 °C for 12 h.

2.2.1.2 Activated Carbon Synthesis by Heat-Conduction Activation

To investigate the influence of temperature-change rate used for activation on the pore formation of activated carbon using the precursor material of CCG-KOH mixture, activated carbon was synthesized by conventional heat-conduction activation with various temperature-elevation programs. A cylindrical electric furnace was used here because it was impossible to intentionally control the temperature-elevation rate in the MiWP-KOH activation. In this experiment, the CCG-KOH mixture was heated to 1000 °C under a nitrogen atmosphere (100 mL min^{-1}). The temperature programs used to prepare activated carbon are shown in **Figure 2.1**.

Figure 2.1 (b) represents the temperature programs made by the cylindrical electric furnace with temperature-elevation rates of 5.6-9.6 °C min^{-1} to 1000 °C. Here, the total heating period of each temperature program was set at a constant value of 195 min by keeping the temperature at 1000 °C. By using these conditions, the influence of the holding time at 1000 °C can be observed in addition to that of the temperature-elevation step. To enable

one to focus on the temperature-elevating step, the conditions are shown in **Figure 2.1 (c1)** and **(c2)** were made. These figures illustrate the temperature programs by the same furnace with the temperature-elevation rate in the range of 2.2-19.1 °C min^{-1} without keeping the temperature after it reaches 1000 °C. **Figures 2.1 (c1)** and **(c2)** shows the same data with different scales of the horizontal axis to clearly exhibit the wide range of temperature-elevation rate.

In addition, these figures show a fast temperature change of 91.5 °C min^{-1} realized by conductive heating using a hand-made plate-shape heater to imitate the temperature change of the CCG-KOH mixture in MIWP-KOH activation. This hand-made heater was made of a graphite plate of 1 mm-thickness with applying DC electric current. CCG-KOH mixture was placed on this graphite-plate heater set in a quartz tube and heated to synthesize activated carbon under nitrogen flow. By this way, the CCG-KOH mixture was heated up to 812 °C. This temperature-changing pattern is similar to that seen in the MIWP-KOH activation. This temperature change was plotted in **Figures 2.1 (a), (c1),** and **(c2)**.

The activated carbon obtained by the heat-conduction was also washed and dried in the same way as the activated carbon prepared by the aforementioned MiWP-KOH activation.

2.2.2 Investigation on Pore Structure of Activated Carbon

Nitrogen adsorption-desorption isotherms on the activated carbon at 77 K were investigated using a specific-surface-area pore-size-distribution analyzer [MicrotracBEL, BELSORP-mini II-S] to analyze pore properties. The nitrogen adsorption isotherms were used to calculate the specific surface area and the micropore volume based on Brunauer-Emmett-Teller (BET) method [84] and *t*-plot method [85], respectively. The mesopore volume of activated carbon was calculated by applying Barrett-Joyner-Helenda (BJH) method [86] to the nitrogen desorption isotherm.

Mass yield percentage of the activated carbon was obtained using the following Eq. (2.1).

$$\text{Mass yield percentage} = \frac{\text{mass of activated carbon}}{\text{mass of CCG}} \times 100\ \% \qquad (2.1)$$

In addition, the micropores including the narrow spaces can not be accessed by nitrogen. Therefore, carbon dioxide adsorption isotherms at 298 K were used to analyze the activated carbon by the abovementioned analyzer based on Dubinin-Radushkevitch (DR) equation [87] on the representative two

specimens from the MiWP-KOH activation and three specimens from the conductive heating method.

2.3 Results and Discussion

2.3.1 Nitrogen adsorption-desorption isotherm

Figure 2.2 illustrates nitrogen adsorption-desorption isotherms of activated carbon prepared using different heating methods. **Figure 2.2 (a)** represents the adsorption-desorption isotherms of activated carbon prepared by MiWP-KOH activation using microwave-irradiation time of 40-600 s. The results show that the volume of nitrogen adsorbed at low relative pressure tends to increase with the increase of microwave-irradiation time. The adsorption of nitrogen at low relative pressure here indicates the formation of highly microporous structures. [88] The results suggest that in the pore formation step, the number of micropores increase with an increase of microwave-irradiation time. In addition, each of the adsorption-desorption isotherms represents a hysteresis loop, which might be associated with capillary condensation taking place in mesopores. [88–90] The results show that the hysteresis loops do not increase with the increase of microwave-irradiation time. This feature is unique in MIWP-KOH activation in comparison to the conventional heat-conduction activation.

It should be reminded that the temperature in MiWP-KOH activation can reach above 800 °C with the a high temperature-elevation rate of approximately 90-700 °C min^{-1}. As reported in Chapter 1, the gas plasma generated above the CCG-KOH mixture has an extremely high temperatures, such as 5500 °C. The contact of this plasma with the CCG-KOH mixture should enable this high temperature-elevation rate. This high temperature-elevation rate should be an important feature in MiWP-KOH activation, and it may be an important factor to determine the pore structure in the produced activated carbon.

To investigate the effect of temperature-elevation rate on the pore formation of activated carbon from the CCG-KOH mixture, the activated carbon was prepared using various temperature programs by the heat-conduction activation as illustrated in **Figure 2.1**. When activated carbon was prepared by varied temperature programs with the controlled total heating period as shown in **Figure 2.1 (b)**, Nitrogen adsorption-desorption isotherm was obtained as represented in **Figure 2.2 (b)** to investigate the pore structure of the activated carbon.

The formation of microporous structure in the activated carbon can be observed owing to the nitrogen adsorption at low relative pressure. The

results show that the hysteresis loops became wider with a decrease in temperature-elevation rate with less time to hold at 1000 °C. It indicates that the number of mesopores increases as the temperature-elevation rate decreases. This is a piece of evidence that keeping the high temperature at 1000 °C level is not the important factor to increase the micropore/mesopore volume ratio in the structures of activated carbon, but the high temperature-elevation rate is one of the improtant factors to achieve its high value. Here, it should be reminded that the temperature-elevation rate of the CCG-KOH mixture is extremely high when MiWP-KOH activation is used to prepare activated carbon. Therefore, one can expect that the microporous structure dominates over the mesopores in the activated carbon prepared by MiWP-KOH activation.

To confirm the above feature, activated carbon was prepared using the various temperature-elevation programs without controlled total heating period as shown in **Figure 2.1 (c)**, and the isotherms from such conditions are shown in **Figure 2.2 (c)**. The nitrogen adsorption-desorption isotherms show that the adsorption amount above 400 cm^3 g^{-1} STP at low relative pressure can be observed in the isotherms of each activated carbon, indicating micropore formation. The microporous structures in activated carbon seemed to be formed in all conditions (except the condition of 91.5 °C min^{-1}, which do not reach 1,000 °C) when the temperature reached 1,000 °C, but the level of the micropore formation does not seem dependent on the temperature-elevation rate so significantly here. The hysteresis loops can be clearly observed only from the isotherms of activated carbon prepared using a low temperature-elevation rate (2.2 to 5.3 °C min^{-1}). In contrast, the isotherms of activated carbon prepared with the high temperature-elevation rate of 19.1 and 91.5 °C min^{-1} do not present any clear hysteresis loops. Since the presence of a hysteresis loop might suggests the formation of mesoporous structures, the results confirm that when a low temperature-elevation rate is used to prepare activated carbon, the mesoporous structures can be formed significantly in activated carbon. These tendencies indicate that the micropores should dominate over the mesopores when the temperature-elevation rate is high. Therefore, when microwave-induced plasma is generated to realize the extremely high temperature-elevation rate in the CCG-KOH mixture, the micropores should be preferably formed in comparison to mesopores.

For comparison, the isotherms of activated carbon prepared by the MiWP-KOH and the heat-conduction method using similar activating conditions including activation temperature, activation time, and temperature-elevation rate are illustrated in **Figure 2.2 (d)**. One can see that

activated carbon prepared by MiWP-KOH activation has a higher pore volume than activated carbon prepared by the conventional heat-conduction activation.

2.3.2 Specific Surface Area and Pore Volume

Nitrogen adsorption-desorption isotherms of the activated carbon prepared by the MiWP-KOH method were used to calculate specific surface area as shown in **Figure 2.3 (a)**. The calculation shows that the specific surface area of activated carbon increases with an increase in microwave-irradiation time. When microwave-irradiation time is longer, more energy should transfer to the CCG-KOH mixture, resulting in more micropore-formation and higher specific surface area. According to the previous report [91], activated carbon prepared using the microwave-irradiation time in the range of 40 – 80 s shows a specific surface area of 43-1263 m^2 g^{-1}. The activated carbon prepared using the microwave-irradiation time in the range of 80-600 s shows a specific surface area in the range of 1132–2500 m^2 g^{-1}. Also, these results suggest that when microwave-irradiation time is shorter than 80 s, the energy transferred to the feed materials is not enough to make activated carbon with a high surface area. The value of 80 s should correspond to the time required to reach about 800 °C in the MiWP-KOH activation, as shown in **Figure 2.1 (a)**.

The mass yield percentage of the activated carbon prepared by MiWP-KOH activation was calculated as shown in **Figure 2.3 (a)**. The results show that the yield of the activated carbon drastically decreases as microwave-irradiation time increases from 40 to 80 s. After that, the yield of the activated carbon decreases as microwave-irradiation time increases from 80 to 600 s. This result suggests that when the temperature is lower than about 800 °C, weak parts in the CCG structure can be consumed without fast small-pore formation, resulting in the decrease of activated carbon yield with low specific surface area. When the MiWP-KOH activation was conducted further after 80 s, the temperature becomes high enough to open micropores at relatively stable parts in the CCG structure, resulting in the high specific surface area and the low additional consumption of the CCG with a relatively retarded decrease of the yield.

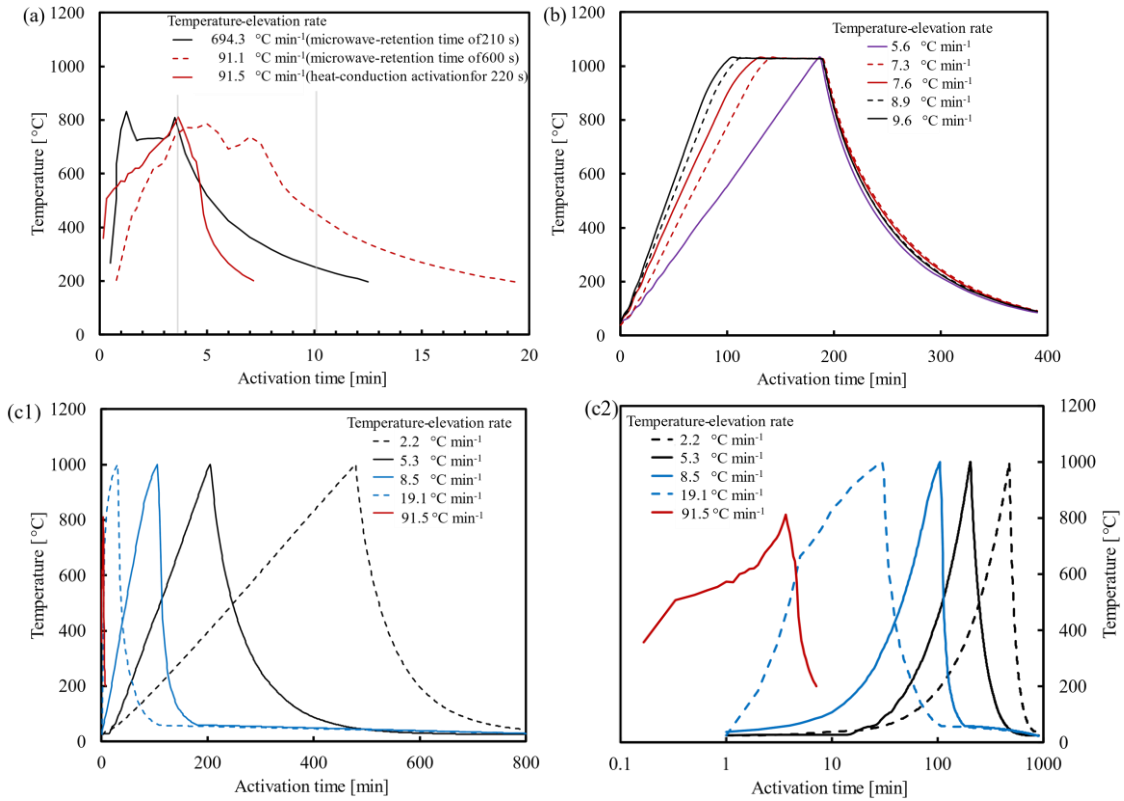

Figure 2.1 Temperature programs used to prepare activated carbon by (a) MiWP-KOH activation and heat-conduction activation using a similar temperature-change pattern, (b) by heat-conduction activation, when the total heating period was controlled, and (c1) by heat-conduction activation, when the total heating period was not controlled in a normal scale of activation time and (c2) in log scale of activation time.

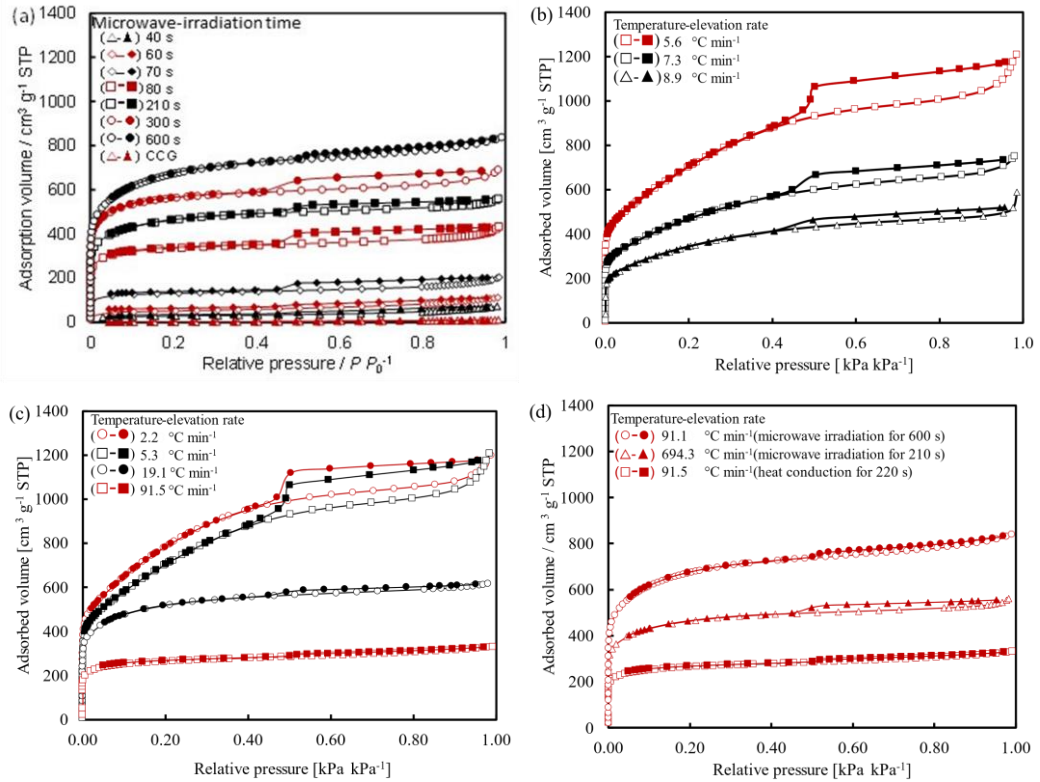

Figure 2.2 Nitrogen adsorption-desorption isotherm of activated carbon prepared by (a) MiWP-KOH method, (b) heat-conduction method using the temperature-elevation pattern of Figure 2.1 (b), (c) heat-conduction method using the temperature-elevation pattern of Figure 2.1 (c), and (d) MiWP-KOH method and heat-conduction with similar temperature-change pattern.

Additionally, the microwave should excite the rotation of molecular dipole to cause the heating. KOH can be heated by this mechanism. Also, a free electrons in conductive materials can absorb the microwave to cause heating. Carbon can be heated by this mechanism. The pores in carbon can be generated by reaction of carbon with KOH ($2C + 6KOH \rightarrow 2K + 3H_2 + 2K_2CO_3$, $2C + K_2CO_3 \rightarrow 2K + 3CO$) at a considerably high temperature [34].

Figure 2.3 (b) presents a specific surface area of the activated carbon prepared from the heat-conduction activation using a variety of temperature-elevation patterns as shown in **Figure 2.1 (b)**. The activated carbon prepared by the temperature-elevation rate of 5.6-9.6 °C min^{-1} shows a specific surface area of 1,208-2,507 m^2 g^{-1}. The results indicate that a specific surface area of the activated carbon tends to decrease with an increase in temperature-elevation rate. Here, it should be reminded that when the heating rate is higher, the holding time at 1000 °C is longer. Namely, an excessively long heating period at 1000 °C can lead to degradation of the porous structures by some reactions, such as sintering, chemical transformations, evaporation, etc. [92], resulting in low specific surface area in activated carbon as illustrated in **Figure 2.3 (c)**.

Moreover, **Figure 2.3 (b)** shows thmass yield percentage of the activated carbon prepared by heat-conduction using different temperature-elevation patterns. The mass yield percentage is in the re ange of 1.5-10.2 %, which tends to slightly decrease as the temperature-elevation rate increases. One should be aware that the yield from MiWP-KOH activation is significantly higher than that from the heat-conduction activation. This would be because the activation time by MiWP-KOH activation is much shorter than that by the conduction activation.

It should be noted that the activated carbon prepared by heat-conduction with the temperature-elevation rate of 91.5 °C min^{-1} and total heating time of 220 s shows a specific surface area of 984 m^2 g^{-1}, while the activated carbon prepared by MiWP-KOH with a similar temperature-change pattern (temperature-elevation rate = 91.1 °C min^{-1} as shown in **Figure 2.1 (a)**) exhibits specific surface area of 1,680 m^2 g^{-1}. Another activated carbon prepared by MiWP-KOH (total activation time of 210 s as shown in **Figure 2.1 (a)**) shows a specific surface area of 1716 m^2 g^{-1}. One can see that activated carbon prepared by MiWP-KOH has a significantly higher specific surface area than that of activated carbon prepared using heat conduction. These results suggest that MIWP-KOH activation should have the microwave-originated effect on the activation of CCG-KOH mixture to

enhance pore formation, resulting in the fast generation of micropore volume in the activated carbon structure.

Micropore and mesopore volumes of the activated carbon were calculated from the nitrogen adsorption-desorption isotherms, and they were used to estimate the ratio of micropore to mesopore volume as represented in **Figure 2.4**. **Figure 2.4 (a)** shows the pore properties of the activated carbon prepared by MiWP-KOH activation. The calculation confirms that both the micropore volume and the mesopore volume tend to increase with an increase of microwave-irradiation time. In addition, the ratio of micropore volume to mesopore volume tends to increase with the increase of microwave-irradiation time. The results indicate that when microwave-irradiation time increases, the microporous structures in the activated carbon become more dominant.

Figure 2.4 (b) represents the pore properties of the activated carbon prepared by the heat-conduction activation with the varied temperature-elevation rate as shown in **Figure 2.1 (b)**. This result shows that the volumes of the micropores and the mesopores decrease with the increase in temperature-elevation rate. It should be recognized that the ratio of micropore to mesopore volume increases with an increase in temperature-elevation rate. This calculation suggests that microporous structures become more dominant when the temperature-elevation rate is high. Since the temperature-elevation rate is extremely high in MiWP-KOH activation, activated carbon with a micropore-dominating structure can be realized.

Table 2.1 represents the micropore volume of activated carbon calculated from nitrogen and carbon dioxide adsorption results based on the DR equation. It seems that the nitrogen-accessible micropore volume becomes about twice by increasing the treatment time is changed from 80 to 600 s in the MiWP-KOH activation, and carbon dioxide-accessible micropore volume becomes four times higher by the same change of the treating time. In the case of the heat-conduction activation, carbon dioxide-accessible pore volume does not change meaningfully, while the nitrogen-accessible pore volume decreases with the increase of the temperature-elevation rate. It should be noted that when the temperature-elevation rate for heat-conduction activation is higher, the time for heating at 1,000 °C is longer. Thus, it is suggested that the carbon dioxide-accessible pores which are smaller than nitrogen-accessible pores may hardly be destroyed by excessively long treatment time at high temperatures. These results would indicate that ultramicropores evaluated by carbon dioxide adsorption experiment can be effectively generated by the MiWP-KOH activation and such pores are considered stable.

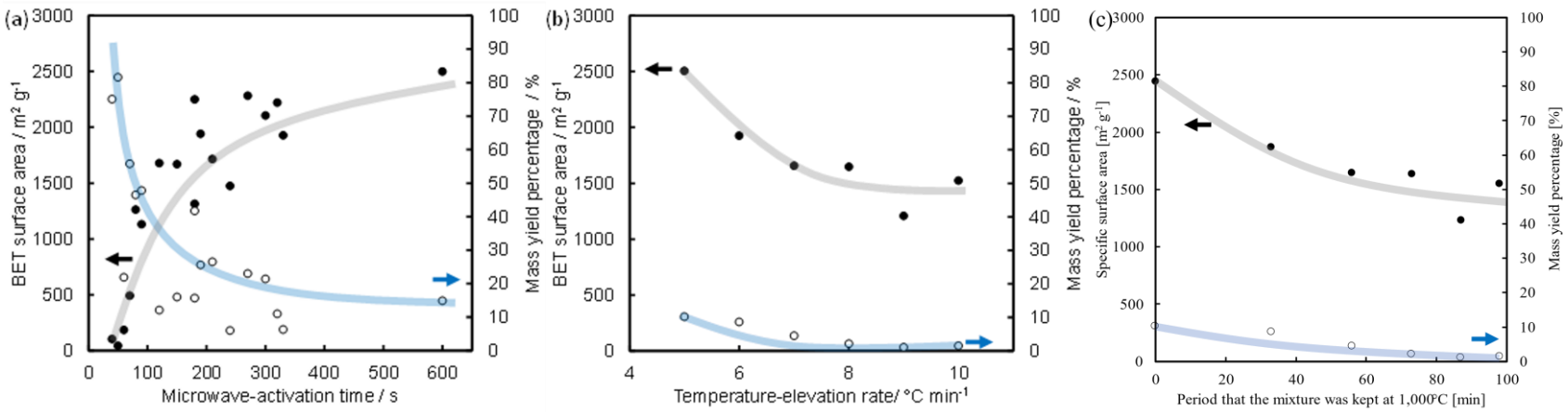

Figure 2.3 Specific surface area and mass yield percentage of activated carbon prepared by (a) MiWP-KOH activation varied with microwave-irradiation time, and by the heat-conduction activation using the temperature-elevation pattern of Figure 2.1 varied by (b) temperature-elevation rate and (c) Period that the mixture was kept at 1,000 °C.

As mentioned earlier, micropores and mesopores are focused to investigate here. If one are interested in the surface morphologies of activated carbon prepared by MiWP-KOH activation related to macropores, one can refer to Chapter 1, showing the observation by scanning electron microscope (SEM) and transmission microscope (TEM) on it. One can see an SEM image there showing that slit pores with the width less than 0.8 μm are generated in activated carbon synthesized by MiWP-KOH activation, while activated carbon synthesized by the conduction heating activation exhibits nearly-circle cross-section pores or random-mesh-like pores, depending on temperature-elevation rate, with diameters less than 0.8 μm.

2.3.3 Mechanism of Pore Formation

Based on the explanation of the results above, the phenomena with the pore formation of the activated carbon in MiWP-KOH activation is illustrated in **Figure 2.5 (a)** in contrast to the one in the conventional conductive activation as in **Figure 2.5 (b)**. Due to the high temperature-elevation rate of the CCG-KOH mixture of 91.1-694.3 °C min^{-1} heated by the microwave-induced plasma, the consumption of CCG occurs within 80 s to start opening pores. From 80 s, mesopores starts to be opened, so that the micropore to mesopore volume ratio is not so high at this stage. Afterward, micropores are increased by time, reaching to the high micropore to mesopore volume ratio. Then, micropore-dominating structure with a large specific surface area of about 2000 m^2 g^{-1} can be formed finally until 5-6 min.

In the case of the activation using the conventional heat-conduction activation, high temperature-elevation rate can cause the micropore-dominating structure. However, the specific surface area of activated carbon prepared by a heat-conduction which has similar temperature-change pattern with MIWP-KOH activation cannot reach the level of 1000 m^2 g^{-1}. This result suggests that microwave-irradiation should have the effect to enhance pore formation at CCG-KOH mixture.

The mechanism of this microwave-originated effect has not yet been clarified. At this stage, we consider that it may be reasonable that the temperature at the interface between carbon and molten KOH may be highly raised by microwave irradiation because carbon is electrically conductive. When microwave is irradiated to conductive materials, eddy current is generated in them. [92] When the sizes of the materials are deeper than the depths of the skin effect of the generated current, the surface of the materials can be locally heated. Therefore, the pore formation on the surface of CCG is considered to be enhanced.

Pore formation in activated carbon prepared by using electric furnace (for example, using the temperature-elevation patterns of **Figure 2.1 (b)**) is illustrated in **Figure 2.5 (**b**)**. Here, the heat transfer occurs only by heat conductivity from outside. The results confirm that microporous structures become more dominant when a high temperature-elevation rate is used. However, specific surface area of the activated carbon decreases as a temperature-elevation rate used to prepare activated carbon increases, owing to long holding period at reaction temperature, resulting in thermal degradation of porous structures [93].

2.4 Conclusion

This study investigates the pore formation of high surface area activated carbon prepared using MiWP-KOH activation by observing the effects of temperature-elevation rate on the pore structure of activated carbon. It is revealed from nitrogen adsorption-desorption isotherms that micropore and mesopore volume and specific surface area of activated carbon can increase as the microwave-irradiation time increases. In addition, microporous structures become more dominant as the microwave-irradiation time is longer.

By the experiment using the heat-conductive activation, it was confirmed that temperature-elevation rate have a significant influence to cause the micropore-dominating activated carbon structures. Thus, the extremely high temperature-elevation rate occurred in MiWP-KOH activation can be used to prepare activated carbon with micropore-dominating structures.

Temperature-change pattern in MiWP-KOH activation was measured. Then, it turned out that the specific surface area of activated carbon prepared by MiWP-KOH activation was significantly larger than that of activated carbon prepared by heat-conductive activation with similar temperature-change pattern. This result suggests that MiWP-KOH activation should have the microwave-originated effect to enhance pore formation.

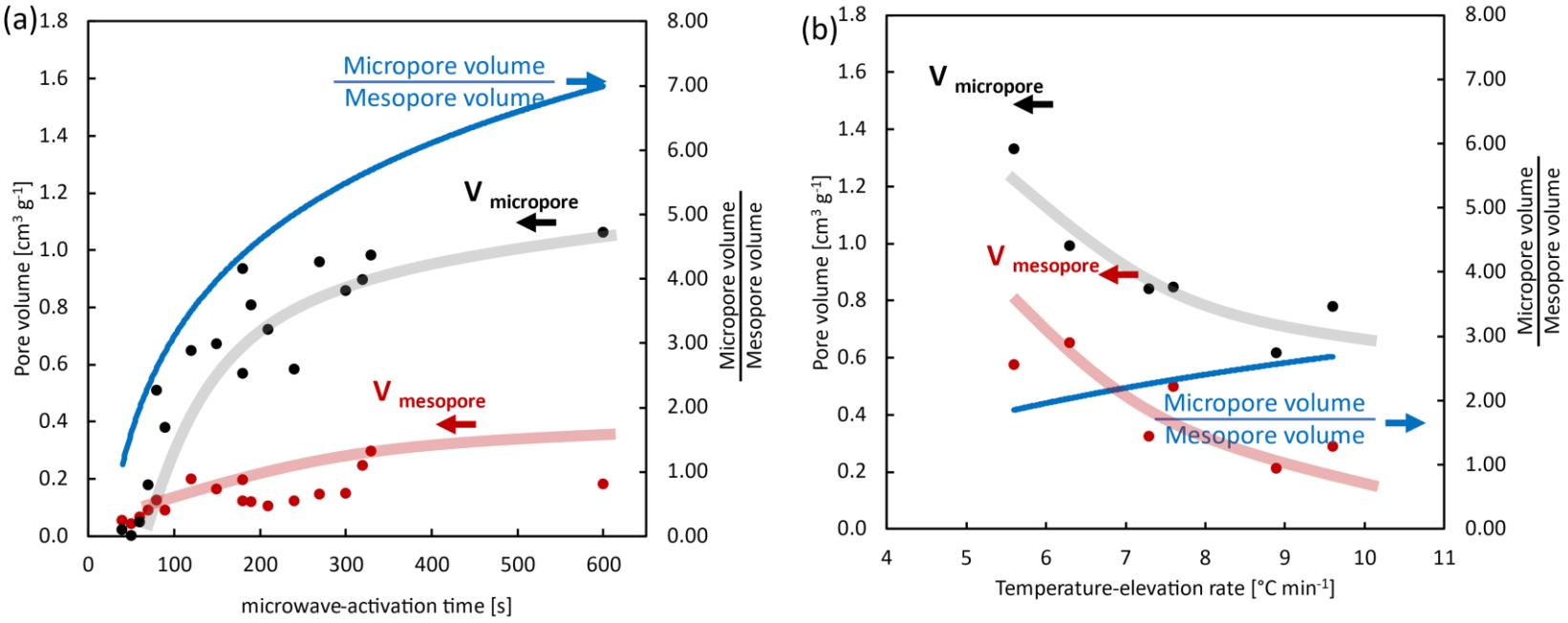

Figure 2.4 Micropore and mesopore volume, ratio of micropore volume to mesopore volume of activated carbon prepared by (a) MiWP-KOH activation, and by (b) heat-conduction activation using temperature-elevation pattern of Figure 2.1 (b).

Table 2.1 Micropore volumes of activated carbon prepared by MiWP-KOH activation and by heat-conduction activation using temperature-elevation patterns of Figure 2.1 (b) measured by adsorption of N_2 and CO_2.

Activation method	Microwave-retention time for MiWP-KOH activation [s] or Temperature-elevation rate for heat-conduction activation [$^oC\ min^{-1}$]	Micropore volume [$cm^3\ g^{-1}$]	
		N_2	CO_2
MiWP-KOH activation	80	0.65	0.64
	600	1.11	2.65
Heat-conduction activation	5.6	1.02	1.24
	6.3	0.79	1.48
	7.3	0.70	1.41

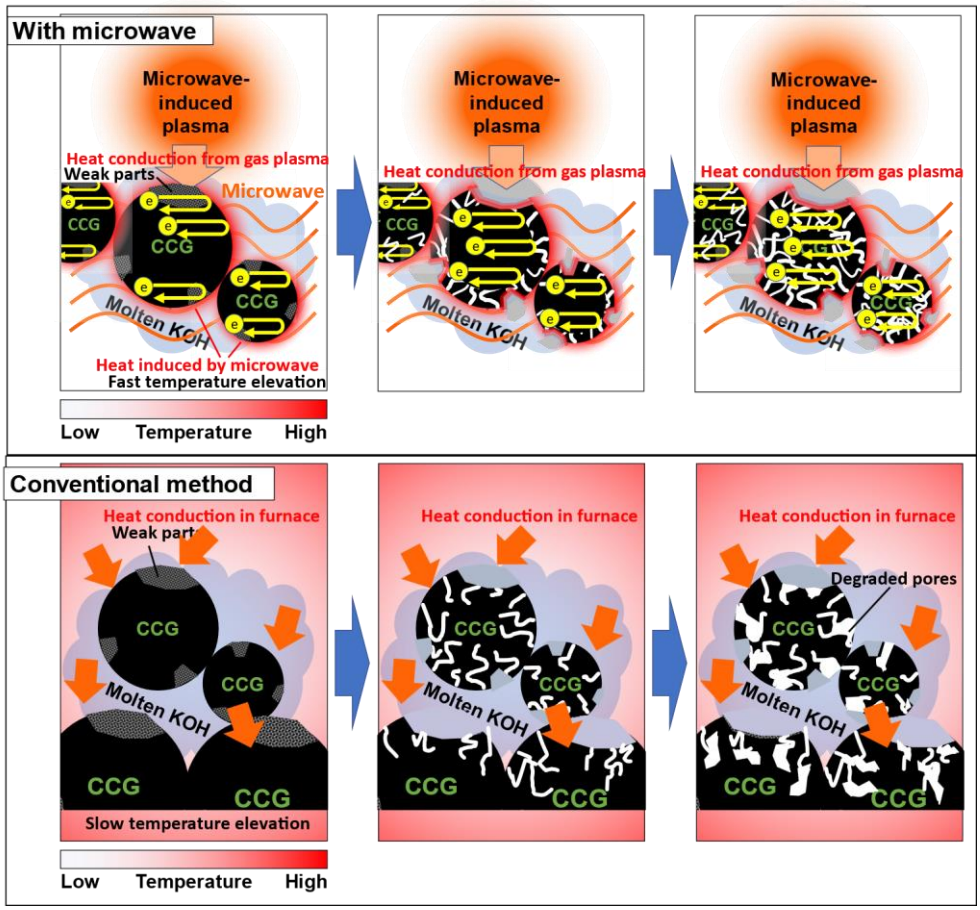

Figure 2.5 Illustration of pore formation of activated carbon prepared by (a) MiWP-KOH activation and (b) conventional heat-conduction activation.

Chapter 3 Effect of KOH Concentration in Feed Mixture

3.1 Introduction

Activated carbon has a hierarchical pore structure consisting of micropores (pore diameter is smaller than 2 nm), mesopores (pore diameter is between 2-50 nm), and macropores (pore diameter is larger than 50 nm) [15–19]. According to its microporous structure, activated carbon has been recognized as a promising adsorbent. Activated carbon can be used to adsorb various kind of molecules such as acetone, dichloromethane, ethyl formate, etc. [94]

To prepare the activated carbon with high surface area, carbon precursors (feed materials) must be mixed with the activating agents and heated at high temperature for several hours. [66,69,95,96] Among various activation methods, KOH activation is a well-established method that can be used to prepare high-surface-area activated carbon in industrial scale. [97] Previous study reported that the high-surface-area activated carbon with microporous and mesoporous structures can be prepared by mixing KOH with the carbon precursor using KOH/carbon mass ratio of 6. [98]

In a conventional process, the mixture of the carbon precursors and the activating agents was heated at 700-850 °C for 0.5-2.5 h to get the activated carbon with specific surface area in the range of 647-2413 $m^2 g^{-1}$. [99–101] The long activation time limits the activated carbon preparation process to be operated in batch systems, which cannot efficiently produce activated carbon in large scale. If the activation time becomes shorter (several minutes), the activated carbon preparation process can be operated in continuous system.

Many researchers have been seeking for a new method to reduce activation time by applying microwave irradiation to the KOH activation. For example, previous study [102] reported that activated carbon can be synthesized using KOH activation with microwave irradiation, suggesting that activated carbon with specific surface area of 729 $m^2 g^{-1}$ can be prepared within 10 min. In another study, activated carbon was prepared by microwave-KOH activation [103], suggesting that the mixture of carbon precursors and KOH was heated by microwave irradiation for 7 min to obtain activated carbon with specific surface area of 752 $m^2 g^{-1}$. Furthermore, activated carbon with specific surface areas of 972 $m^2 g^{-1}$ and 1229 $m^2 g^{-1}$ can be prepared within 12 min [98] and within 3 min, [97] respectively, using microwave-KOH activation. In these studies, the preparation methods required at least 3 min to get high-surface-area activated carbon, and none of them report the synthesis of activated carbon of which the specific surface area is above 2000 $m^2 g^{-1}$.

And, none of them report the generation of the plasma in the reaction zone, but only electromagnetic heating of the feed.

Recently, we found that the MiWP-KOH activation can be used to prepare activated carbon with high-surface-area of 1007 and 2084 m^2 g^{-1} using microwave-irradiation time of 80 and 330 s, as suggested in Chapter 1. Economically, the consumed energy and the cost for the preparation of activated carbon should depend on the activation time. The preparation of high surface area activated carbon with microporous and mesoporous structures in a short time is considered to be very important from an energy point of view.

Previous studies suggested that activation time and concentration of the activating agents in the feed mixture play an important role in pore formation of activated carbon prepared by a conventional method. [43,104,105] Therefore, the work in this Chapter 3 aims to investigate the influence of the concentration of the activating agents, KOH, to use MiWP-KOH activation for the preparation of activated carbon with high specific surface area (higher than 2000 m^2 g^{-1}) and hierarchical pore structures with micropores and mesopores. Also the effect of the microwave-irradiation time was investigated on the pore structures, with relating to the effects of the KOH concentration.

3.2 Materials and Methods

3.2.1 Preparation of Activated Carbon

A carbonized carbon gel (CCG) has been used as a carbon precursor here. Synthesis procedure of CCG is explained in Chapter 1. CCG was activated by MiWP-KOH activation as descripted in previous chapters by adjusting the microwave-irradiation time (80, 180, and 270 s) as well as KOH concentration (9-91 wt-%) in the feed mixture, which is CCG-KOH mixture. The MiWP-KOH activation was carried out in a modified household microwave oven [Sanyo Electric, EM-LA1(HL)] under nitrogen atmosphere with a flowrate of 300 cm^3 min^{-1} in a quartz tube. The microwave oven was operated at 500 W and 2.45 GHz. The mixture was cooled to ambient temperature under nitrogen atmosphere. Then, the mixture was washed with distilled water until the filtrate became neutral (pH ~7). The activated carbon was dried at 50 °C for 12 h before being collected and measured its weight to evaluate mass yield percentage using Eq. (2.1).

3.2.2 Investigation of Activation Temperature

Microwave-induced plasma can be clearly observed as a uniquely bright plasma above the CCG-KON mixture bed. As mentioned in Chapter 1, the temperature of this plasma was estimated to be above 5000 °C from the analysis of the emission spectra. The contact of this hot plasma with the CCG-KOH mixture bed should enhance the fast increase of its temperature.

It was observed that thermocouples were corroded heavily by KOH at high temperature, suggesting that commonly-used thermocouples protected by metallic sheath cannot be used to measure the temperature of the CCG-KOH mixture in the MiWP-KOH activation. Therefore, the temperature-change of the CCG-KOH mixture was observed using a radiation thermometer [Japan Sensor, FTHX-0200S V-1563].

3.2.3 Investigation on Pore Structure of Activated Carbon

Pore structures of the activated carbon was studied by obtaining nitrogen adsorption-desorption isotherms using an automated physisorption surface area analyzer [MicrotracBEL, BELSORP-miniII-S]. The samples were outgassed at 200 °C in vacuum for 4 h before the measurements. The nitrogen adsorption-desorption isotherm was used to evaluate pore properties of the activated carbon.

The total pore volume was assessed, corresponding to volume of nitrogen adsorbed at relative pressure (P/P_0) of 0.9. Micropore volume was calculated by applying *V-t* plot method [85] to nitrogen adsorption data. Mesopore volume was calculated from nitrogen desorption isotherms using Barrett-Joyner-Helenda (BJH) method. [86] Specific surface area was calculated by Brunauer–Emmett–Teller (BET) equation [84] using nitrogen adsorption isotherms. The calculation considered the molecular cross-sectional area of nitrogen at 77 K to be 0.162 nm^2. Microporosity was calculated by Eq. (3.1) to indicate the degree of micropore-domination in structure of activated carbon.

$$\text{Microporosity} = \frac{\text{micropore volume}}{\text{total pore volume}} \times 100\ \% \qquad (3.1)$$

3.3 Results and Discussion

3.3.1 Activation Temperature

The temperature-change of CCG-KOH mixture was recorded as illustrated in **Figure 3.1**. It is shown that the temperature rises along with

microwave-irradiation time to about 450 °C by 80-90 s with almost same temperature-elevating rate in all KOH-concentration cases, and the difference can be seen in the temperature-elevation rate after this time range. The result shows that the maximum activation temperature was 505, 787, and 860 °C when KOH to CCG ratio is 4:1, 6:1, and 10:1, respectively. It indicates that the maximum activation-temperature increases along with the increasing of KOH concentration in feed material.

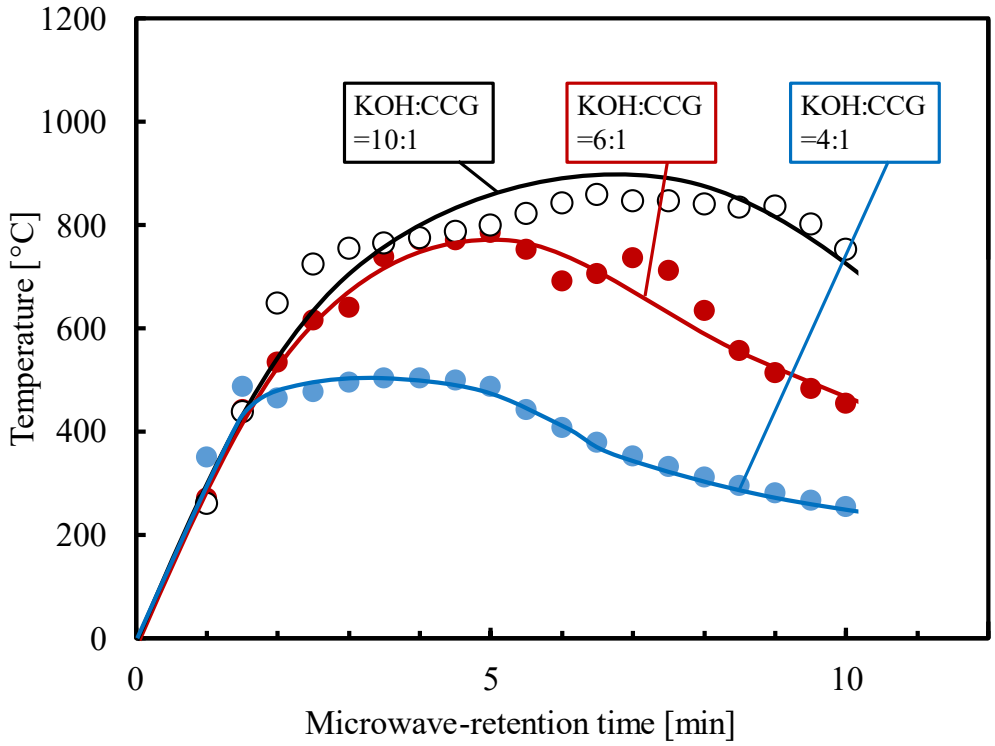

Figure 3.1 Temperature-change of CCG-KOH mixture in the MiWP-KOH activation with varied KOH:CCG ratio.

3.3.2 Pore Formation of Activated Carbon

Figure 3.2 represents nitrogen adsorption-desorption isotherms of the activated carbon prepared using various KOH concentration in the feed mixture. **Figures 3.2 (a)**, **(b)**, and **(c)** show adsorption-desorption isotherms of the activated carbon prepared using microwave-irradiation time of 80, 180, and 270 s, respectively. The adsorption-desorption isotherms show adsorption of nitrogen at low relative pressure ($P/P_0 < 0.01$), indicating microporous structure in activated carbon. [76,88] The results suggested that the adsorbed volume of nitrogen at low P/P_0 tends to increase with an increase in the KOH concentration, leading to an increase in micropore volume. In addition, each isotherm shows a hysteresis loop, indicating mesoporous

structure. [76,88–90] The size of the hysteresis loops seem to be wider as the KOH concentration increases. It can imply that the volume of mesopores increases with the increase of the KOH concentration in the feed mixture.

Figure 3.3 represents the specific surface area of activated carbon prepared using different KOH concentrations in the feed mixture and the microwave-irradiation times. **Figure 3.3 (a)**, **(b)**, and **(c)** show specific surface area of the activated carbon prepared using microwave-irradiation time of 80, 180, and 270 s, respectively. It can be shown that the maximum specific surface area are 1,266, 2,189, and 2,332 m^2 g^{-1} in activated carbon obtained by microwave-irradiation time of 80, 180, and 270 s, respectively. The results illustrate that specific surface area tends to increase as the KOH concentration increases.

Here, "reproducible zone" is defined as the operating conditions used to produce activated carbon with pore properties that have narrow fluctuation-range. The reproducible zone can be observed in the results of activated carbon prepared by microwave-irradiation time of 180 and 270 s. However, no reproducible zone can be seen in the results of activated carbon prepared by microwave-irradiation time of 80 s. This tendency suggests that it takes time more than 80 s to realize uniformity of heating. It should be noted that the electrical conductivity of carbon increases with temperature, [106] and the electrical conductivity of CCG may become high enough to cause the uniform plasma at higher than 450 °C of CCG temperature, when the microwave-irradiation time exceed 80 s. It can be observed in the experiments that when the average CCG temperature is not high enough, the plasma above the GGC-KOH mixture becomes narrowly localized, so that the CCG can be activated just in non-uniform manner.

One should remind that, unless the KOH concentration is substantially high, the reproducible zone can not be seen even if the average temperature of CCG-KOH is high enough. It seems that KOH is vaporized during the MiWP-KOH activation. Thus, if the amount of KOH in GGC-KOH mixture is not high enough, the uniformly-occuring reaction between carbon and KOH can not be preserved during the MiWP-KOH activation.

Similarly to the study reported in Chapter 1, it can be shown here that the specific surface area of activated carbon significantly increases as microwave-irradiation time increases until microwave-irradiation time becomes 120 s. When microwave-irradiation time is longer than 120 s, the specific surface area of the activated carbon seems to increase very slowly with an increase of microwave-irradiation time. This tendency might be due to the loss of KOH from CCG-KOH mixture by the vaporization of KOH.

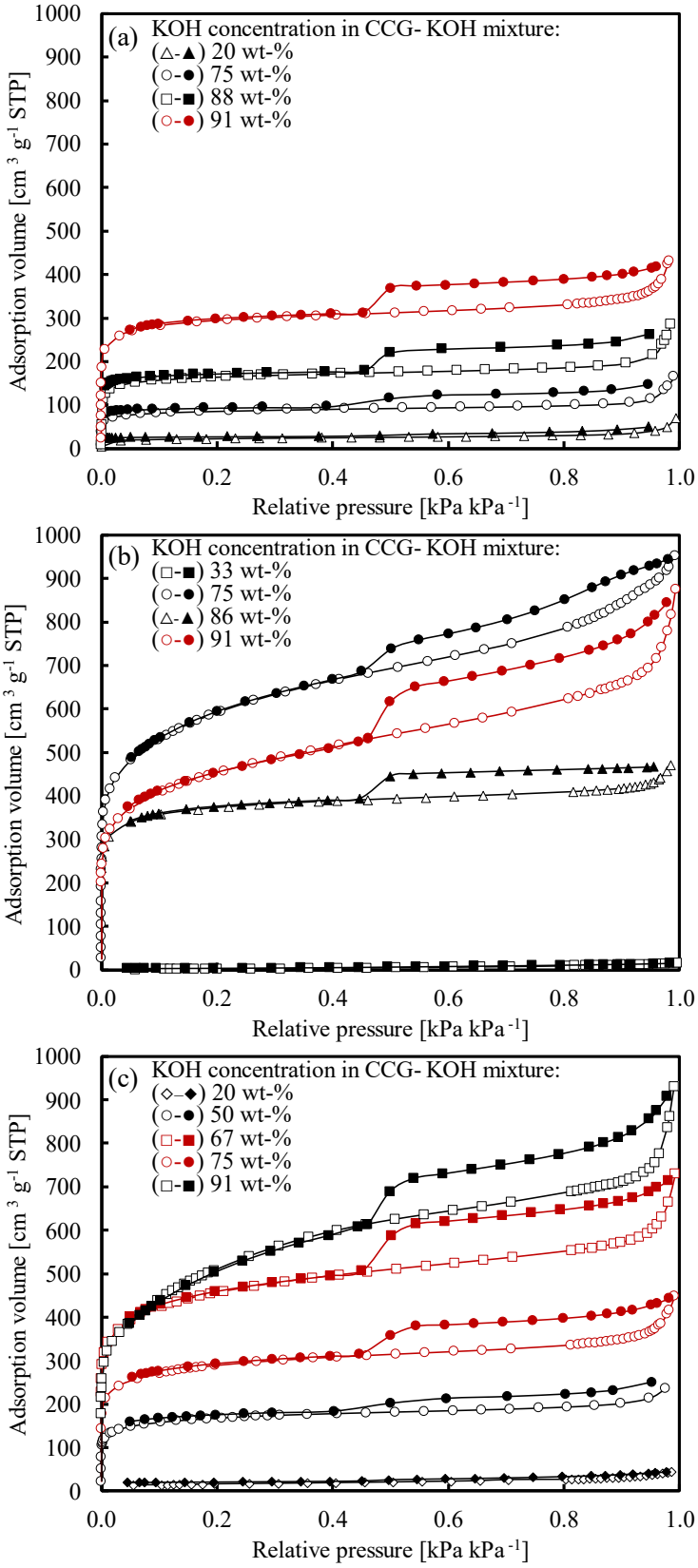

Figure 3.2 Nitrogen adsorption-desorption isotherms of activated carbon prepared by MiWP-KOH activation with microwave-irradiation time of (a) 80, (b) 180, (c) 270 s.

The analytical results of micropore volume show the similar tendency with those of the specific surface area. **Figure 3.4** shows the micropore volume of activated carbon prepared using different KOH concentration and the microwave-irradiation times. **Figures 3.4 (a)**, **(b)**, and **(c)** show the micropore volume of the activated carbon prepared using microwave-irradiation time of 80, 180, and 270 s. The results show that micropore volume tends to increase as the KOH concentration increases. Moreover, the reproducible zone can be observed in the results of the activated carbon prepared by microwave-irradiation time of 180 and 270 s at the high KOH concentration range. However, no reproducible zone is shown in the results of activated carbon prepared by microwave-irradiation time of 80 s. The results indicate that in the suitably high ranges of KOH concentration in feed mixture and microwave-irradiation time, the reproducible zone can be secured for specific surface area and micropore volume.

Figure 3.5 represents mesopore volume of the activated carbon prepared using different concentrations of KOH in feed mixture and microwave-irradiation times. **Figures 3.5 (a)**, **(b)**, and **(c)** show mesopore volume of the activated carbon prepared using microwave-irradiation time of 80, 180, and 270 s, respectively. The results show that mesopore volume increases with an increase of the KOH concentration. Also, the mesopore volume increases with increasing the microwave-irradiation time. The influence of the microwave-irradiation time seems similar to the cases of the specific surface area and the micropore volume. However, differently from the cases of the specific surface area and the micropore volume, the mesopore volume does not exhibit the reproducible values even in the high KOH concentration range, which corresponds to the reproducible zone observed in the results of the specific surface area and the micropore volume.

Figure 3.6 shows the nitrogen adsorption-desorption isotherms of activated carbon synthesized at 82 and 86 wt-% of KOH concentration with 270 s of the microwave-irradiation time. These conditions are categorized into the reproducible zone to obtain the stable values of high specific surface area and the micropore volume. One can notice that the shapes of these isotherms are different in the relatively high pressure range, where the one synthesized at 82 wt-% of KOH concentration is expected to contain well-grown mesopores and the other should not contain significant volume of the mesopores. The reason why mesopore volume is difficult to control can be explained as follows.

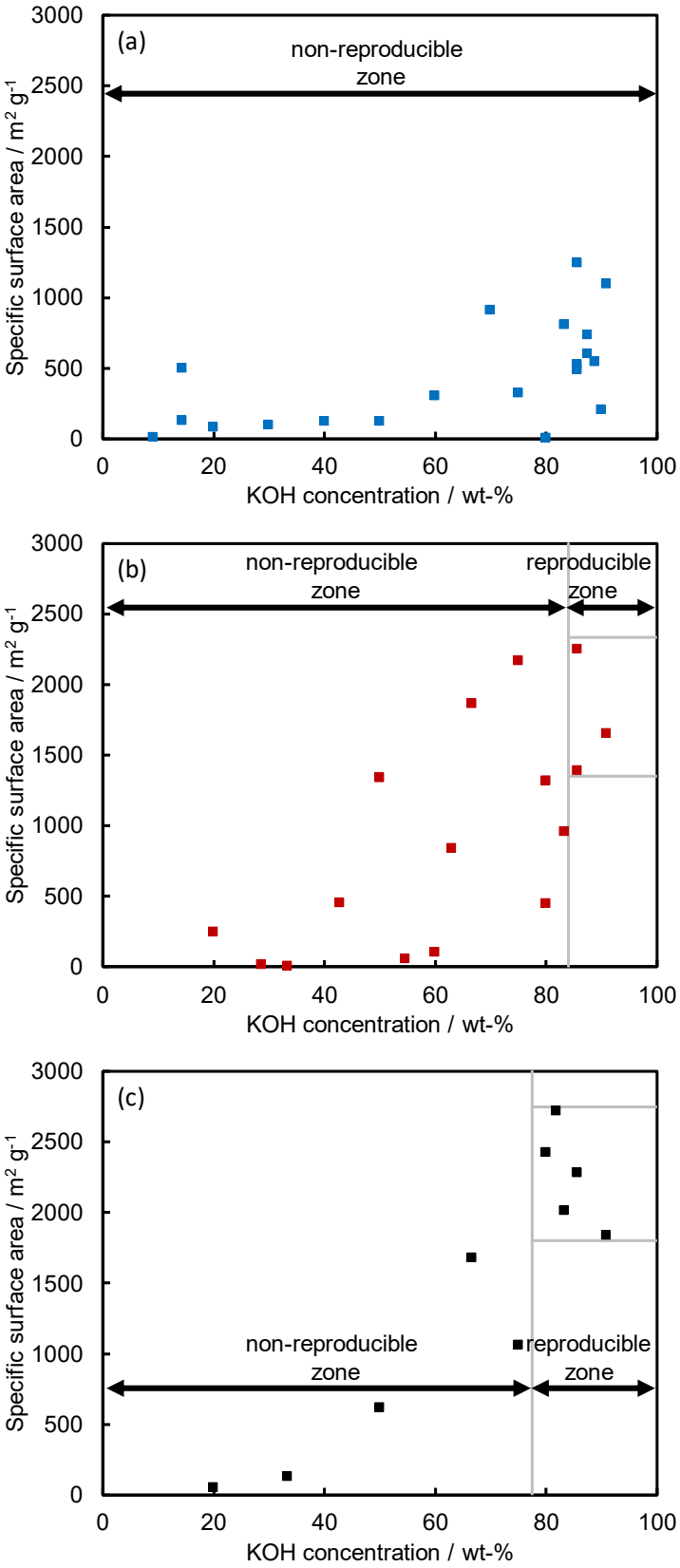

Figure 3.3 Effect of KOH concentration in feed mixture on specific surface area of activated carbon prepared by MiWP-KOH activation using different KOH concentration and microwave-irradiation time of (a) 80, (b) 180, (c) 270 s.

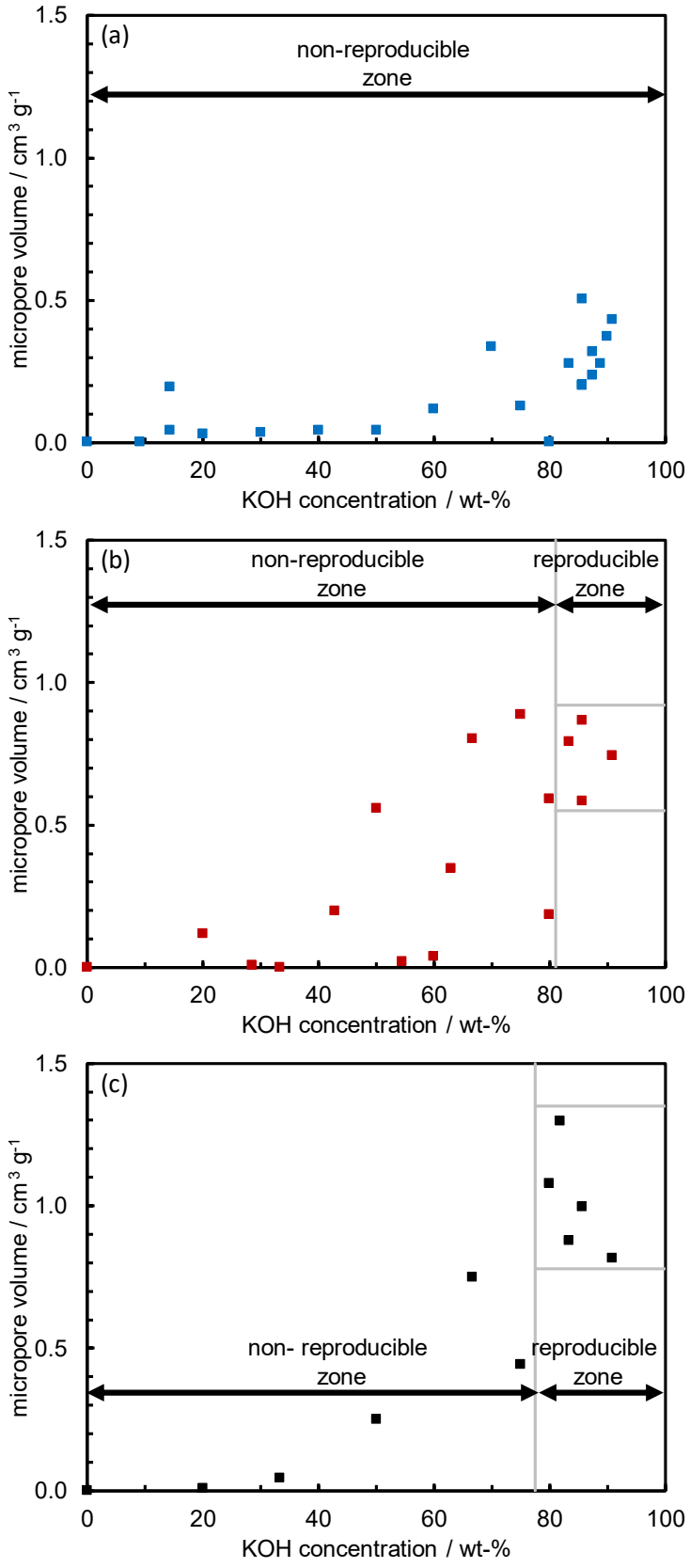

Figure 3.4 Effect of KOH concentration in feed mixture on micropore volume of activated carbon prepared by MiWP-KOH activation using different KOH concentration and microwave-irradiation time of (a) 80, (b) 180, (c) 270 s.

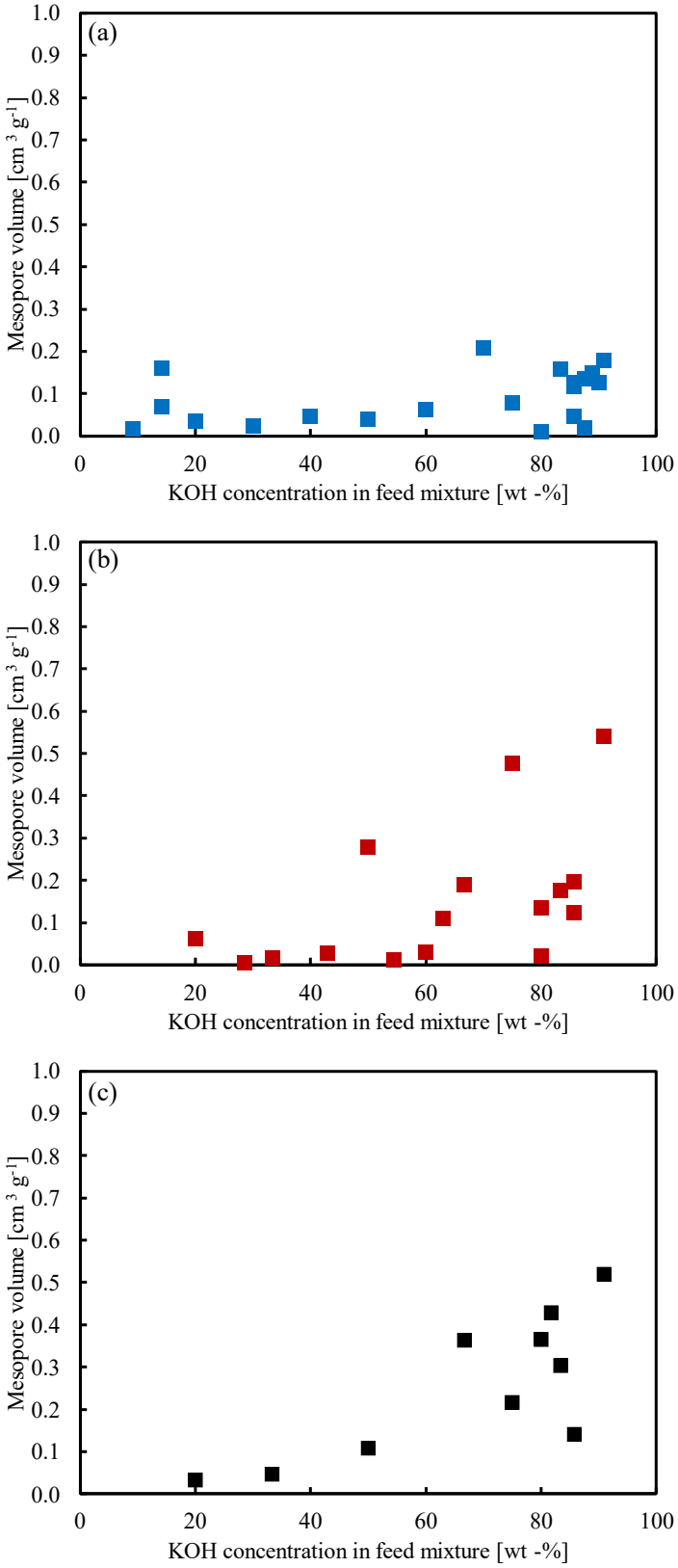

Figure 3.5 Effect of KOH concentration in the feed mixture on mesopore volume of activated carbon prepared by MiWP-KOH activation using different KOH concentration and microwave-irradiation time of (a) 80, (b) 180, (c) 270 s.

In the MiWP-KOH activation, the growth of micropores can proceed since activation time is short, but mesopores grow much slower at the high temperature while the CCG-KOH is heated by the plasma. In fact, the timing to start stable plasma that can heat CCG-KOH mixture uniformly is not well repeatable. Therefore, if the timing to obtain such stable plasma is late, the duration of such plasma until the activation is terminated is not long enough to obtain well-grown mesopores, but this duration can be long enough to form well-grown micropores. If the timing to start such stable plasma is early, the both of micro and mesopores can be grown well. To improve the stability of mesopore volume, further study to investigate the reaction conditions to stabilize the timing to obtain such stable plasma will be necessary.

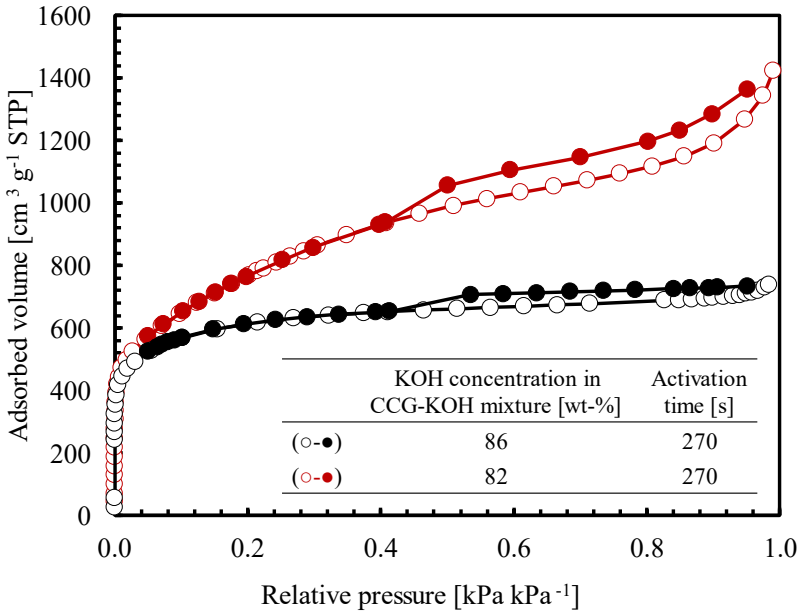

Figure 3.6 Nitrogen adsorption-desorption isotherms of activated carbon prepared by MiWP-KOH activation with two KOH concentrations, 86 and 82 wt-% and microwave-irradiation time of 270 s.

3.3.3 Mass yield percentage in MiWP-KOH activation

Figure 3.7 illustrates the mass yield percentage of activated carbon prepared using microwave-irradiation time of 180 and 270 s. The mass yield percentage was calculated using Eq. (2.1). The average value of the mass yield percentage for the condition when high-surface-area activated carbon with surface area higher than 1500 m^2 g^{-1} was synthesized in the stabilized zone is 12.3 wt.-%. It is similar to the mass yield percentage of the activated

carbon prepared by conventional conduction heating in Chapter 2, which is 9.3 wt-% in average.

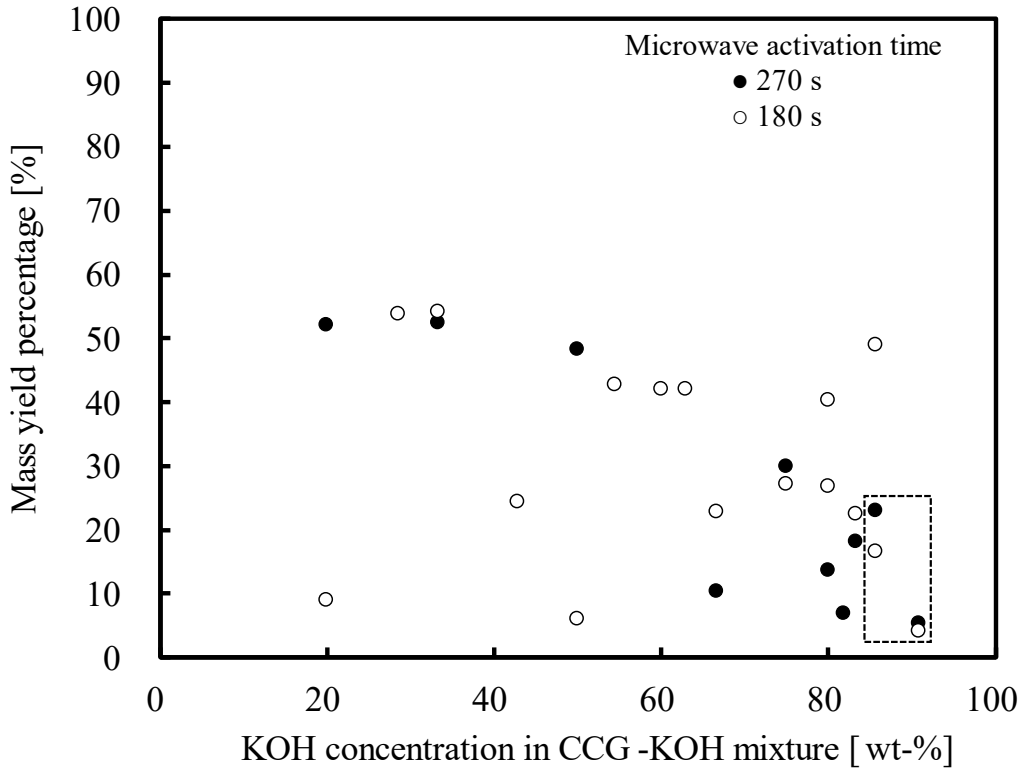

Figure 3.7 Effect of KOH concentration on mass yield percentage of activated carbon prepared by MiWP-KOH activation using microwave-irradiation time of 180 and 270 s. The plots marked by square are the one obtained when high-surface-area activated carbon with surface area higher than 1500 m^2 g^{-1} was synthesized in the stabilized zone.

3.3.4 Comparison with Past Studies

A comparison of the present study with past studies about the use of microwave to produce activated carbon is summarized in **Table 3.1**. Here, the values of the maximum specific surface area of activated carbon obtained by each of the past studies are shown. This table also shows the information of some reports of the conventional activation. By looking at the comparison in this table, it could be said that the present study exhibits the best microwave performance. Koyuncu *et al.* [107] reported that activated carbon with specific surface area of 1021 m^2 g^{-1} was obtained within 40 s, but the power to generate microwave used by them was 900 W. On the other hand, the power used by the present MiWP-KOH activation to produce the activated carbon

with similar surface area was only 500 W. Liu *et al.* [108] used the even lower power, 350 W, to obtain activated carbon with specific surface area of 1410 m^2 g^{-1}, but a long microwave-irradiation time such as 20 min was required there. Other works used longer time and higher power to make the microwave activation. And importantly, none of the microwave activation methods except MiWP-KOH activation realized the synthesis of activated carbon of which specific surface area was above 2000 m^2 g^{-1}.

One can see in this table that the conventional methods can be used to prepare activated carbon with high specific surface area, but they need 60-90 min to finish the activation [109–111]. One may imagine that such time-consuming activation of MiWP-KOH may result in high energy consumption. As a feature of the pore structure of activated carbon prepared by MiWP-KOH activation, the microporosity seems to be relatively high. The characteristics of the MiWP-KOH activation which need relatively short activation time and less power to generate microwave may indicate the potential to realize the energy saving process to produce high-surface-area activated carbon.

3.3.5 Controllability of Microporosity

Figure 3.8 shows the microporosity calculated by Eq. (3.1) for the results obtained with all of KOH concentration in feed mixture and microwave-irradiation time adopted in this study. The results suggest that the microporosity tends to increase as the KOH concentration increases. On the other hand, the influence of the microwave-irradiation time is not clearly seen.

The relation between the microporosity and KOH concentration within the observed KOH concentration range seem to be described by a linear equation, although relatively large variations from this correlation line can be seen. This correlation line can be written as (Microporosity) = (0.529)(KOH concentration [wt-%]) + 22.65%, where coefficient of determination R^2 is 0.414.

The microporosity defined here is considered to be a kind of criteria to know how much the micropores dominate the porous structures. When one needs to use activated carbon to adsorb relatively large molecules, or wants quick adsorption with high diffusivity of adsorbate molecules in activated carbon, the activation condition with high KOH concentration can be recommended. The result here can be used to synthesize activated carbon by MiWP-KOH activation to answer such demands for the pore structure of activated carbon. Schematic summary of pore formation can be summarized as shown in **Figure 3.9**.

Table 3.1 Comparison of pore properties of various activated carbon prepared from microwave and conventional activation.

Carbon precursor	Activation method	Activating agent	Activation time [min]	Activation temperature [°C]	Microwave power [W]	Surface Area [m^2 g^{-1}]	Micro-porosity/ [g g^{-1}]	References
CCG	Microwave	KOH	1:20		500	1266	90.8	This study
			3:00		500	2189	80.6	
			4:30		500	2238	74.9	
Mandarin shells	Microwave	H_3PO_4	0:40		900	1021	3.1	[107]
Orange peel	Microwave	K_2CO_3	6:00		600	1104	40.2	[42]
Rice husks	Microwave	K_2CO_3	7:00		600	1165	42.3	[103]
Rice husks	Microwave	KOH	7:00		600	752	40.6	[103]
Cotton stalk	Microwave	K_2CO_3	8:00		660	621	29.0	[102]
Cotton stalk	Microwave	KOH	10:00		680	729	68.4	[102]
Rambutan	Microwave	KOH	12:00		600	972	25.2	[98]
Bamboo	Microwave	H_3PO_4	20:00		350	1432	72.3	[108]
Palm kernel shells	Microwave	steam	30:00		700	419	76.1	[116]
Tuncbilek lignite	Conventional	KOH	60:00	800		1001	74.6	[110]
Anthracite	Conventional	NaOH	60:00	850		1200	94.0	[111]

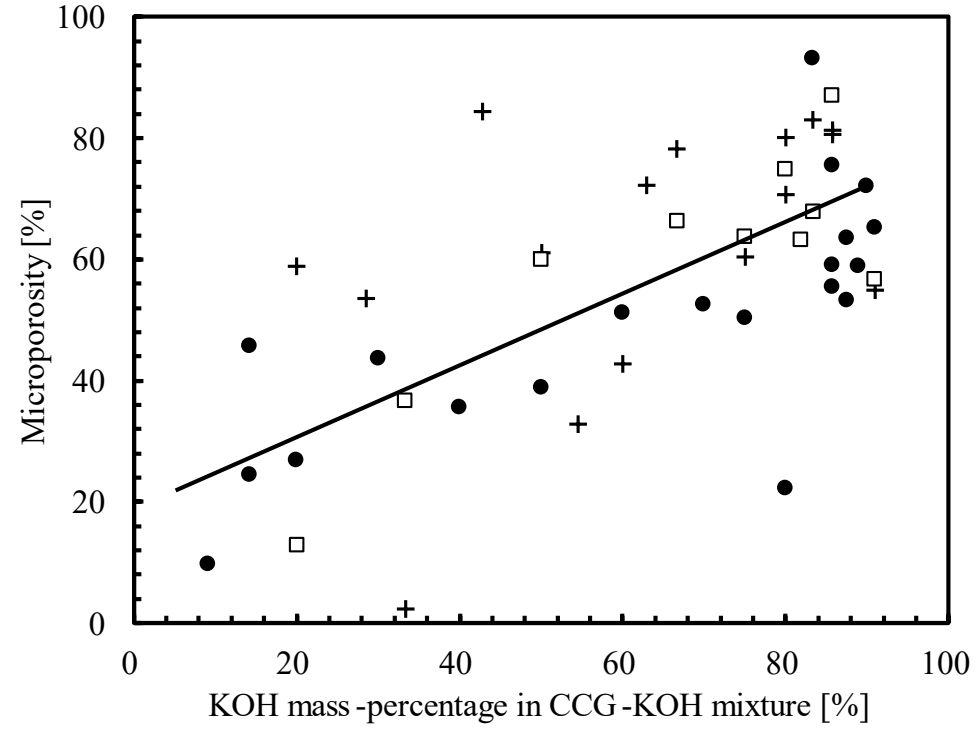

Figure 3.8 Microporosity of activated carbon prepared by MiWP-KOH activation defined by Eq. (3.1) related with KOH concentration in feed-material and microwave-irradiation time of (●) 80, (+) 180, (□) 270 s.

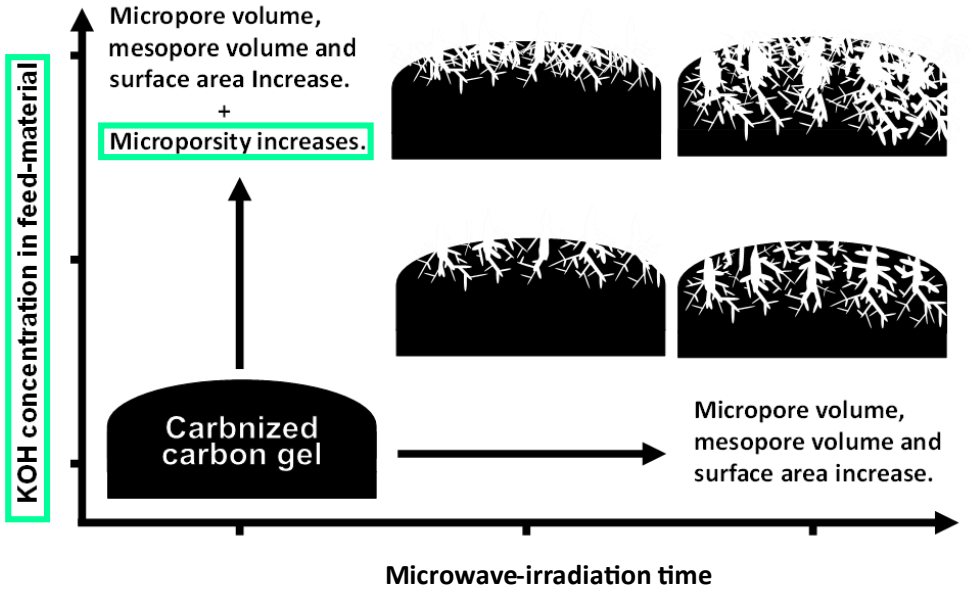

Figure 3.9 Schematic summary of pore formation in activated carbon prodeced by MiWP-KOH activation.

3.4 Conclusion

MiWP-KOH activation can be used to prepare a high-surface-area activated carbon with specific surface area of 1,251, 2,250, and 2,718 m^2 g^{-1} within 80, 180, and 270 s. The MiWP-KOH activation can be done rapidly because the high-temperature plasma, as mentioned in Chapter 1, may support the quick heating of the feed material. It was suggested that the increases in the microwave-irradiation time and KOH concentration in the feed mixture resulted in the increase in micropore and mesopore volumes, but excessively long activation time was not useful to increase these volumes. It was observed that the concentration of KOH should be high enough to stabilize the high values of the micropore volume and the specific surface area of the activated carbon. This condition is referred to as "reproducible zone" in this study. The reproducible zone can not be observed for mesopore volume at this stage. The mass yield percentage of the activated carbon prepared by MiWP-KOH activation was 12.3 wt-% in average in the stable condition. This mass yield percentage is higher than the mass yield percentage of the activated carbon prepared by the conventional activation.

The result about microporosity indicates that the microporous structure becomes more dominant when KOH concentration becomes higher. The results obtained here may be useful to control the pore structures of activated carbon with high specific surface area for various demands for adsorption applications.

Chapter 4 MiWP-KOH Activation: Pseudo Continuous Operation

4.1 Introduction

Conventionally, activated carbon with high specific surface area can be made by mixing carbon precursor with activating agents and heated at high temperature for several hours [112]. Since the mixture of carbon precursors and activating agents must be heated for a long period, such activated carbon preparation process is limited to be operated in batch system, leading to the difficulty to produce activated carbon in fast way. If the activation time can be shortened, this process can be improved to be continuous operation. Then, fast and energy-saving production of activated carbon can become possible.

Previous study reported that some types of electrical plasma can be used to modify surface structure of carbon materials. For example, Su *et al.*[113] reported that atmospheric dielectric barrier discharge plasma can be used to modify $LiMn_{0.8}Fe_{0.2}PO_4$/nitrogen-doped carbon, which is a part of lithium-ion battery. Moreover, work of Das *et al.* [114] shows that microwave-induced plasma can successfully use to synthesize of multiwall carbon nanotubes.

A microwave-induced plasma can be generated by irradiating microwave onto electrically conductive materials with suitable shape such as a metal needle with sharp-edge or porous carbon materials. For the porous carbon materials, the microwave-induced plasma can be generated because electron is discharged in micropores of the porous carbon materials. Zheng *et al.* [83] reported that activated carbon with specific surface area of 1036 $m^2\ g^{-1}$ can be prepared using microwave irradiation in carbon dioxide environment within 90 min. As explained in the previous chapters, the MiWP-KOH activation used microwave-induced plasma with KOH activation had been successfully developed to prepare activated carbon with surface area of 2000 $m^2\ g^{-1}$ or higher within several minutes. Due to the significantly short activation time, the results can contribute to the development of continuous reactor system for the preparation of high surface area activated carbon.

As a first step toward the development of the continuous reactor, this research has developed a new activation method using pseudo continuous reactor system with feeding carbon precursor (carbonized carbon gel; CCG) mixed with KOH under microwave-induced plasma, so called MiWP-KOH activation, to prepare high surface-area activated carbon.

4.2 Materials and Methods

4.2.1 Activated Carbon Preparation by Pseudo Continuous Reactor

Firstly, the CCG was mixed with KOH at 86 wt-% and ground thoroughly. Then, the mixture of CCG-KOH was activated using a pseudo continuous microwave reactor, which was developed as represented in **Figure 4.1**. An L-shape quartz tube was placed in a microwave oven, and motor was driven to move a ceramic boat containing the CCG-KOH mixture. The moving speed was controlled in the range of 0.03-0.12 mm s^{-1}. The path of this moving boat was adjusted so that the carbon precursor was carried through the microwave-concentrated zone. The length of the microwave reaction zone in the moving direction was estimated to be 14.3 mm. Microwave was generated at 2.45 GHz and 500 W there. The retention time of the carbon precursor in the microwave reaction zone is defined by the reaction zone length divided by the boat moving speed. This microwave-retention time was varied for 120-510 s. Nitrogen gas was introduced to the quartz tube at 300 mL min^{-1} so that the activation reaction can occur in inert gas environment. After the precursor-contained ceramic boat passed the microwave reaction zone, the boat was dropped down at the L-shape part in the quartz tube. After the activation, the resulted activated carbon was washed with distilled water until the filtrate became neutral (pH ~7) before being dried at 50 °C for 12 h.

A radiation thermometer [Japan Sensor, FTHX-0200S V-1563] was used to observe the temperature-change of the CCG-KOH mixture in this reactor. This measurement was conducted in batch mode when the moving speed of the precursor-contained boat was stopped, so that the time-dependency of the precursor temperature could be obtained. When the pseudo continuous operation is conducted in this reactor, the temperature of the precursor at the microwave reaction zone can be estimated by the microwave-retention time related with this time-dependency of the precursor temperature.

4.2.2 Investigation on Pore Structure of Activated Carbon

An automatic physisorption-based surface area analyzer [MicrotracBEL, BELSORP-mini II-S] was used to observe nitrogen adsorption-desorption isotherms of the activated carbon. The adsorption-desorption isotherms have been used to investigate pore properties. Specific surface area, micropore volume, and total pore volume of the activated carbon can be calculated from the nitrogen adsorption-desorption isotherms. Micropore volume was calculated from *t*-plot method. Mesopore volume was calculated from the

difference between total pore volume and micropore volume. Mass yield percentage of activated carbon is defined by Eq. (2.1).

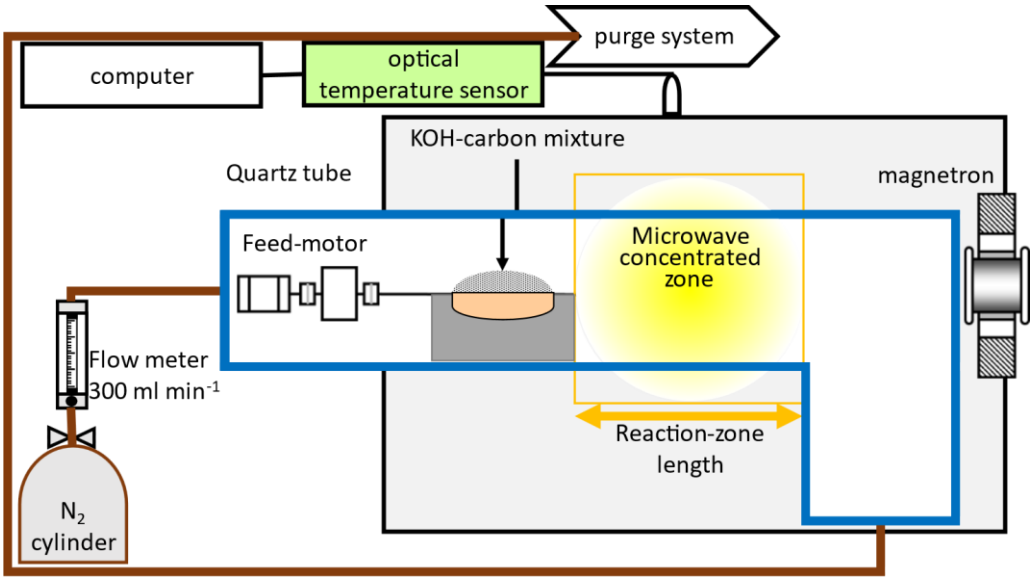

Figure 4.1 Pseudo continuous microwave reactor system used for activated carbon preparation.

4.3 Results and Discussion

4.3.1 Heating Feed Mixture by Microwave

The temperature-change of the carbon precursor in batch mode was measured as presented in **Figure 4.2**. The result suggests that the maximum of activation temperature is 787 °C. The temperature-elevation rate is 90 °C min^{-1}, as calculated from the period of time used to rise temperature from 500 to 787 °C.

It should be noted that the temperature of the CCG cannot reach the activation temperature unless KOH is mixed. When microwave was irradiated to 0.1-0.7 g of ground CCG without mixing KOH for 10 min, its temperature could not reach above 200 ºC, which is the minimum limit of the radiation thermometer used here. Then, further temperature increase was not observed even when the microwave-retention time was prolonged. From this result, KOH seems to play a role not only for reaction to open pores on carbon but also for increasing the temperature of the feed to activate the carbon. When microwave is irradiated to pure KOH, the temperature became 450 ºC at maximum.

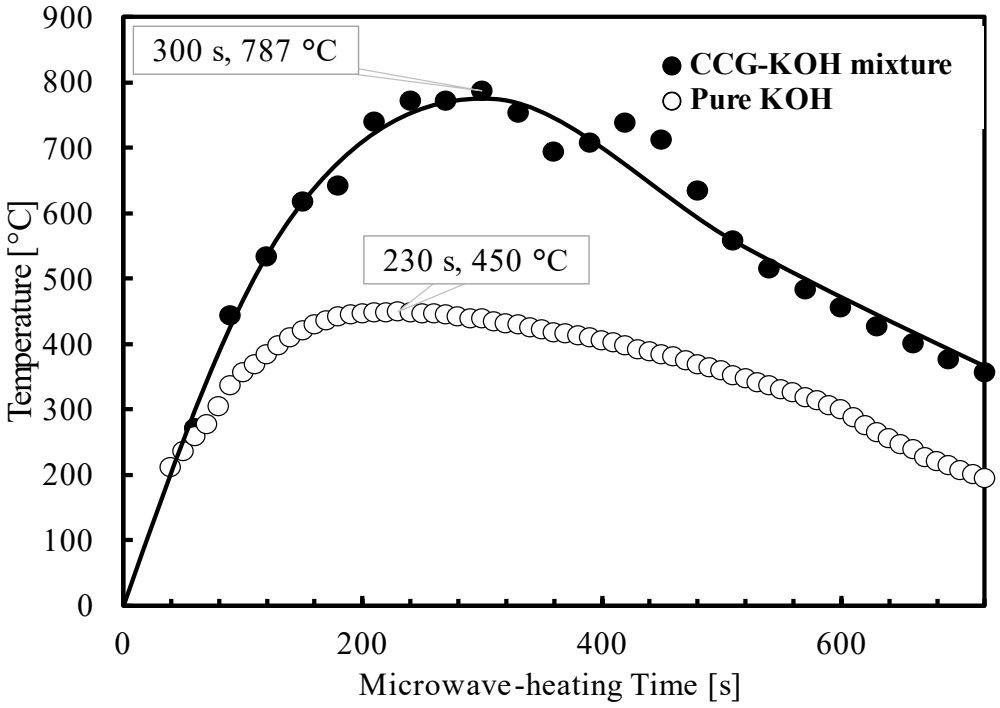

Figure 4.2 Temperature-change of CCG-KOH mixture placed at the microwave-reaction zone in the batch mode.

The electrically-conductive high-crystallinity carbon can absorb microwave by its free electrons, and electric current induced in such carbon causes Joule heating [115]. However, if the carbon material does not have high electrical conductivity due to its inclusion of amorphous structures, the microwave heating may not be so efficient. The analyses using X-ray diffractometer were conducted on the CCG, as presented in **Figure 4.3**. The results suggested that the signals to prove the existence of graphitic structures was not clear. Thus, the main structure of the CCG should be amorphous, and such structure should lead to the difficulty of the temperature-elevation of the CCG without KOH at ambient temperature.

Nevertheless, it should be noted that the electrical conductivity of carbon significantly increase with temperature [106]. When microwave is absorbed by KOH by its dipole excitation, it can cause the temperature-elevation of CCG-KOH mixture. Then, the CCG can be conductive enough at such high temperature to be heated by the microwave-induced electric current.

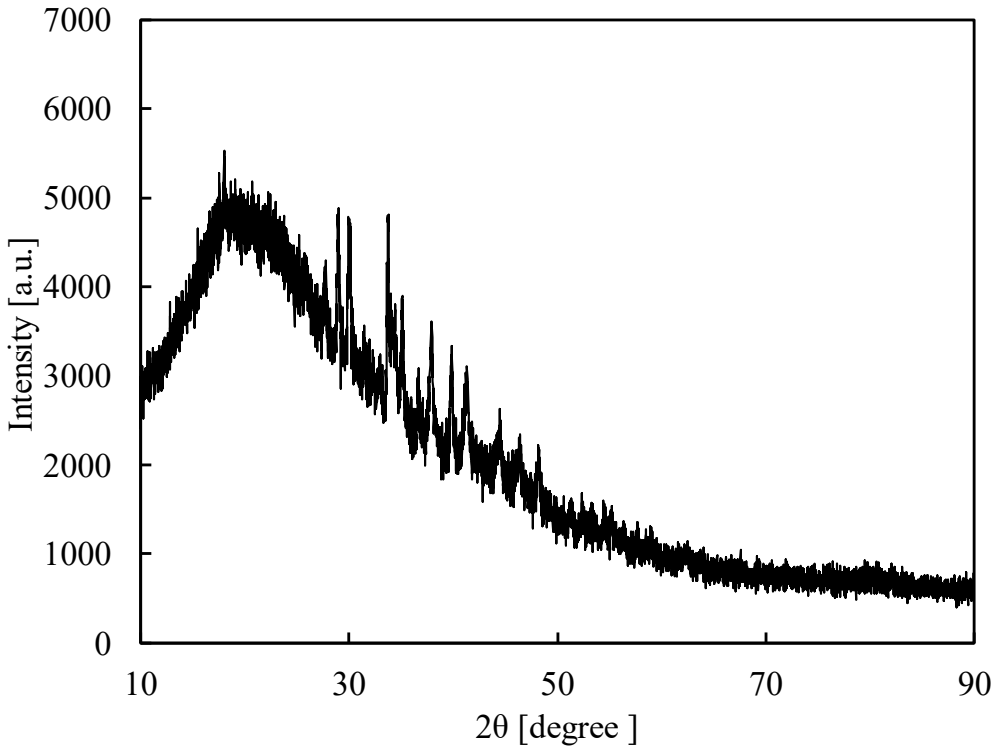

Figure 4.3 X-ray diffractometer of activated carbon prepared by MiWP-KOH activation.

4.3.2 Nitrogen Adsorption-Desorption Isotherm

The nitrogen adsorption-desorption isotherms of the activated carbon prepared from the pseudo continuous microwave-reactor is shown in **Figure 4.4**. The results indicate that the products obviously have micropores when the microwave-retention time is longer than 210 s, suggested by the sharp slope at the low-pressure range seen in the products with the retention time from 210 to 510 s. In this range, the microporous structure of the activated carbon seems to increase as microwave-retention time increases. Considering with the result of the temperature change shown in **Figure 4.2**, it should be necessary to experience the temperature higher than about 730 ℃ to generate micropores.

The result shown in **Figure 4.4** also indicates that the micropore volume increases as microwave-retention time prolongs. This trend seems significant. Moreover, each isotherm shows a hysteresis loop, which might be related to capillary condensation taking place in mesoporous structure. This hysteresis loop also tends to increase when the microwave-retention time prolongs. However, the trend of the hysteresis loop depending on the microwave-retention time does not seem so significant compared with the trend of the micropore volume. The quantitative comparison between these trends is explained later.

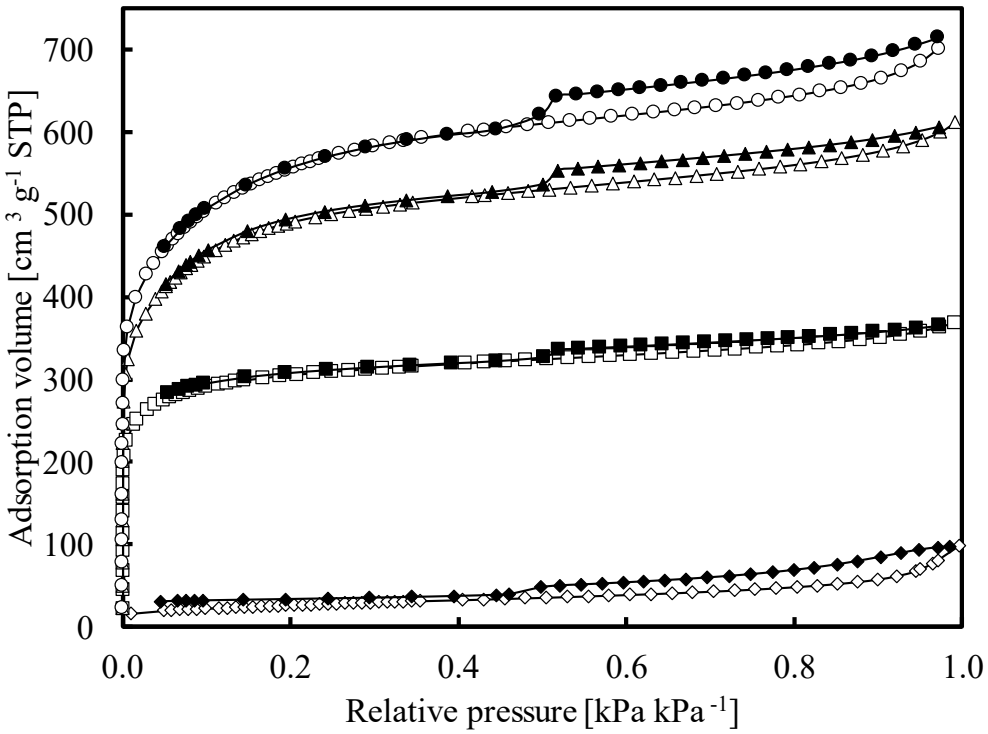

Figure 4.4 Nitrogen adsorption-desorption isotherm of activated carbon prepared by pseudo continuous microwave-reactor using microwave-retention time of (◇-◆) 120 s, (□-■) 210 s, (△-▲) 300 s, and (○-●) 450 s.

4.3.3 Specific Surface Area, Micropore and Mesopore Volume

Figure 4.5 represents the specific surface area of the activated carbon prepared by the pseudo continuous microwave-reactor system. The results indicate that the specific surface area of the activated carbon increases as the microwave-retention time is prolonged. It should be noted that the specific surface area can continue growing even after 300 s, when the temperature becomes maximum at 787 °C. At the microwave-retention time of 510 s, when the specific surface area becomes the largest, the temperature of the carbon precursor may become down to about 500 °C, as suggested in **Figure 4.2**. This result indicates that under the irradiation of the microwave, the growth of the pores can continue in the temperature range, 500-788 °C. This temperature range is considered to be lower compared with typical temperature for activation in conventional ways by ordinary heat-conduction. From this fact, one may consider that there would be unique effects of microwave irradiation to enhance pore formation reactions.

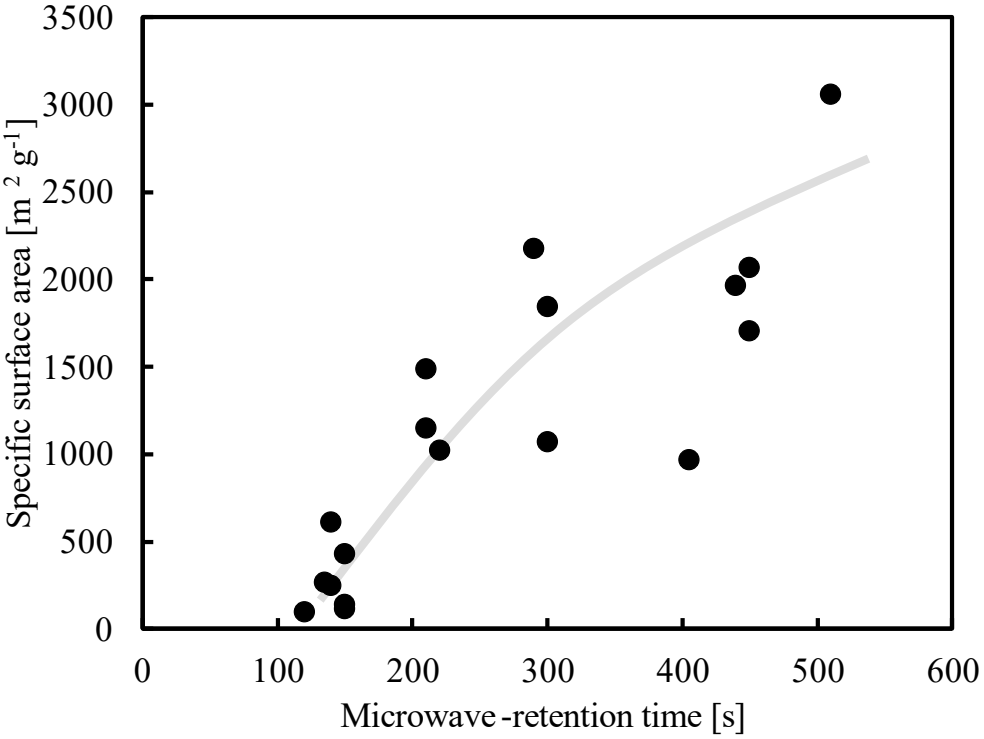

Figure 4.5 Specific surface area of activated carbon prepared by pseudo continuous microwave-reactor.

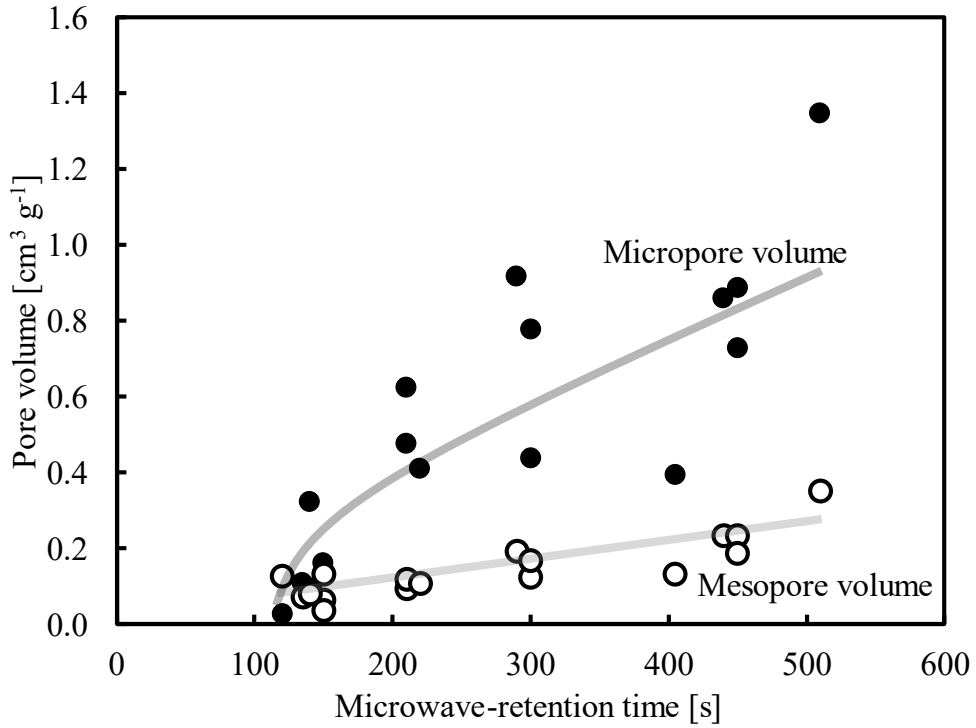

Figure 4.6 Micropore and mesopore volume of activated carbon prepared by the pseudo continuous microwave-reactor

From the nitrogen adsorption-desorption isotherms, micropore and mesopore volume of the activated carbon prepared from the pseudo continuous microwave reactor system can be calculated as shown in **Figure 4.6**. The results indicate that the both of micropore and mesopore structure increase as microwave-retention time prolongs. In the conditions when the microwave-retention time is long enough to clearly exhibit pore volumes, namely when microwave retention time is longer than 210 s, the ratio of the micropore volume to mesopore volume does not seem to depend on the microwave retention time. Overall, the micropore volume is about three times larger than mesopore volume.

4.3.4 Length of the microwave reaction zone

The effective retention time for microwave irradiation on the moving KOH-carbon mixture in the pseudo continuous system was calculated by the assumed reaction zone length divided by the speed of the motion of the KOH-carbon mixture. This assumed reaction zone length was changed so that the results from batch and pseudo continuous systems seemed the same with consideration of the experimental error.

Nitrogen adsorption-desorption isotherms of the activated carbon obtained from batch and pseudo continuous systems were used to calculate specific surface area and micropore volume as shown in **Figure 4.7** and **Figure 4.8**, respectively. It should be noted that the batch and pseudo continuous system exhibits the same trend in the relationship of the specific surface area and the micropore volume to the retention time of the microwave irradiation, when the reaction zone length is set to be 1.43 cm.

The calculation results reveal that the length of the reaction zone is 1.43 cm. It should be noted that the motion of the KOH-carbon mixture does not affect the pore structures of the AC products. The results here can contribute to development of a continuous microwave-reactor system for activated carbon preparation.

4.3.5 Mass Yield Percentage of Activated carbon

Figure 4.9 shows the mass yield percentage of the activated carbon prepared using the pseudo continuous microwave reactor system. In this work, activated carbon using the microwave-retention time of 120-510 s shows the mass yield percentage of 21.7-71.2 wt-%. The yield of the activated carbon significantly decreases as microwave-retention time increase from 120 to 210 s. However, the yield of the activated carbon shows the slightly decrease as the microwave-retention time increases from 210 to 510 s, although the

temperature of the feed mixture may become about 787 °C at 300 s within this time range as stated earlier.

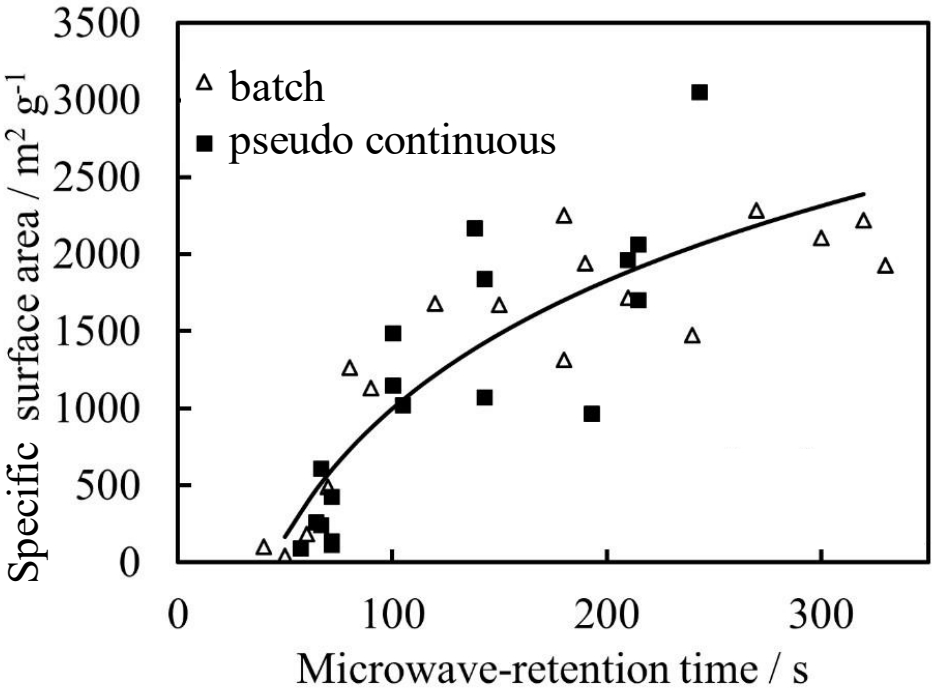

Figure 4.7 Specific surface area of activated carbon prepared by batch and pseudo continuous reactor system.

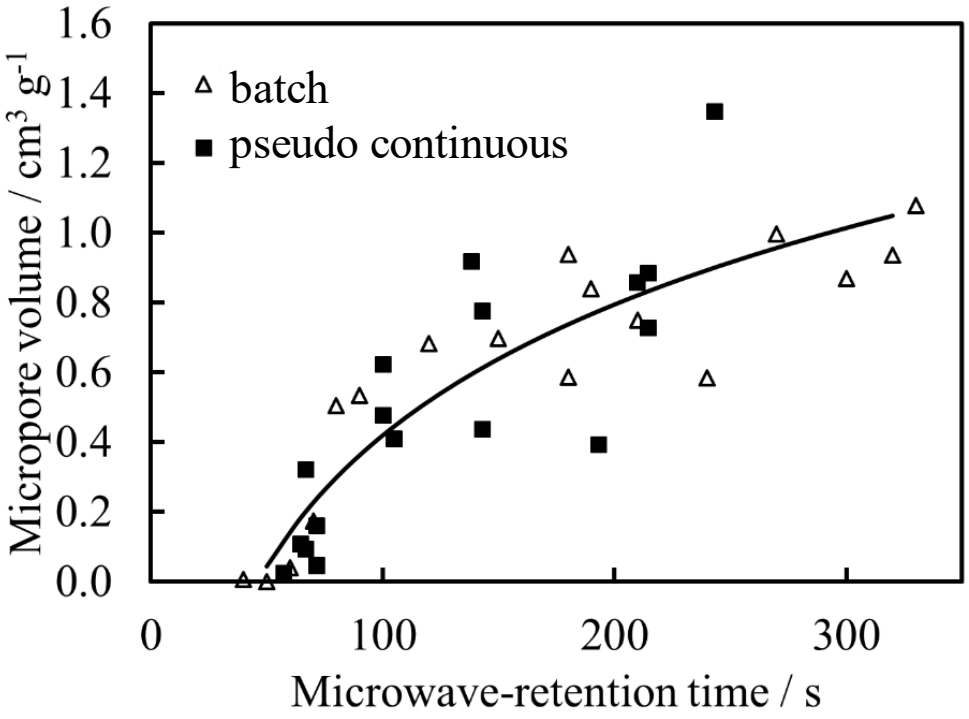

Figure 4.8 Micropore volume of AC prepared by batch and semi-batch reactor system.

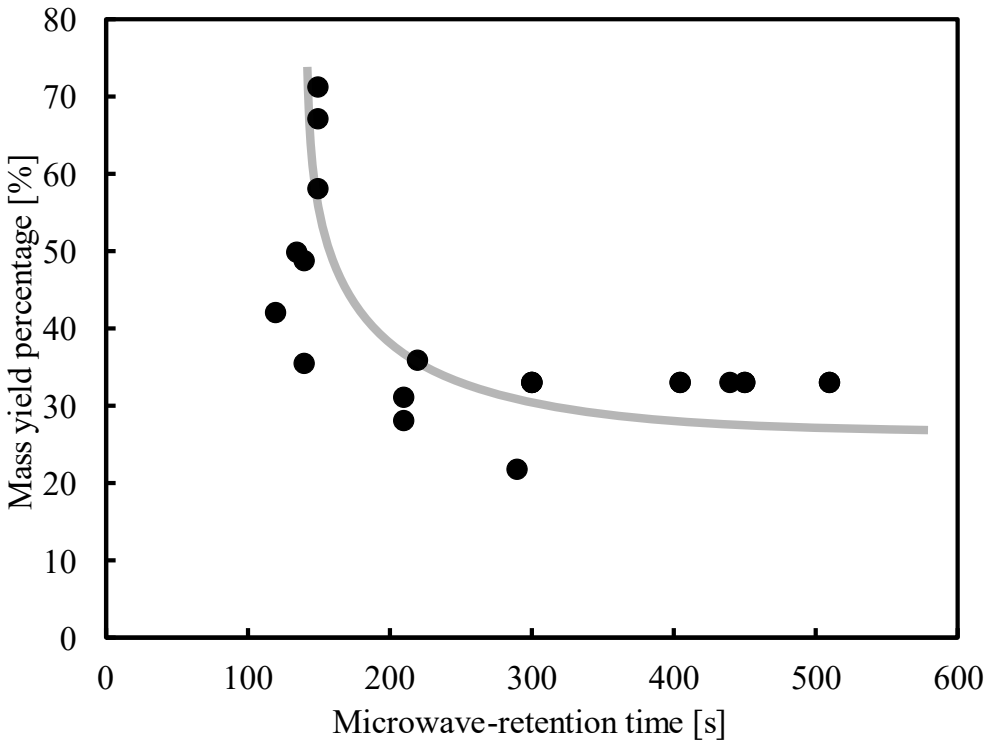

Figure 4.9 Mass yield percentage of activated carbon prepared by the pseudo continuous microwave-reactor.

This tendency can be explained by considering that the CCG consists of stable structures and relatively weak structures. Within 210 s of the microwave-retention time, the weak structure could be reacted with KOH, leading to the drastic decrease in the mass yield percentage. This consumption does not generate pores so much without the significant increase of specific surface area of the activated carbon. After this time range, the temperature of the carbon precursor becomes higher than about 700 °C as mentioned above, which can be high enough to generate micropores and mesopores at the remaining stable parts in the structure of CCG. Therefore, the yield-decreasing rate while the pores are generated at high temperature after 210 s can be obviously lower than that while the weak parts are consumed within 210 s.

The average mass yield percentage of the activated carbon was calculated for the conditions when specific surface area becomes higher than 1,000 m^2 g^{-1}. The calculation results show that the average yield of the activated carbon is 24.2%.

4.3.6 Mechanism of Pore Formation

According to the results mentioned earlier, model of pore formation of activated carbon prepared by pseudo continuous microwave reactor system

can be summarized as illustrated in **Figure 4.9**. The consumption of CCG can start at its weak parts in the short retention time range within 210 s without generating significant amount of pores. After the microwave retention time reaches 210 s, the microporous and mesoporous structures start to be generated on the stable parts of the CCG. One should be reminded that micropore volume is dominant over mesopore volume during the pore generation. Finally, the activated carbon with high specific surface area of 3000 m^2 g^{-1} with micropore-dominant structure can be achieved within 8-9 min.

4.4 Conclusion

Toward the development of a continuous reactor system to produce high-surface-area activated carbon, the pseudo continuous microwave reactor system is firstly investigated. Here, CCG mixed with KOH is used as a feed material to produce activated carbon. The results regarding the surface area, the pore volume, and the production yield have been discussed based on the microwave-retention time defined by the reaction zone length divided by the feed moving-speed through the microwave reaction zone. The nitrogen adsorption-desorption isotherms of the activated carbon produced by the proposed system reveal that pore volume and specific surface area can increase significantly when the microwave retention time is long enough to achieve about 700 °C of the temperature at the carbon precursor. Overall, micropore volume becomes more dominant over mesopore volume. The production yield decreases drastically in the short microwave retention time range when the temperature of the carbon precursor is lower than about 700 °C, and this decrease becomes slight when the microwave retention time is long enough to reach above about 700 °C. This tendency can be explained by considering that the fed CCG consists of weak parts and stable parts, and the weak parts are consumed when the microwave-retention time is short. When the microwave-retention time was set to 510 s, the specific surface area of the activated carbon reached 3054 m^2 g^{-1} by use of the proposed system. The fast rate and high yield shown here should contribute to energy-saving process.

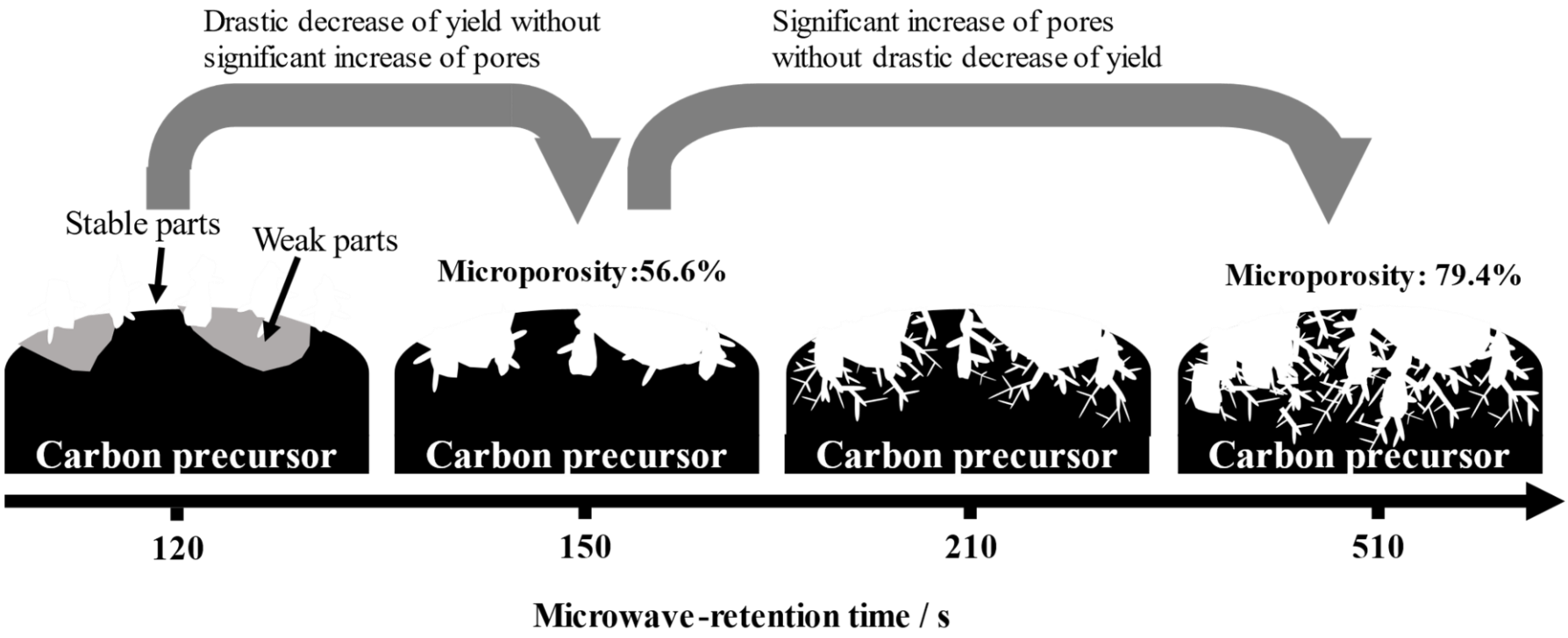

Figure 4.9 Illustration of pore formation of activated carbon prepared by pseudo continuous microwave reactor.

Conclusion and Outlook

Summary of the key thesis contribution

This dissertation contributes to the development of a continuous reactor system to synthesize activated carbon with high specific surface area by microwave-induced plasma with KOH activation, so-called MiWP-KOH activation. To develop this continuous microwave reactor system, systematic investigation on the parameters that could have an influent on the pore formation of activated carbon had been conducted. Firstly, it was proved that activated carbon with a specific surface area larger than 2,000 m^2 g^{-1} can be synthesized in a short time using MiWP-KOH activation (Chapter 1). The pore formation mechanism of activated carbon prepared by MiWP-KOH had been investigated by studying influences of temperature-elevation rate (Chapter 2) and KOH concentration in the feed mixture (Chapter 3) on pore properties of the activated carbon. Finally, the pseudo continuous microwave reactor system was investigated (Chapter 4).

In Chapter 1, it was experimentally confirmed that high-surface-area activated carbon can be synthesized within several minutes using MiWP-KOH method. In this method, a plasma gas was generated above the mixture of powdery CCG and KOH. The temperature of the plasma was estimated to be higher than 5000 °C. This high temperature plasma could lead to the energy input to the precursors to realize the extremely-fast activation. The analytical results of emission spectra indicate that the plasma should be a non-thermal plasma. By using this fast activation, the activated carbon with specific surface area of 1007, 1888, and 2084 m^2 g^{-1} can be obtained within 80, 270, and 330 s. In comparison to a conventional activation, MiWP-KOH method can reduce the activation time by one to two orders of magnitude. Moreover, nitrogen adsorption-desorption isotherm and micropore observation show that temperature-elevation rate could have significant effects on pore structure of the activated carbon. The results also indicate that activated carbon with pore structure that the micropores dominate the mesopores can be obtained by MiWP-KOH with appropriate KOH/carbon ratio.

In Chapter 2, the effects of temperature-elevation rate on pore structure of activated carbon prepared by MiWP-KOH have been investigated to realize pore formation mechanism. The results reveal that as the microwave retention time prolongs, microporous structure becomes more dominant in the structure of the activated carbon. For comparison, activated carbon was prepared by conventional conduction activation method. The experimental results confirm that temperature-elevation rate is one of important factors to

generate micropore-dominating structures in activated carbon. Therefore, activated carbon with micropore-dominating structures can be prepared by MiWP-KOH, which has the extremely high temperature-elevation rate. In addition, temperature-change pattern of the mixture of powdery CCG and KOH during MiWP-KOH activation occurred had been measured. In comparison with the activated carbon prepared using conventional activation with similar temperature-change pattern, the activated carbon prepared by MiWP-KOH activation has a higher specific surface area. This suggests that MiWP-KOH activation should have the microwave-originated effect to enhance pore formation.

In Chapter 3, the investigation of the pore formation of high-surface-area activated carbon prepared by MiWP-KOH activation by observing the effects of KOH concentration in the feed mixture on pore structure of activated carbon is discussed. In this experiment, the "reproducible zone" in pore properties of the activated carbon can be observed when an appropriate range of microwave-retention time and the KOH concentration was used to prepare activated carbon. Here, microwave-irradiation time and the KOH concentration were optimized to realize the reproducible zone in pore properties of the activated carbon, leading to more repeatability of activated carbon properties. The experimental results show that microporosity of the activated carbon indicates that the microporous structure becomes more dominant as the microwave-retention time and the KOH concentration prolongs, resulting in the activated carbon with higher specific surface area.

In Chapter 4, development of a pseudo continuous reactor with MiWP-KOH activation for production of activated carbon with high specific surface area was reported. The specific surface area, pore volume, and production yield of the activated carbon have been discussed based on the microwave-retention time. The study revealed that pore volume and specific surface area of the activated carbon produced by continuous activation can become as 3,054 m^2 g^{-1} when the microwave-retention time is long enough for the temperature of the carbon mixture to achieve about 700 °C. In addition, micropore volume becomes more dominant over mesopore volume as the microwave-retention time prolongs. Since CCG consists of weak and stable parts, and the weak parts might be consumed when the temperature is lower than about 700 °C. Then, the stable parts could be consumed when the microwave retention time is long enough to reach above about 700 °C. Therefore, when the temperature of the carbon precursor is low, the mass yield percentage significantly decreases in the short microwave-retention time range. Decreasing the yield becomes slight when the microwave-retention time is long enough.

In this dissertation, an original method, MiWP-KOH activation, which can be operated in batch and pseudo continuous systems had been developed. The feature of the production method is using microwave-induced plasma to prepare high-surface-area activated carbon with micropore-dominating structure in a short time. This kind of activated carbon has been used as a superior adsorbent for separation units in chemical industries, cleaning of water and air for environmental protection, energy storage capacitors, and so forth.

There are five achievements therein.

(1) Ultra-fast pore formation (270 s) to produce activated carbon (2,718 m^2 g^{-1}) is realized by MiWP-KOH activation operated in batch system.
(2) Extremely high temperature-elevation rate (> 90 °C min^{-1}) in MiWP-KOH activation is essential to realize minute-level activated carbon synthesis.
(3) Micropore domination can be seen in activated carbon made by MiWP-KOH activation.
(4) It is possible to control micropore-volume to mesopore-volume ratio.
(5) Pore formation model on the carbonize carbon gel is proposed for MiWP-KOH activation.

The novel point in this research is the development of MiWP-KOH activation for the preparation of activated carbon that has a specific surface area above 2,000 m^2 g^{-1}. Although the activating conditions in many kinds of literature can use microwave to produce activated carbon with a high surface area, none of the previous literature reported the fast production by consuming low microwave power as this study. Furthermore, this MiWP-KOH method can successfully prepare activated carbon with a high specific surface area and remarkably reduce activation time by one or two orders of magnitude compared to the conventional activation method. In terms of generation of high surface area activated carbon with significant reduction of reaction time, MiWP-KOH activation can be a promising method.

Energy consumption in MiWP-KOH activation and activation by heat conduction using electric furnace can be simply compared based on experimental result in Chapter 2 using Eq.C.1. The calculation results are summarized in **Table C.1**.

$$\text{Energy Consumption [J g}^{-1}\text{]} = \frac{\text{Supplied Power [J s}^{-1}\text{]} \times \text{Heating time [s]}}{\text{Amount of produced activated carbon [g]}} \qquad \text{(C.1)}$$

The calculation shows that energy needed to be consumed to produce activated carbon by MiWP-KOH activation and heat conduction activation is

20.13 and 261.34 MJ g^{-1}, respectively. MiWP-KOH activation can consume less energy than heat conduction activation because MiWP-KOH activation requires less activation time to produce activated carbon with high specific surface area. Therefore, the pseudo continuous system that had been developed could open the possibility to develop continuous system, which might result in less energy consumption and be more environmental friendly.

Table C.1 Energy consumption in MiWP-KOH activation and activation by heat conduction using electric furnace

		MiWP-KOH	Heat conduction
Temperature-elevation rate	°C min^{-1}		19
Specific surface area	m^2 g^{-1}	2,500	2,507
Mass yield percentage	%	14.9	10.2
Total heating time	s	600	11,760 (196 min)
Amount of produced activated carbon	g	0.015	0.031
Supplied Power	W = J s^{-1}	500	680
Energy Consumption	J g^{-1}	2.01E+07	2.61E+08
	MJ g^{-1}	20.13	261.34

Outlook for future research

To realize industrial production, more operating parameters must be investigated. For example, flow rate of inert gas, inert gases, activating agents, particle size of the carbon precursor, and carbon precursors. The carbon precursors can have an influence on both properties of activated carbon and production cost. Our previous study shows that this MiWP-KOH activation can be used to make activated carbon from Water hyacinth, which is well-known biomass in Thailand. More study on this biomass and the others should be done further. In addition, the stability and repeatability of plasma should be improved. Our preliminary study shows that moisture content in the mixture of carbon precursor and activating agents could have an influence on the stability and repeatability of the plasma. More investigation is needed to improve plasma generation. Moreover, analysis of activated carbon properties such as surface functional group and hydrophobicity can expand the range of application of the activated carbon.

Bibliography

1. Danish M, Ahmad T. A review on utilization of wood biomass as a sustainable precursor for activated carbon production and application. *Renewable and Sustainable Energy Reviews*. 2018;87:1-21. doi:10.1016/j.rser.2018.02.003

2. Sreńscek-Nazzal J, Kiełbasa K. Advances in modification of commercial activated carbon for enhancement of CO2 capture. *Applied Surface Science*. 2019;494:137-151. doi:10.1016/j.apsusc.2019.07.108

3. Sreńscek-Nazzal J, Kamińska W, Michalkiewicz B, Koren ZC. Production, characterization and methane storage potential of KOH-activated carbon from sugarcane molasses. *Industrial Crops and Products*. 2013;47:153-159. doi:10.1016/j.indcrop.2013.03.004

4. Menéndez JA, Arenillas A, Fidalgo B, et al. Microwave heating processes involving carbon materials. *Fuel Processing Technology*. 2010;91(1):1-8. doi:10.1016/j.fuproc.2009.08.021

5. Oladimeji TE, Odunoye BO, Elehinafe FB, Obanla OR, Odunlami OA. Production of activated carbon from sawdust and its efficiency in the treatment of sewage water. *Heliyon*. 2021;7(1). doi:10.1016/j.heliyon.2021.e05960

6. Cardoso BS, Forte MBS. Purification of biotechnological xylitol from Candida tropicalis fermentation using activated carbon in fixed-bed adsorption columns with continuous feed. *Food and Bioproducts Processing*. 2021;126:73-80. doi:10.1016/j.fbp.2020.12.013

7. Roegiers J, Denys S. Development of a novel type activated carbon fiber filter for indoor air purification. *Chemical Engineering Journal*. 2021;417. doi:10.1016/j.cej.2020.128109

8. Zakaria R, Jamalluddin NA, Abu Bakar MZ. Effect of impregnation ratio and activation temperature on the yield and adsorption performance of mangrove based activated carbon

for methylene blue removal. *Results in Materials*. 2021;10:100183. doi:10.1016/j.rinma.2021.100183

9. Kupila R, Lappalainen K, Hu T, Romar H, Lassi U. Lignin-based activated carbon-supported metal oxide catalysts in lactic acid production from glucose. *Applied Catalysis A: General*. 2021;612:118011. doi:10.1016/j.apcata.2021.118011

10. Li L, Chen J, Zhang Q, Yang Z, Sun Y, Zou G. Methane dry reforming over activated carbon supported Ni-catalysts prepared by solid phase synthesis. *Journal of Cleaner Production*. 2020;274:122256. doi:10.1016/j.jclepro.2020.122256

11. China Activated Carbon Water Filter Cartridge for Pre-Filtration - China Cartridge Filter, Water Filter. Accessed July 15, 2021. https://darlly.en.made-in-china.com/product/WvjQFnArboYe/China-Activated-Carbon-Water-Filter-Cartridge-for-Pre-Filtration.html

12. Hydroponic Control Activated Carbon Air Filter - Buy Carbon Filter,Activated Carbon Air Filter,Activated Carbon Air Filter Product on Alibaba.com. Accessed July 15, 2021. https://www.alibaba.com/product-detail/Hydroponic-Control-Activated-Carbon-Air-Filter_1620651335.html

13. Activated carbon from rice husks provide superior substrates for palladium and other catalysts in organic syntheses – yet2. Accessed July 15, 2021. https://www.yet2.com/active-projects/activated-carbon-rice-husks/

14. Tsao CS, Liu Y, Chuang HY, et al. Hydrogen spillover effect of pt-doped activated carbon studied by inelastic neutron scattering. *Journal of Physical Chemistry Letters*. 2011;2(18):2322-2325. doi:10.1021/JZ2010368

15. Rashidi NA, Yusup S. Potential of palm kernel shell as activated carbon precursors through single stage activation technique for carbon dioxide adsorption. *Journal of Cleaner Production*. 2017;168:474-486. doi:10.1016/j.jclepro.2017.09.045

16. Ahmed MB, Zhou JL, Ngo HH, Guo W, Chen M. Progress in the preparation and application of modified biochar for improved contaminant removal from water and wastewater. *Bioresource Technology*. 2016;214:836-851. doi:10.1016/j.biortech.2016.05.057

17. Aroua MK, Daud WMAW, Yin CY, Adinata D. Adsorption capacities of carbon dioxide, oxygen, nitrogen and methane on carbon molecular basket derived from polyethyleneimine impregnation on microporous palm shell activated carbon. *Separation and Purification Technology*. 2008;62(3):609-613. doi:10.1016/j.seppur.2008.03.003

18. Ahmed MB, Zhou JL, Ngo HH, Guo W. Insight into biochar properties and its cost analysis. *Biomass and Bioenergy*. 2016;84:76-86. doi:10.1016/j.biombioe.2015.11.002

19. Lozano-Castelló D, Alcañiz-Monge J, de La Casa-Lillo MA, Cazorla-Amorós D, Linares-Solano A. Advances in the study of methane storage in porous carbonaceous materials. *Fuel*. 2002;81(14):1777-1803. doi:10.1016/S0016-2361(02)00124-2

20. Thommes M, Kaneko K, Neimark A v, et al. Physisorption of gases, with special reference to the evaluation of surface area and pore size distribution (IUPAC Technical Report). *Pure and Applied Chemistry*. 2015;87(9-10):1051-1069. doi:10.1515/pac-2014-1117

21. Celzard A, Fierro V, Marêché JF, Furdin G. *Advanced Preparative Strategies for Activated Carbons Designed for the Adsorptive Storage of Hydrogen †*.

22. Chen J, Lin Y, Liu J, et al. Outstanding supercapacitor performance of nitrogen-doped activated carbon derived from shaddock peel. *Journal of Energy Storage*. 2021;39:102640. doi:10.1016/j.est.2021.102640

23. Khuongab DA, Nguyen HN, Tsubota T. Activated carbon produced from bamboo and solid residue by CO2 activation utilized as CO2 adsorbents. *Biomass and Bioenergy*. 2021;148:106039. doi:10.1016/j.biombioe.2021.106039

24. Guclu C, Alper K, Erdem M, Tekin K, Karagoz S. Activated carbons from co-carbonization of waste truck tires and spent tea leaves. *Sustainable Chemistry and Pharmacy*. 2021;21:100410. doi:10.1016/j.scp.2021.100410

25. Naganathan KK, Faizal ANM, Zaini MAA, Ali A. Adsorptive removal of Bisphenol a from aqueous solution using activated carbon from coffee residue. *Materials Today: Proceedings*. Published online March 26, 2021. doi:10.1016/j.matpr.2021.02.802

26. Hwang B, Yi SH, Chun SE. Dual-role of ZnO as a templating and activating agent to derive porous carbon from polyvinylidene chloride (PVDC) resin. *Chemical Engineering Journal*. 2021;422:130047. doi:10.1016/J.CEJ.2021.130047

27. Rodrigues R, Santos MS, Nunes RS, Carvalho WA, Labuto G. Solvent-free solketal production from glycerol promoted by yeast activated carbons. *Fuel*. 2021;299:120923. doi:10.1016/j.fuel.2021.120923

28. Kongsune P, Rattanapan S, Chanajaree R. The removal of Pb2+ from aqueous solution using mangosteen peel activated carbon: Isotherm, kinetic, thermodynamic and binding energy calculation. *Groundwater for Sustainable Development*. 2021;12:100524. doi:10.1016/J.GSD.2020.100524

29. Tian H, Pan J, Zhu D, et al. Innovative one-step preparation of activated carbon from low-rank coals activated with oxidized pellets. *Journal of Cleaner Production*. 2021;313:127877. doi:10.1016/J.JCLEPRO.2021.127877

30. Lopes GKP, Zanella HG, Spessato L, et al. Steam-activated carbon from malt bagasse: Optimization of preparation conditions and adsorption studies of sunset yellow food dye. *Arabian Journal of Chemistry*. 2021;14(3):103001. doi:10.1016/j.arabjc.2021.103001

31. Ahmadpour A, Do DD. The preparation of active carbons from coal by chemical and physical activation. *Carbon*. 1996;34(4):471-479. doi:10.1016/0008-6223(95)00204-9

32. Pallarés J, González-Cencerrado A, Arauzo I. Production and characterization of activated carbon from barley straw by physical activation with carbon dioxide and steam. *Biomass and Bioenergy*. 2018;115:64-73. doi:10.1016/j.biombioe.2018.04.015

33. Kwiatkowski M, Vargas Delgadillo DP. Computer analysis of the effect of the type of activating agent on the formation of the porous structure of activated carbon monoliths. *Journal of Materials Research and Technology*. 2019;8(5):4457-4463. doi:10.1016/j.jmrt.2019.07.058

34. Lillo-Ródenas MA, Cazorla-Amorós D, Linares-Solano A. Understanding chemical reactions between carbons and NaOH and KOH: An insight into the chemical activation mechanism. *Carbon*. 2003;41(2):267-275. doi:10.1016/S0008-6223(02)00279-8

35. Yue Z, Economy J, Bordson G. Preparation and characterization of NaOH-activated carbons from phenolic resin. *Journal of Materials Chemistry*. 2006;16:1456-1461. doi:10.1039/b513267c

36. Chen R, Li L, Liu Z, et al. Preparation and characterization of activated carbons from tobacco stem by chemical activation Preparation and characterization of activated carbons from tobacco stem by chemical activation. *Journal of the Air & Waste Management Association*. 2017;67(6):713-724. doi:10.1080/10962247.2017.1280560

37. Molino A, Donatelli A, Marino T, Aloise A, Rimauro J, Iovane P. Waste tire recycling process for production of steam activated carbon in a pilot plant. *Resources, Conservation and Recycling*. 2018;129:102-111. doi:10.1016/j.resconrec.2017.10.023

38. Lobato-Peralta DR, Duque-Brito E, Ayala-Cortés A, et al. Advances in activated carbon modification, surface heteroatom configuration, reactor strategies, and regeneration methods for enhanced wastewater treatment. *Journal of Environmental Chemical Engineering*. 2021;9(4):105626. doi:10.1016/j.jece.2021.105626

39. Satya Sai PM, Ahmed J, Krishnaiah K. Production of Activated Carbon from Coconut Shell Char in a Fluidized Bed Reactor. *Industrial & engineering chemistry research*. 1997;36:3625-3630. doi:10.1021/ie970190v

40. Mohaddespour A, Atashrouz S, Munir MT, Farag S, Jaradat KT. Carbon aerogels activation by CO2 using an induction heated fluidized bed reactor. *Chemical Engineering Science*. 2021;229:116123. doi:10.1016/j.ces.2020.116123

41. Tiegam RFT, Tchuifon Tchuifon DR, Santagata R, et al. Production of activated carbon from cocoa pods: Investigating benefits and environmental impacts through analytical chemistry techniques and life cycle assessment. *Journal of Cleaner Production*. 2021;288:125464. doi:10.1016/j.jclepro.2020.125464

42. Foo KY, Hameed BH. Preparation, characterization and evaluation of adsorptive properties of orange peel based activated carbon via microwave induced K 2CO 3 activation. *Bioresource Technology*. 2012;104:679-686. doi:10.1016/j.biortech.2011.10.005

43. Zhu X, Gao Y, Yue Q, Kan Y, Kong W, Gao B. Preparation of green alga-based activated carbon with lower impregnation ratio and less activation time by potassium tartrate for adsorption of chloramphenicol. *Ecotoxicology and Environmental Safety*. 2017;145:289-294. doi:10.1016/j.ecoenv.2017.07.053

44. Canales-Flores RA, Prieto-García F. Taguchi optimization for production of activated carbon from phosphoric acid impregnated agricultural waste by microwave heating for the removal of methylene blue. *Diamond and Related Materials*. 2020;109:108027. doi:10.1016/j.diamond.2020.108027

45. Brazil TR, Gonçalves M, Junior MSO, Rezende MC. A statistical approach to optimize the activated carbon production from Kraft lignin based on conventional and microwave processes. *Microporous and Mesoporous Materials*. 2020;308:110485. doi:10.1016/j.micromeso.2020.110485

46. Tripathi NK, Sathe M. Pilot Scale Production of Activated Carbon Spheres Using Fluidized Bed Reactor and Its Evaluation for the Removal of Hexavalent Chromium from Aqueous Solutions. *Journal of The Institution of Engineers (India): Series E*. 2017;98(2):141-147. doi:10.1007/s40034-017-0100-5

47. Chen X, Cheng Y, Li T, Cheng Y. Characteristics and applications of plasma assisted chemical processes and reactors. *Current Opinion in Chemical Engineering*. 2017;17:68-77. doi:10.1016/J.COCHE.2017.07.001

48. Why a stream of plasma makes chemical reactions more efficient: Modeling shows that plasmas may activate the metal catalyst in a packed bed reactor, resulting in faster chemical reactions -- ScienceDaily. Accessed July 15, 2021. https://www.sciencedaily.com/releases/2018/11/181106133243.htm

49. Rizk SA, El-Hashash MA, Youssef AA, Elgendy AT. A green microwave method for synthesizing a more stable phthalazin-1-ol isomer as a good anticancer reagent using chemical plasma organic reactions. *Heliyon*. 2021;7(3):e06220. doi:10.1016/J.HELIYON.2021.E06220

50. Cheng B, Ishihara K. Formation of stable polydopamine layer on polytetrafluoroethylene substrate by hybrid process involved plasma treatment and spontaneous chemical reactions. *Materials Today Communications*. 2020;22:100774. doi:10.1016/J.MTCOMM.2019.100774

51. al Zoubi W, Putri RAK, Ko YG. Understanding the metal ion-ligand responsible in the plasma-assisted electrochemical reactions for optimizing chemical stability. *Journal of Molecular Liquids*. 2021;321:114756. doi:10.1016/J.MOLLIQ.2020.114756

52. Kabouzi Y, Calzada MD, Moisan M, Tran KC, Trassy C. Radial contraction of microwave-sustained plasma columns at atmospheric pressure. *Journal of Applied Physics*. 2002;91(3):1008-1019. doi:10.1063/1.1425078

53. Itaya Y, Matsubara K, Tanaka R, Kobayashi N. Optical analysis during reduction of nitric oxide in microwave-induced plasma promoted by activated cokes at atmospheric pressure. *Fuel*. 2019;242:382-388. doi:10.1016/j.fuel.2018.12.133

54. Domínguez A, Fernández Y, Fidalgo B, Pis JJ, Menéndez JA. Biogas to syngas by microwave-assisted dry reforming in the presence of char. *Energy and Fuels*. 2007;21(4):2066-2071. doi:10.1021/ef070101j

55. Fidalgo B, Domínguez A, Pis JJ, Menéndez JA. Microwave-assisted dry reforming of methane. *International Journal of Hydrogen Energy*. 2008;33(16):4337-4344. doi:10.1016/j.ijhydene.2008.05.056

56. Hoseinzadeh Hesas R, Wan Daud WMA, Sahu JN, Arami-Niya A. The effects of a microwave heating method on the production of activated carbon from agricultural waste: A review. *Journal of Analytical and Applied Pyrolysis*. 2013;100:1-11. doi:10.1016/j.jaap.2012.12.019

57. Ao W, Fu J, Mao X, et al. Microwave assisted preparation of activated carbon from biomass: A review. *Renewable and Sustainable Energy Reviews*. 2018;92:958-979. doi:10.1016/j.rser.2018.04.051

58. Brea P, Delgado JA, Águeda VI, Uguina MA. Comparison between MOF UTSA-16 and BPL activated carbon in hydrogen purification by PSA. *Chemical Engineering Journal*. 2019;355:279-289. doi:10.1016/j.cej.2018.08.154

59. Zuo Q, Zhang Y, Zheng H, et al. A facile method to modify activated carbon fibers for drinking water purification. *Chemical Engineering Journal*. 2019;365:175-182. doi:10.1016/j.cej.2019.02.047

60. Santos-Clotas E, Cabrera-Codony A, Ruiz B, Fuente E, Martín MJ. Sewage biogas efficient purification by means of lignocellulosic waste-based activated carbons. *Bioresource Technology*. 2019;275:207-215. doi:10.1016/j.biortech.2018.12.060

61. Ishihara T, Miyahara M, Yamada T, Yamamoto K. Innovative next-generation monoclonal antibody purification using activated carbon: A challenge for flow-through and column-free processes. *Journal of Chromatography B: Analytical Technologies in the Biomedical and Life Sciences*. 2019;1121:72-81. doi:10.1016/j.jchromb.2019.05.009

62. Wawrzyńczak D, Panowski M, Majchrzak-Kucęba I. Possibilities of CO2 purification coming from oxy-combustion for enhanced oil recovery and storage purposes by adsorption method on activated carbon. *Energy*. 2019;180:787-796. doi:10.1016/j.energy.2019.05.068

63. Arneli, Safitri ZF, Pangestika AW, Fauziah F, Wahyuningrum VN, Astuti Y. The influence of activating agents on the performance of rice husk-based carbon for sodium lauryl sulfate and chrome (Cr) metal adsorptions. In: *IOP Conference Series: Materials Science and Engineering*. Vol 172. Institute of Physics Publishing; 2017:012007-undefined. doi:10.1088/1757-899X/172/1/012007

64. le Van K, Luong Thi Thu T. Preparation of pore-size controllable activated carbon from rice husk using dual activating agent and its application in supercapacitor. *Journal of Chemistry*. 2019;2019:4329609-undefined. doi:10.1155/2019/4329609

65. Ravichandran P, Sugumaran P, Seshadri S, Basta AH. Optimizing the route for production of activated carbon from Casuarina equisetifolia fruit waste. *Royal Society Open Science*. 2018;5(7):171578-undefined. doi:10.1098/rsos.171578

66. Selvaraju G, Bakar NKA. Process conditions for the manufacture of highly micro-mesoporous eco-friendly activated carbon from artocarpus integer bio-waste by steam activation. *Journal of the Taiwan Institute of Chemical Engineers*. 2018;93:414-426. doi:10.1016/j.jtice.2018.08.011

67. Sivakumar B, Kannan C, Karthikeyan S. Preparation and characterization of activated carbon prepared from Balsamodendron caudatum wood waste through various

activation processes. *RASĀYAN Journal of Chemistry*. 2012;5(3):321-327. http://www.rasayanjournal.com

68. Das D, Samal DP, BC M. Preparation of Activated Carbon from Green Coconut Shell and its Characterization. *Journal of Chemical Engineering & Process Technology*. 2015;06(05). doi:10.4172/2157-7048.1000248

69. Loya-González D, Loredo-Cancino M, Soto-Regalado E, et al. Optimal activated carbon production from corn pericarp: A life cycle assessment approach. *Journal of Cleaner Production*. 2019;219:316-325. doi:10.1016/J.JCLEPRO.2019.02.068

70. Mukai SR, Tamitsuji C, Nishihara H, Tamon H. Preparation of mesoporous carbon gels from an inexpensive combination of phenol and formaldehyde. *Carbon*. 2005;43(12):2628-2630. doi:10.1016/j.carbon.2005.05.004

71. Liu S, Cai Y, Yu YL, Wang JH. A miniature liquid electrode discharge-optical emission spectrometric system integrating microelectrodialysis for potassium screening in serum. *Journal of Analytical Atomic Spectrometry*. 2017;32(9):1739-1745. doi:10.1039/c7ja00111h

72. Lim M, Zulazalan A, Zulkifli S, Hassan H. Biomass Combustion: Potassium and Sodium Flame Emission Spectra and Composition in Ash. *Journal of the Japan Institute of Energy*. 2017;96:367-371.

73. Element Potassium | AtomTrace. Accessed June 6, 2021. https://www.atomtrace.com/elements-database/element/19

74. Bird RB, Stewart WE, Lightfoot EN. *Transport Phenomena*. Vol 1. John Wiley & Sons; 2006.

75. Bruggeman PJ, Iza F, Brandenburg R. Foundations of atmospheric pressure non-equilibrium plasmas. *Plasma Sources Science and Technology*. 2017;26(12). doi:10.1088/1361-6595/aa97af

76. Sing KSW. Reporting physisorption data for gas/solid systems with special reference to the determination of surface area and porosity (Recommendations 1984). *Pure and Applied*

Chemistry. 1985;57(4):603-619. doi:10.1351/pac198557040603

77. Dollimore D, Heal GR. An improved method for the calculation of pore size distribution from adsorption data. *Journal of Applied Chemistry*. 1964;14(3):109-114. doi:10.1002/jctb.5010140302

78. Horvath G, Kawazoe K. Method for the calculation of effective pore size distribution in molecular sieve carbon. *Journal of Chemical Engineering of Japan*. 1983;16(6):470-475.

79. Glonek K, Wróblewska A, Makuch E, et al. Oxidation of limonene using activated carbon modified in dielectric barrier discharge plasma. *Applied Surface Science*. 2017;420:873-881. doi:10.1016/j.apsusc.2017.05.136

80. de Velasco Maldonado PS, Hernández-Montoya V, Montes-Morán MA. Plasma-surface modification vs air oxidation on carbon obtained from peach stone: Textural and chemical changes and the efficiency as adsorbents. *Applied Surface Science*. 2016;384:143-151. doi:10.1016/j.apsusc.2016.05.018

81. Konno K, Oike Y, Ohba Y, et al. Short-Time Preparation of NaOH-Activated Carbon from Sugar Cane Bagasse Using Microwave Plasma Heating. *Green and Sustainable Chemistry*. 2017;07(04):259-269. doi:10.4236/gsc.2017.74020

82. Boudou JP, Martinez-Alonzo A, Tascon JMD. Introduction of acidic groups at the surface of activated carbon by microwave-induced oxygen plasma at low pressure. *Carbon*. 2000;38(7):1021-1029. doi:10.1016/S0008-6223(99)00209-2

83. Zheng Z qiang, Xia H ying, Srinivasakannan C, Peng J hui, Zhang L bo. Utilization of Crofton weed for preparation of activated carbon by microwave induced CO2 activation. *Chemical Engineering and Processing: Process Intensification*. 2014;82:1-8. doi:10.1016/j.cep.2014.05.001

84. Brunauer S, Emmett PH, Teller E. Adsorption of Gases in Multimolecular Layers. *Journal of the American Chemical Society*. 1938;60(2):309-319. doi:10.1021/ja01269a023

85. Lippens MBC, de Boer JH. Studies on pore systems in catalysts: V. The t method. *Journal of Catalysis*. 1965;4(3):319-323. doi:10.1016/0021-9517(65)90307-6

86. Barrett EP, Joyner LG, Halenda PP. The Determination of Pore Volume and Area Distributions in Porous Substances. I. Computations from Nitrogen Isotherms. *Journal of the American Chemical Society*. 1951;73(1):373-380. doi:10.1021/ja01145a126

87. Dubinin MM, Plavnik GM. Microporous structures of carbonaceous adsorbents. *Carbon*. 1968;6(2):183-192. doi:10.1016/0008-6223(68)90302-3

88. Schneider P. Adsorption isotherms of microporous-mesoporous solids revisited. *Applied Catalysis A, General*. 1995;129(2):157-165. doi:10.1016/0926-860X(95)00110-7

89. Thommes M. Physical Adsorption Characterization of Nanoporous Materials. *Chemie Ingenieur Technik*. 2010;82(7):1059-1073. doi:10.1002/cite.201000064

90. Cychosz KA, Thommes M. Progress in the Physisorption Characterization of Nanoporous Gas Storage Materials. *Engineering*. 2018;4(4):559-566. doi:10.1016/j.eng.2018.06.001

91. Kuptajit P, Sano N. Application of microwave-induced plasma for extremely fast synthesis of large surface area activated carbon. *Applied Physics Express*. 2019;12(8):086001-undefined. doi:10.7567/1882-0786/ab29e5

92. Mishra RR, Sharma AK. Microwave-material interaction phenomena: Heating mechanisms, challenges and opportunities in material processing. *Composites Part A: Applied Science and Manufacturing*. 2016;81:78-97. doi:10.1016/j.compositesa.2015.10.035

93. Moulijn JA, van Diepen AE, Kapteijn F. Catalyst deactivation: is it predictable? What to do? *Applied Catalysis A: General*. 2001;212:3-16. doi:10.1016/S0926-860X(00)00842-5

94. Benhouria A, Islam MA, Zaghouane-Boudiaf H, Boutahala M, Hameed BH. Calcium alginate-bentonite-activated carbon composite beads as highly effective adsorbent for methylene blue. *Chemical Engineering Journal*. 2015;270:621-630. doi:10.1016/j.cej.2015.02.030

95. Zabaniotou A, Madau P, Oudenne PD, Jung CG, Delplancke M-P, Fontana A. Active carbon production from used tire in two-stage procedure: industrial pyrolysis and bench scale activation with H2O–CO2 mixture. *Journal of Analytical and Applied Pyrolysis*. 2004;72(2):289-297. doi:10.1016/j.jaap.2004.08.002

96. Zhang Y, Song X, Xu Y, Shen H, Kong X, Xu H. Utilization of wheat bran for producing activated carbon with high specific surface area via NaOH activation using industrial furnace. *Journal of cleaner production*. 2019;210:366-375.

97. Liang J, Qu T, Kun X, et al. Microwave assisted synthesis of camellia oleifera shell-derived porous carbon with rich oxygen functionalities and superior supercapacitor performance. *Applied Surface Science*. 2018;436:934-940. doi:10.1016/j.apsusc.2017.12.142

98. Njoku VO, Foo KY, Asif M, Hameed BH. Preparation of activated carbons from rambutan (Nephelium lappaceum) peel by microwave-induced KOH activation for acid yellow 17 dye adsorption. *Chemical Engineering Journal*. 2014;250:198-204. doi:10.1016/j.cej.2014.03.115

99. Li K, Zhou M, Liang L, Jiang L, Wang W. Ultrahigh-surface-area activated carbon aerogels derived from glucose for high-performance organic pollutants adsorption. *Journal of Colloid and Interface Science*. 2019;546:333-343. doi:10.1016/j.jcis.2019.03.076

100. Nasrullah A, Saad B, Bhat AH, et al. Mangosteen peel waste as a sustainable precursor for high surface area mesoporous activated carbon: Characterization and application for methylene blue removal. *Journal of Cleaner Production*. 2019;211:1190-1200. doi:10.1016/j.jclepro.2018.11.094

101. Sulaiman NS, Hashim R, Mohamad Amini MH, Danish M, Sulaiman O. Optimization of activated carbon preparation from cassava stem using response surface methodology on surface area and yield. *Journal of Cleaner Production*. 2018;198:1422-1430. doi:10.1016/j.jclepro.2018.07.061

102. Deng H, Li G, Yang H, Tang J, Tang J. Preparation of activated carbons from cotton stalk by microwave assisted KOH and K2CO3 activation. *Chemical Engineering Journal*. 2010;163(3):373-381. doi:10.1016/j.cej.2010.08.019

103. Foo KY, Hameed BH. Utilization of rice husks as a feedstock for preparation of activated carbon by microwave induced KOH and K 2CO 3 activation. *Bioresource Technology*. 2011;102(20):9814-9817. doi:10.1016/j.biortech.2011.07.102

104. Huber L, Hauser SB, Brendlé E, et al. The effect of activation time on water sorption behavior of nitrogen-doped, physically activated, monolithic carbon for adsorption cooling. *Microporous and Mesoporous Materials*. 2019;276:239-250. doi:10.1016/j.micromeso.2018.09.025

105. Üner O, Bayrak Y. The effect of carbonization temperature, carbonization time and impregnation ratio on the properties of activated carbon produced from Arundo donax. *Microporous and Mesoporous Materials*. 2018;268:225-234. doi:10.1016/j.micromeso.2018.04.037

106. Morgan M. Electrical conduction in amorphous carbon films. *Thin Solid Films*. 1971;7(5):313-323. doi:10.1016/0040-6090(71)90049-6

107. Koyuncu F, Güzel F, Sayğılı H. Role of optimization parameters in the production of nanoporous carbon from mandarin shells by microwave-assisted chemical activation and utilization as dye adsorbent. *Advanced Powder Technology*. 2018;29(9):2108-2118. doi:10.1016/j.apt.2018.05.019

108. Liu QS, Zheng T, Wang P, Guo L. Preparation and characterization of activated carbon from bamboo by microwave-induced phosphoric acid activation. *Industrial*

Crops and Products. 2010;31(2):233-238. doi:10.1016/j.indcrop.2009.10.011

109. Lv Y, Zhang F, Dou Y, et al. A comprehensive study on KOH activation of ordered mesoporous carbons and their supercapacitor application. *Journal of Materials Chemistry*. 2012;22(1):93-99. doi:10.1039/c1jm12742j

110. Erdoğan S, Akmil Başar C, Önal Y. Particle size effect of raw material on the pore structure of carbon support and its adsorption capability. *Particulate Science and Technology*. 2017;35(3):330-337. doi:10.1080/02726351.2016.1154911

111. Boujibar O, Ghamouss F, Ghosh A, Achak O, Chafik T. Activated carbon with exceptionally high surface area and tailored nanoporosity obtained from natural anthracite and its use in supercapacitors. *Journal of Power Sources*. 2019;436:226882-undefined. doi:10.1016/j.jpowsour.2019.226882

112. Wang H, Xu J, Liu X, Sheng L. Preparation of straw activated carbon and its application in wastewater treatment: A review. *Journal of Cleaner Production*. 2021;283:124671-undefined. doi:10.1016/j.jclepro.2020.124671

113. Su C-Y, Wu C-Y, Hsu S-Y, Wu C-Y, Duh J-G. Improving the electrochemical performance of LiMn0. 8Fe0. 2PO4 cathode with nitrogen-doped carbon via dielectric barrier discharge plasma. *Materials Letters*. 2020;272:127880. doi:10.1016/j.matlet.2020.127880

114. Das D, Roy A. Synthesis of diameter controlled multiwall carbon nanotubes by microwave plasma-CVD on low-temperature and chemically processed Fe nanoparticle catalysts. *Applied Surface Science*. 2020;515:146043. doi:10.1016/j.apsusc.2020.146043

115. Zhao Y, He J. Superfast microwave synthesis of hierarchically porous rGO by graphite ignited reduction propagation. *Carbon*. 2021;178:734-742. doi:https://doi.org/10.1016/j.carbon.2021.03.048

116. Lam SS, Su MH, Nam WL, et al. Microwave Pyrolysis with Steam Activation in Producing Activated Carbon for Removal of Herbicides in Agricultural Surface Water. *Industrial and Engineering Chemistry Research*. 2019;58(2):695-703. doi:10.1021/acs.iecr.8b03319

Acknowledgement

This dissertation is a summary of my research activities at Separation Engineering Laboratory, Department of Chemical Engineering, Kyoto University from 2018 to 2021.

I would like to express my special gratitude and thanks to my supervisor, Dr. Noriaki Sano, Professor of Department of Chemical Engineering, Kyoto University. He did not only gave me his knowledge, suggestion, and expertise for this research but also gave me full supports to help me overcome countless challenges.

I am deeply grateful to Dr. Minoru Miyahara and Dr. Motoaki Kawase, Professor of the Department of Chemical Engineering, Kyoto University for their time and affords to review this thesis. Their critical questions and insightful comments enriched my knowledge and improved this dissertation.

I would like to thank Dr. Kyuya Nakagawa, Associate Professor, and Dr. Tetsuo Suzuki, Assistant Professor of Department of Chemical Engineering, Kyoto University. Their support helps me continuous this research.

I gratefully acknowledge the Asahi Glass Foundation (AF) for a scholarship. This scholarship helps me gain more confidence in my research and gain more self-esteem. Therefore, the speed of improving both my research and myself was accelerated.

I appreciate the Horiguchi scholarship for granting the travel fee to participate in FOA2019. At this conference, I had a chance to learn the most recent knowledge in the field of adsorption science from world-leading experts.

My deep gratitude goes to all members of Separation Engineering Laboratory. This place gave me a lot of memorable moments. I am thankful to my colleagues, Mr. Hiroaki Ueno for his time and affords to teach me how to use an automated physisorption surface area analyzer. Special thanks to Mr. Taku Tsujioka and Mr. Daiki Komuta for their kind helps with TEM and SEM observations for my first publication. I also would like to thank Ms. Mayumi Uchimura, a secretary of the laboratory, for her helpful office works and kindly serving confections. Her kindly support always bright up my day.

Finally, my thanks and appreciations also go to my family and friends who have helped me unconditionally.

Purichaya Kuptajit

Kyoto,

August 2021

List of Publications

Parts of this thesis have been published in the following journal papers:

1. Purichaya Kuptajit, Noriaki Sano, "Application of microwave-induced plasma for extremely fast synthesis of large surface area activated carbon" *Appl. Phys. Express* **12**, 086001 (2019).

[Parts of **Chapter 1** of the thesis are reproduced from this paper with permission. This paper is available online at: https://doi.org/10.7567/1882-0786/ab29e5. Copyright 2019 The Japan Society of Applied Physics.]

2. Purichaya Kuptajit, Kyuya Nakagawa, Tetsuo Suzuki, Noriaki Sano, "A study on pore formation of high surface area activated carbon prepared by microwave-induced plasma with KOH (MiWP-KOH) activation: Effect of temperature-elevation rate" *Chem. Eng. Process* **167,** 108511 (2021).

[Parts of **Chapter 2** of the thesis are reproduced from this paper with permission. This paper is available online at: https://doi.org/10.1016/j.cep.2021.108511.
Copyright 2021 Elsevier B.V.]

3. Purichaya Kuptajit, Kyuya Nakagawa, Tetsuo Suzuki, Noriaki Sano, "Microwave-induced plasma with KOH (MiWP-KOH) activation for preparation of high-surface-area activated carbon: Controllability of pore structures by KOH-to-carbon ratio in feed and activating time" **submitted.**

[This paper is based on parts of **Chapter 3** of this thesis.]

4. Purichaya Kuptajit, Kyuya Nakagawa, Tetsuo Suzuki, Noriaki Sano, "Pseudo continuous reactor with microwave-plasma for preparation of high surface area activated carbon" accepted by **Jpn. Inst. Energy**.

[This paper is based on parts of **Chapter 4** of this thesis.]

International Conferences

1. Purichaya Kuptajit, Tawatchai Charinpanitkul, Noriaki Sano, "Extremely fast activation method to synthesize activated carbon using KOH with microwave irradiation". *JCREN2018*, **IN_13**, Ube, Japan, December 2018 (Oral presentation).

2. Purichaya Kuptajit, Tawatchai Charinpanitkul, Noriaki Sano, "Ultrafast activation method to prepare activated carbon with a large specific surface area using microwave irradiation with KOH". *#13FOA*, **87**, Cairns, Australia, May 2019 (Poster presentation).

3. Purichaya Kuptajit, Noriaki Sano, "Development of extremely fast activation method by using microwave heating for activated carbon preparation from carbon gel". *APCChE2019*, **C217**, Sapporo, Japan, September 2019 (Oral presentation).

4. Purichaya Kuptajit, Noriaki Sano, "Utilization of microwave-induced plasma in extremely fast activation for preparation of activated carbon with large surface area". *MRM2019*, **H2-O12-005**, Yokohama, Japan, December 2019 (Oral presentation).

5. Purichaya Kuptajit, Kyuya Nakagawa, Tetsuo Suzuki, Noriaki Sano, "Preparation of high surface area activated carbon using semi-batch reactor". *JCREN2020*, **JCREN30**, Khon Kaen, Thailand, October 2020 (Oral presentation, Online).